

CONTROLS ON RESERVOIR CHARACTER IN CARBONATE-CHERT STRATA,
MISSISSIPPIAN (OSAGEAN-MERAMECIAN), SOUTHEAST KANSAS

BY

Erin Megan Young
B.S., The University of Nebraska at Omaha, 2007

Submitted to the graduate degree program in Geology
and the Graduate Faculty of the University of Kansas
in partial fulfillment of the requirements for the degree of
Master of Sciences

2010

Robert H. Goldstein, Co-chairperson

Evan K. Franseen, Co-chairperson

Michael Taylor, Committee member

Date defended: _____

The Thesis Committee for Erin M. Young certifies
that this is the approved version of the following thesis:

CONTROLS ON RESERVOIR CHARACTER IN CARBONATE-CHERT STRATA,
MISSISSIPPIAN (OSAGEAN-MERAMECIAN), SOUTHEAST KANSAS

Committee:

Robert H. Goldstein, Co-chairperson

Evan K. Franseen, Co-chairperson

Michael Taylor, Committee member

Date approved: _____

ABSTRACT

Erin Megan Young
Department of Geology, November 2010
The University of Kansas

Osagean-Meramecian strata in southeast Kansas were investigated to determine structural, relative sea level, diagenetic, and depositional controls on stratigraphy, lithofacies distribution, and reservoir character.

Lithofacies include echinoderm-rich bioclastic wacke-packstone, sponge-spicule-rich packstone, dolomitic bioclastic wackestone, argillaceous dolomite, tripolitic chert, and chert breccia. Four cores are used to construct a ten-mile long southwest-northeast cross section, which assists in interpretation of three genetic units. Paragenesis reveals that early and late dissolution enhance porosity in chert. Fluid inclusion microthermometry from megaquartz and baroque dolomite reveals variable but increasing homogenization temperatures (70°C-160°C) that increase in salinity through time.

Data indicate that reservoir character is an interplay of depositional through late diagenetic events. The best reservoirs may be controlled by depositional setting that led to large amounts of chert and carbonate grains in grain support, alteration associated with subaerial exposure, and a hydrologic and structural setting that led to enhanced hydrothermal fluid flow for later dissolution.

TABLE OF CONTENTS

ACCEPTANCE PAGE.....	II
ABSTRACT.....	III
TABLE OF CONTENTS	IV
LIST OF FIGURES & TABLES.....	VI
ACKNOWLEDGMENTS	VII
INTRODUCTION.....	1
Methodology	3
GEOLOGIC SETTING	4
LITHOFACIES AND DEPOSITIONAL ENVIRONMENT	11
Echinoderm-rich bioclastic wacke-packstone.....	11
Sponge-spicule-rich packstone	12
Dolomitic bioclastic wackestone	14
Argillaceous wackestone	15
Tripolitic chert	16
Variable chert breccia	17
Ooid packstone.....	19
Dark shale	20
GENETIC STRATIGRAPHY.....	30
Unit 1	30
Unit 2	38
Unit 3	42
DIAGENESIS.....	46
FLUID INCLUSIONS	57
Megaquartz	57
Baroque dolomite.....	59
DISCUSSION	66
Hydrothermal system.....	66
Subaerial versus hydrothermal porosity enhancement in chert	74
Localization of best reservoir facies	79

CONCLUSIONS	79
REFERENCES CITED	83
APPENDIX	94
Appendix I Core descriptions	94
PM-17	96
PM-12	116
PM-21	136
PM-8	155
Appendix II Thin section descriptions	171
Appendix III Fluid inclusion data	196

LIST OF FIGURES AND TABLES

Figure 1	Location map.....	6
Figure 2	Mississippian stratigraphic nomenclature.....	7
Figure 3	Paleogeographic map.....	10
Figure 4	Core photographs and thin section photomicrographs of echinoderm-rich bioclastic wacke-packstone and sponge-spicule-rich packstone.....	26
Figure 5	Core photographs and thin section photomicrographs of dolomitic bioclastic wackestone, argillaceous wackestone, and tripolitic chert.....	27
Figure 6	Core photographs of variable chert breccia.....	29
Figure 7	Legend for Figures 8, 9, 10, and 11.....	33
Figure 8	Stratigraphic cross section of four cores described in study area.....	34
Figure 9	Stratigraphic cross section of Unit 1.....	36
Figure 10	Stratigraphic cross section of Unit 2.....	41
Figure 11	Stratigraphic cross section of Unit 3.....	45
Figure 12	Paragenetic sequence.....	47
Figure 13	Photomicrographs illustrating characteristics leading to interpretation of diagenetic stages 1-14.....	54
Figure 14	Photomicrographs illustrating characteristics leading to interpretation of diagenetic stages 14-17.....	55
Figure 15	Photomicrographs illustrating characteristics leading to interpretation of diagenetic stages 10-22.....	56
Figure 16	Photomicrographs of fluid inclusions in quartz and baroque dolomite.....	61
Figure 17	Fluid inclusion data.....	62
Figure 18	FIA transects of fluid inclusion homogenization temperatures.....	64
Figure 19	Homogenization temperatures of fluid inclusions through time.....	65
Figure 20	Schematic diagrams illustrating diagenetic fluid flow scenarios.....	72
Table 1	Characteristics of lithofacies.....	25

ACKNOWLEDGMENTS

First and foremost, I would like to thank my advisors Dr. Robert Goldstein and Dr. Evan Franseen for taking me under their wings and guiding this project. I thank you for your time, effort, and willingness to teach me not only all things geology but life lessons I will take with me on my journey. I am forever grateful to you for accepting me into this department for I am so lucky and proud to be G-Hawker. A special thank you also goes to Dr. W. Lynn Watney with all of his help with everything Mississippian in Kansas; without his previous work this project would not have been possible.

I would like to thank the Department of Geology at The University of Kansas, Kansas Geological Survey, Kansas Geological Foundation, American Association of Petroleum Geologists Grants-In-Aid, and the Croatian Cultural Society of Omaha for all their generous funding throughout this project. Without their gracious support, this project would not have been possible.

Thank you to all the Kansas Geological Survey staff for their exceptional assistance. Dave Laflen for his manual labor taking out core and putting it back again, and again, and again. Janice Sorensen for finding me every article, book, or map I ever asked for and doing it with a smile on her face. Wayne Dickerson for assistance with fluid inclusion thick section preparation. Karen Dawber for making sure I could always afford to eat and have health insurance. Also, thank you to Yolanda, Liz, Gwethalyn, and Jenna for all their support with everything paperwork related; you ladies are great.

I would also like to thank my undergraduate geology department at The University of Nebraska at Omaha. Dr. Robert Shuster played the most important role in introducing me to

geology and without him I would have never applied to graduate school. Dr. Harmon Maher Jr. and Dr. George Engelmann also played an enormous role in my geology foundation. I thank all three of them for taking the time on a semi-non-traditional student in a small geology department who had no idea what she wanted to do with her life. You completely led me in the right direction and I will be forever grateful for that.

My family has stood by my side no matter what decision I made. I love them more deeply than words can express and would not be here if it wasn't for them. Thank you Mom and Dad for all the sacrifices you made along the way, thank you for instilling all your values and ethics into me, and shaping me into this wonderful human being. You are the greatest fans a kid could ask for. To my two beautiful sisters Audrey and Jill, you are both so inspiring and motivating, and I don't know how I got so lucky to have you both in my life. I can't imagine growing up without you girls (maybe fewer bruises). Andy is the greatest brother I could ask for, he is so kind and loving, and just out right hilarious; I look forward to his dinner table stories every time. Gracie is the most precious gift our family has received and I look forward to teaching her all about earth sciences when she gets a little bit older. Also, special thank you to Grandma Murcek, Grandma Young, Uncle Ted and Aunt Sharon, Uncle Bill, and Uncle Dan for your support system and positive motivation. Let's not forget Scooby (RIP), Jersey, Dewey, Sienna, and Winston for all the kisses and smiles along the way.

No graduate degree is complete without an extended support system of friends. These people have listened to all the gripes and groans along the way and provided endless hours of support and guidance; Sarah Trout, Jackie and Jacob Belt, Mackenzie Parker, Annie Hoover, Leah Thrasher, Karla Leslie, Erin Dempsey, Celina and Marina Suarez, Steve and Becky Sloan, Natalie Ciaccio, Sarah Evans, Arne Sturm, Daniel Doolittle, Justin Fairchild, Jesse Thompson,

Joe Miller, Ben Rickards, Breanna Huff, Jessica Clatterbuck, C.J. Lipinski, Eugene Szymanski, Mallory and Ian Bowen, Markella Hoffman, Kayla Manzel, Anya Hess, Kathryn Hoffmiester, Juli Emry, Jeff Schroeder, and Paul Kenward.

Most of all, I would like to thank my best friend and love of my life Benjamin Ramaker. Your constant motivation and inspiration have fueled me through these last few months. Thank you for sticking by my side and helping me through the difficult phases of this milestone. I love you with all my heart and I cannot wait to spend the rest of my life with you.

INTRODUCTION

Porous chert reservoir facies are documented throughout North America in the Permian basin, Appalachian basin, and the southern midcontinent (Thomas, 1982; Rogers et al., 1995; Colleary et al., 1997; Montgomery et al., 1998; Luebking et al., 2001; Packard et al., 2001; Rogers, 2001; Rogers and Longman, 2001; Ruppel and Barnaby, 2001; Watney et al., 2001; Franseen, 2006; Watney et al., 2008; Mazzullo et al., 2009). Understanding porous chert formation and production from chert reservoirs is important because trillions of cubic feet of natural gas and hundreds of millions of barrels of oil have been, and will continue to be, produced from chert reservoirs (Rogers and Longman, 2001). Several authors have documented porosity development and retention in Mississippian, Pennsylvanian, and Devonian chert reservoirs. The Lower Devonian Thirtyone Formation of west Texas and New Mexico is one of the largest chert reservoir successions in the world, with chert porosity formed by molds, intercrystalline pores within chert matrix, and fractures (Ruppel and Barnaby, 2001). The best reservoir facies of the Pennsylvanian Amsden Formation of central Montana is solution-collapse chert breccia that formed after dissolution of evaporites, with later diagenetic alteration changing reservoir quality (Luebking et al., 2001). The hydrothermal chert reservoir of the Upper Devonian Wabamun Formation of British Columbia, Canada retains most of the reservoir pore volume by microintercrystalline porosity within replacement chert (Packard et al., 2001).

Mississippian reservoirs of Kansas, including porous chert facies, represent over 40% of the 35 million barrels of annual oil production (<<http://www.kgs.ku.edu>>). Middle Mississippian (Osagean-Meramecian) carbonate and chert strata that form these important reservoirs were deposited in ramp-margin settings bordering the northern Anadarko and Arkoma

basins. These reservoirs are informally termed “chat”, which describes the characteristic chattering sound made by the bit as it cuts through hard chert (Colleary et al., 1997). The largest Mississippian chat oil and gas fields are Glick and Spivey-Grabs-Basil in south-central Kansas (Watney et al., 2001). The most productive and economic chat reservoir is a high-porosity, low-resistivity tripolitic chert facies, exhibiting variable amounts of sponge-spicule molds, chert microporosity, vuggy porosity, and autoclastic breccia (Rogers et al., 1995; Montgomery et al., 1998). Tripolitic chert is a light colored, porous siliceous rock that has been interpreted to result from the weathering of chert or siliceous limestone in a subaerial environment (Tarr, 1938; Pettijohn, 1975).

Understanding historical production and future potential of chat reservoirs requires an understanding of depositional environment, diagenesis, structure, and lithofacies controls. Many contributors have addressed some of these issues, yet several questions remain (Lane and De Keyser, 1980; Thomas, 1982; Peeler, 1985; Choquette et al., 1992; Rogers et al., 1995; Colleary et al., 1997; Montgomery et al., 1998; Franseen, 1999, 2006; Rogers, 2001; Watney et al., 2001; Watney et al., 2008; Mazzullo et al., 2009; Boardman et al., 2010).

This study focuses on cores in a Mississippian ramp margin location with the purpose of examining: (1) the structural, relative sea level, and depositional controls on stratigraphy and lithofacies distribution; and (2) the diagenetic controls on reservoir character. Determining the paragenesis can provide a better understanding of porosity development in these reservoirs. The diagenetic, structural, and stratigraphic controls evaluated in this study can aid in delineating additional conventional and unconventional gas reservoirs as well as increasing our ability to predict areas of enhanced reservoir porosity.

Methodology

This study focused on four cores from northwest Cherokee County, Kansas (Fig. 1). Core descriptions identified lithology, sedimentary structures, grain types, and grain size, which provided the basis for the interpretations of depositional environment. Core lithologies were described using the Dunham (1962) classification (Appendix 1). Core descriptions were used to construct a ten-mile long southwest-northeast trending cross section. Cross section correlations were used for stratigraphic interpretation and facies geometries. Previous structural interpretations, including fault locations and subsurface structure maps, were utilized to investigate the structural setting and its control on facies geometry, facies distribution, and porosity development (Blair et al., 1992).

One hundred and twenty-five thin sections were prepared for transmitted light and cathodoluminescence petrography (Appendix 2). Thin sections, prepared by Petrographic Services in Montrose, CO, were impregnated with blue epoxy and doubly polished to 30 microns. Combined alizarin red S and potassium ferricyanide stain was used to distinguish between calcite, ferroan calcite, dolomite, and ferroan dolomite (Dickson, 1966). Only a portion of each thin section was stained in order to preserve unstained material for cathodoluminescence microscopy. Thin section analysis was completed using a binocular petrographic microscope, Olympus BX60. Thin sections were used for characterization of lithofacies, interpretation of depositional environment, and paragenetic sequence.

Cathodoluminescence petrography (e.g. Meyers, 1974) was performed using a Cambridge Image Technology LTD Clmk4 stage mounted on a Leitz SM-LUX-POL

microscope. Operating conditions for luminescence were 14kV acceleration potential and ~0.5mA gun current.

Thick section sample preparation and fluid inclusion petrography was conducted using low-temperature techniques outlined by Goldstein and Reynolds (1994). Five thick sections of megaquartz and five of baroque dolomite were prepared; the samples were chosen based on position in the paragenesis. Primary fluid inclusion assemblages were chosen for microthermometry to determine minimum entrapment temperature during crystal growth, and chemistry and concentration of salts of inclusion fluids. Microthermometric analyses were performed using a Linkam THMSG 600 stage (Appendix 3).

GEOLOGIC SETTING

The study area is located in Cherokee County of southeast Kansas (Fig. 1). Cherokee County is situated within the Cherokee basin which is an extension of the Arkoma basin; it is bounded to the north by the Bourbon Arch and to the west by the Nemaha Anticline (Fig. 1). The Cherokee basin developed in pre-Desmoinesian-post-Mississippian time in the area of the older Chautauqua arch. The Chautauqua arch was an anticlinal-broad feature in pre-Mississippian time but consequent subsidence, deposition, deformation, and erosion occurred before deposition of Mississippian strata, forming the post-Mississippian Cherokee basin (Merriam, 1963).

From Cambrian through middle Mississippian time, the area of the Arkoma basin and Ouachita foldbelt were part of a stable shelf and passive continental margin of southern North America (Byrnes and Lawson, 1999). By the late Paleozoic the proto-Atlantic Ocean was

closing due to subduction beneath Gondwana, which resulted in the Marathon-Ouachita orogenic event (Ziegler, 1989). During the middle Mississippian, the stable Arkoma shelf began subsiding under the load of Ouachita thrust sheets advancing from the south. In Kansas, Late Mississippian-Early Pennsylvanian structural uplift of the Central Kansas uplift (CKU) is related to the Ouachita orogenic event, which, together with eustatic fall, resulted in an extensive period of subaerial exposure in the Midcontinent, that lasted for approximately 10 million years and caused erosion of Mississippian strata (Merriam, 1963; Ross and Ross, 1988; Montgomery et al, 1998; Watney et al., 2001; Franseen, 2006).

Osagean-Meramecian strata in Kansas consist of cherty, partially dolomitized skeletal (especially crinoidal) packstones and grainstones and cherty, partially dolomitized and argillaceous wackestones and mudstones (Fig. 2; Watney et al., 2001; Franseen, 2006). In particular, Osagean-Meramecian strata contain siliceous sponge-dominated and heterozoan carbonate facies that developed in inner ramp, ramp margin, and basinal settings under subtropical/tropical conditions (Fig. 3; Lane and De Keyser, 1980). Although previous literature refers to this area of the mid-continent during the Osagean-Meramecian as a shelf (Lane and De Keyser, 1980), ramp terminology has been adopted for this study. This is because shallow water deposits make up the inner “shelf” and pass downslope to the slope break around the mid- to outer “shelf” in relatively deep water, defining a distally steepened ramp morphology. During the Mississippian an extensive carbonate ramp covered much of the central United States, and during the Osagean-Meramecian, the outer ramp and ramp margin extended through southern Kansas (Lane and De Keyser, 1980). A deep seaway lay south of the carbonate ramp edge along

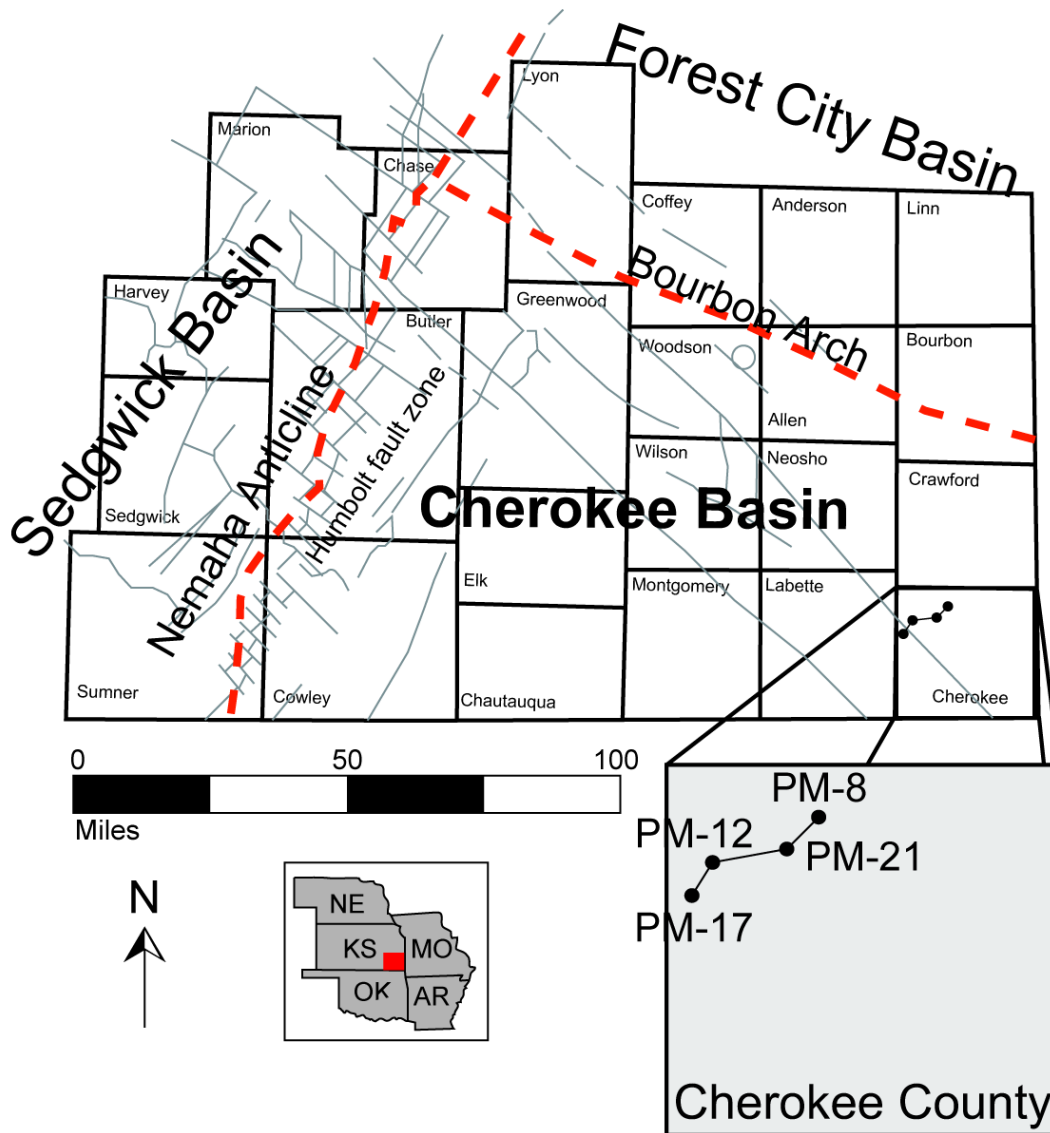


Figure 1. Location of study area in northwest Cherokee County (gray box), Kansas within the Cherokee basin. The Cherokee basin is bounded to the north by the Bourbon arch and to the west by the Nemaha anticline. Core locations marked by black circles. Line of cross section (Figures 8-11) marked with black line. Gray lines are inferred structures affecting the Precambrian basement. Northwest-southeast faults are along the Bourbon arch fault complex. The north-northeast-south-southwest faults are along the Humboldt fault zone. These fault systems have characteristics of intersecting conjugate wrench-fault zones of late Precambrian age (modified from Baars and Watney, 1991).

System	Stage	Formations/Members Goebel, 1968	Formations/Members Maples, 1994		Stage	System	
MISSISSIPPIAN	Meramecian	Ste. Genevieve Limestone	Ste. Genevieve Limestone		Meramecian	MISSISSIPPIAN	
		St. Louis Limestone	St. Louis Limestone	Stevens Mb. Hugoton Mb.			Cowley Formation
		Salem Limestone	Salem Limestone				
		Warsaw Limestone	Warsaw Limestone				
	Osagean	Keokuk Limestone	Burlington-Keokuk Limestone	Short Creek Oolite Mb.		Osagean	
				Keokuk Limestone	Burlington-Keokuk Limestone		
		Burlington Limestone	Burlington Limestone	Elsley Fm.			
		Fern Glen Limestone	Reeds Spring Ls. Mbr.		Reeds Spring Ls. Mbr.		
		St. Joe Ls. Mbr.	Pierson Limestone				

Figure 2. Mississippian stratigraphic nomenclature used in Kansas focused on Osagean and Meramecian stratigraphy (modified from Maples, 1994).

a converging plate boundary between Gondwana and North America, (Scotese, 1999). During the Osagean-Meramecian, Kansas was located at approximately 20° south latitude (Witzke, 1990), and the warm climate associated with lower latitudes allowed widespread carbonate accumulation (Fig. 3).

Vail et al., (1977) proposed global cycles of relative sea-level change for the Mississippian system to consist of two 3rd-order cycles ranging from ~1-10 m.y., with each cycle punctuated by major unconformities. Two 3rd order cycles are also recognized in northern Arkansas and southwestern Missouri by biostratigraphers, (Gordon, 1964; Thompson and Fellows, 1970; Thompson, 1972; Saunders et al., 1977). Ross and Ross (1987) proposed that the Mississippian system in the Mississippi Valley region was deposited during 14-15 3rd-order cycles of sea-level change ranging from ~1-3 m.y. Rygel et al. (2008) proposed that the Mississippian system consists of at least 4 distinct phases of glacioeustatic fluctuations lasting 5-15 m.y. All recognize a worldwide sea-level fall near the end of the Mississippian and continuing through the Early Pennsylvanian resulting in subaerial exposure of Mississippian strata.

Extensive evidence for the migration of hydrothermal fluid has been documented near the study area (Brannon et al., 1996; Banner et al., 1998a; Banner et al., 1998b; Coveney, 1992, Coveney, 1999). These hydrothermal fluids are responsible for the occurrence of the Mississippi Valley Type (MVT) Pb-Zn deposits in Missouri, Kansas, and Oklahoma, commonly referred to as the Tri-State district. Successful radiometric dating, paleomagnetic age dating, and fluid inclusion studies indicate the formation of MVT ores during and soon after the late Paleozoic

Alleghenian-Ouachita orogeny (Gregg, 1985; Leach & Rowan, 1986; Shelton et al., 1986; Brannon et al., 1996). Hydrothermal fluid migration continued later, giving rise to radiometric dates of mineralizing fluids of 251 Ma, 165 Ma, 137 Ma, 67 Ma, 65 Ma, and 39 Ma (Brannon et al., 1996; Coveney et al., 2000; Blackburn et al., 2008). The presence of MVT mineralization, coarse baroque dolomite, hydrothermal geochemical signatures, and elevated thermal maturity of organic matter in the Osagean-Meramecian chert indicate hydrothermal fluids may have preferentially migrated through the top of the Mississippian section (Wojcik et al., 1992; Wojcik et al., 1994; Wojcik et al., 1997; Watney et al., 2008).

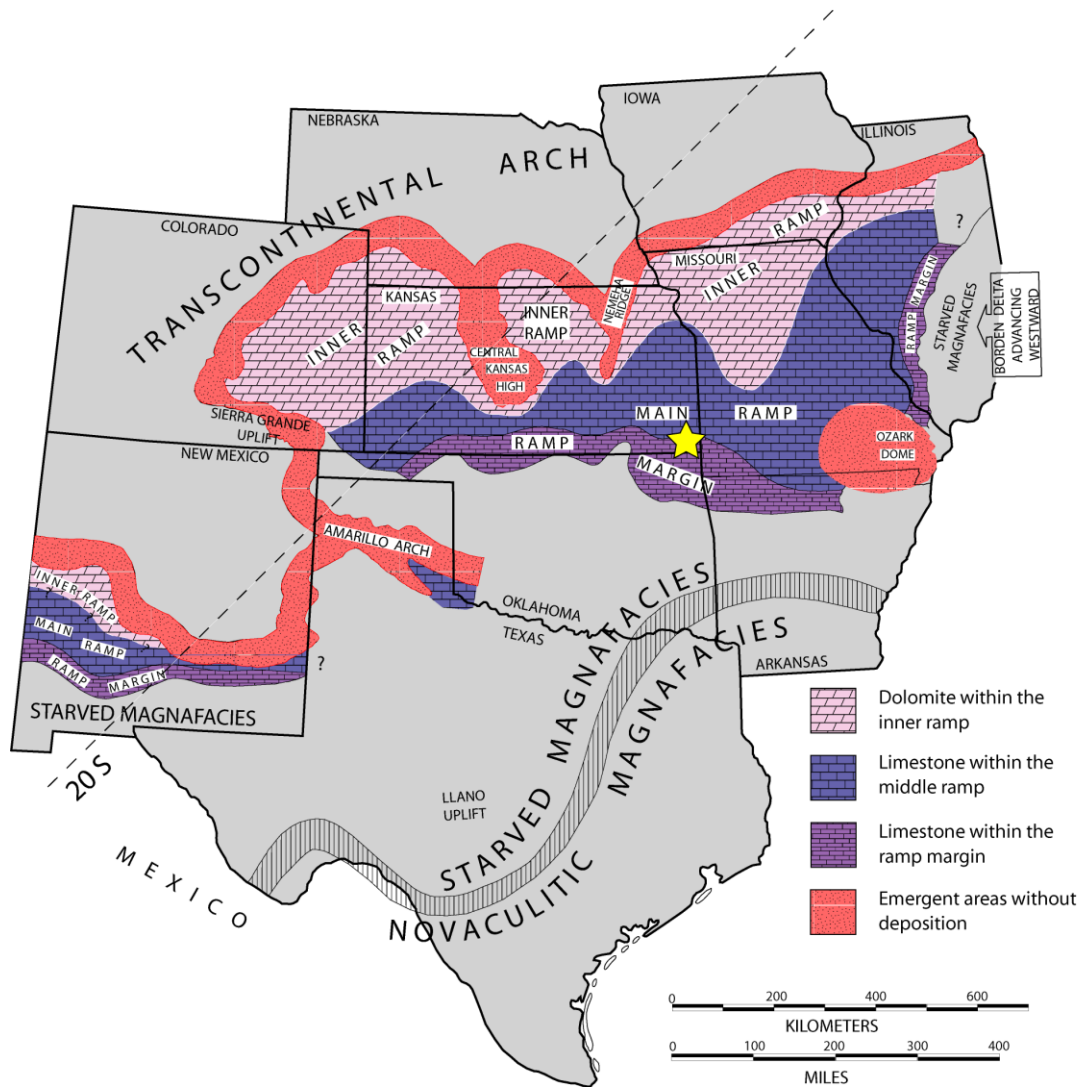


Figure 3. Paleogeographic map during the Osagean-Meramecian for parts of the Kansas ramp. Map depicts inner or upper ramp, main or lower ramp, ramp margin, and starved basin to the south (modified from Lane and De Keyser, 1980; Watney et al., 2001). Yellow star indicates study area.

LITHOFACIES AND DEPOSITIONAL ENVIRONMENT

Osagean-Meramecian strata in the study area are subdivided into eight lithofacies on the basis of core description and thin section analysis. Percentages of skeletal constituents are from visual estimates of thin sections. The term 'silica' is used loosely to refer to opal-A, opal-CT, cryptocrystalline quartz or chalcedony, and microcrystalline quartz. Lithofacies characteristics are summarized in Table 1, core photographs and thin section photomicrographs are shown in Figure 4, 5, and 6, and interpretation of depositional environment is presented below.

Echinoderm-Rich Bioclastic Wacke-Packstone

This facies is characterized by highly disarticulated, unabraded, and diverse skeletal fragments with an abundance of echinoderms. There is an overall lack of primary sedimentary structures except for alternating stratification of coarse-grained bioclastic wackestone and fine-grained bioclastic packstone. Fossil content is consistent with normal marine subtidal conditions. Muddy fabrics alternating with grainy and sorted interbeds are consistent with an environment below fair weather wave base that was subjected to times of higher energy. The higher energy is likely related to storms or prevalent currents, which others (e.g. Heckel, 1972) have shown to create fabrics similar to those found in this facies.

Johnson and Budd (1994) describe similar grainstone facies dominated by echinoderms and fenestrate bryozoans in Meramecian strata in Bindley field, Hodgman County, Kansas and interpreted those strata to represent deposition in a normal-marine, low-to-high energy ramp environment that was periodically winnowed by storms. Witzke (1990) described crinoid-bryozoan packstone intervals of Keokuk Limestone in Iowa and interpreted them to represent

episodic bottom agitation during storm events within middle-ramp environments. Franseen (2006) described echinoderm-dominated facies in Osagean strata of Schaben field, Ness County, Kansas and interpreted these strata to represent deposition on an inner ramp environment in relatively shallow subtidal, normal-marine conditions with fluctuating energy.

Interpreted depositional water-depth of echinoderm-rich bioclastic wacke-packstone is based off of stratigraphic relationships with adjacent facies of sponge-spicule-rich packstone and dolomitic bioclastic wackestone and previous studies. Elrick and Read (1991) investigated Lower Mississippian-ramp deposits in Wyoming, western Montana, and eastern Idaho and described similar crinoidal-skeletal packstone/grainstone facies and interpreted them to represent deposition in 49-82 feet (15-25 m) water depth (assuming a 131 ft (40 m) storm-wave base). Their interpretations were based off of stratigraphic relationships with adjacent facies and modern analogs in the Persian Gulf (e.g. Wagner and van der Togt, 1973). Elrick and Read (1991) thought the Persian Gulf was the most appropriate modern analog for the Mississippian-ramp system in their study. However, the Mississippian ramp system in my study area likely had a more gentle slope resulting in wider facies belts and was probably less restricted than the Persian Gulf. Despite these differences, the water depths for facies and storm-wave base from the Persian Gulf still seem to be the most appropriate for comparison, and therefore are used in my study for interpretations.

Sponge-Spicule-Rich Packstone

This facies is characterized by disarticulated, unabraded, and diverse skeletal fragments with an abundance of siliceous sponge spicules. It is mostly found massively bedded, commonly

with a mottled texture, and scarce wispy laminations. Diverse fossil content, bioturbation, and fine grain size are consistent with a normal marine, subtidal environment below fair weather wave base. Mazzullo et al. (2009) interpreted bedded spiculitic facies in upper Osagean deposits of south-central Kansas to be deposited in shallow-water, inner-ramp, nearshore to somewhat offshore settings under moderate-energy conditions. They did not identify in-situ sponge colonies or bioherms in the cores they examined, but inferred spicules were derived from demosponges.

The regional setting for these deposits in southeastern Kansas is that of a distal portion of a ramp (Fig. 3). Modern siliceous-sponge spicules, however, do not dominate in middle to outer portions of ramps in low-nutrient, subtropical and tropical environments, most likely due to lack of elevated nutrient and silica levels along with competition from warm-water photozoans (Gammon et al., 2000). To accumulate sponges and other heterozoan carbonates in a tropical/subtropical location, elevated nutrient and dissolved silica supplies are required to prevent the development of photozoans (James, 1997). Elevated nutrient and dissolved silica influx required for the accumulation of sponges can occur from terrestrial or oceanic sources. Gammon et al. (2000) attributed sponge accumulations in mid-latitude, shallow-water environments to nutrient-rich and silica-rich runoff from rivers entering protected waters. As the Osagean-Meramecian setting in southeast Kansas was near a ramp margin lacking a source of siliciclastics (Fig. 3), this is an unlikely explanation for the sponge-spicule-rich facies.

An alternative explanation is that sponges accumulated in deeper open marine settings in association with upwelling. Oceanic upwelling delivers cool nutrient-rich and silica-rich waters

to ramp-margin locations and has been documented as an active process during the Osagean-Meramecian (Lane and DeKeyser, 1980; Gutschick and Sandberg, 1983; Lumsden, 1988; Wright, 1991; Lasemi et al., 1998, 2003; Franseen, 2006; Mazzullo et al., 2009).

Bioherms or mounds have been described in other spiculitic units throughout Kansas and were interpreted to represent deposition near ramp margin locations, below storm-wave base (Rogers et al., 1995; Montgomery et al., 1998). The regional distribution of cherty lithofacies similar to those in southeastern Kansas (Rogers et al., 1995; Montgomery et al., 1998; Watney et al., 2001) indicate concentration near a ramp margin. Because of this relationship it seems most reasonable to interpret oceanic upwelling in relatively seaward of, or at, a deep break in slope as the dominant source for nutrients and silica. In the cores described for this study there was no evidence of constructional mound growth or whole sponges.

Dolomitic Bioclastic Wackestone

This facies is characterized by slightly disarticulated, unabraded, diverse, and unsorted skeletal fragments in mud support. The original lime-mud matrix has been replaced by crystalline-subhedral dolomite. Burrow structures are common, but there are also undulose to wispy laminations present. The dolomitic bioclastic wackestone facies is differentiated from the echinoderm-rich bioclastic wacke-packstone facies by lack of coarse-grained beds, lower percentage of bioclasts, and presence of dolomite. Dolomitization may preferentially replace mud-rich fabrics as opposed to grain-supported fabrics based on reactive surface area (e.g. Katz and Matthews, 1977; Sibley and Bartlett, 1987; Sibley et al., 1987). Through comparison to echinoderm-rich bioclastic wacke-packstone, characteristics are consistent with a normal marine,

quiet-water subtidal environment, below fair-weather wave base, downslope of the environment for echinoderm-rich bioclastic wacke-packstone.

Johnson and Budd (1994) described similar facies in Meramecian rocks in Bindley field, western Kansas. They interpreted echinoderm-bryozoan dolomud-wackestone with common bioturbation to be deposited in a subtidal, normal marine, low-energy environment. Interpreted depositional water-depth of dolomitic bioclastic wackestone is based off of stratigraphic relationships with adjacent facies of echinoderm-rich bioclastic wacke-packstone and argillaceous wackestone and previous studies. Elrick and Read (1991) described similar skeletal wackestone/packstone facies and interpreted them to represent deposition in 65-114 feet (25-40 m) water depth (assuming a 131 ft (40 m) storm-wave base). Previous studies and argument of comparison is discussed in the echinoderm-rich bioclastic wacke-packstone facies above.

Argillaceous Wackestone

This facies is characterized by a low percentage of identifiable skeletal fragments in mud support. The original lime-mud matrix has been replaced by crystalline-subhedral dolomite encapsulated in argillaceous material. There is an abundance of centimeter-scale, dark-colored, sub-circular burrows with traceable anastomosing burrow traces. There are also rare wispy laminations where burrowing is not abundant. There is abundant silicification in the form of rounded and small lenticular-shaped chert nodules, which may suggest selective silicification of burrows (Watney et al., 2001). Low percentage of bioclasts, argillaceous material, burrows, and wispy laminations provide evidence for a subtidal, quiet, open-marine, deep-water environment below storm-wave base.

Johnson and Budd (1994) described argillaceous dolomudstone in Meramecian rocks in Bindley field, of western Kansas to be deposited in a subtidal, restricted environment. Watney et al. (2001) described argillaceous cherty dolomite mudstone in Osagean-Meramecian rocks of south-central Kansas and they interpreted this facies as their deepest water facies in shallowing-upward, transgressive-regressive cycles. The regional setting of the Osagean-Meramecian of southeast Kansas favors the deepwater interpretation of Watney et al. (2001) in this case. Interpreted depositional water-depth of argillaceous wackestone is based off of stratigraphic relationships with adjacent facies of dolomitic bioclastic wackestone and dark shale and previous studies. Elrick and Read (1991) described similar argillite facies and interpreted them to represent deposition in no more than 213 feet (65 m) water depth but at least 131 feet (40 m), the assumed depth to storm-wave base. Previous studies and argument of comparison is discussed in the echinoderm-rich bioclastic wacke-packstone facies above.

Tripolitic Chert

This facies is characterized by highly disarticulated, unabraded, and diverse skeletal fragments with an abundance of siliceous-sponge-spicules. It is mostly massively bedded, commonly with a mottled texture, with subround elongate burrows, and scarce wispy laminations. This facies is commonly autoclastically brecciated consisting of angular to subangular clasts, highly siliceous, and microporous. Tripolitic chert is the most porous chert facies described in this study. The tripolitic chert facies is differentiated from the sponge-spicule-rich packstone facies by the autoclastic fabric, more silicification, and more microporosity. As the facies is similar to sponge-spicule packstone, the depositional environment is likewise interpreted as forming distally on ramp, in a normal marine, subtidal

environment, below fair-weather wave base and associated with upwelling. Autoclastic brecciation is attributed to burial compaction as opposed to solution collapse breccia, because breccia matrix lithology is similar to clast lithology. Mechanisms of silicification and creation of microporosity will be discussed in further detail in the Diagenesis section.

Watney et al. (2001) described similar facies in Osagean-Meramecian rocks of south-central Kansas that had undergone significant diagenetic alteration, including silicification, dissolution, fracturing, and autobrecciation. They recognized that dissolution of chert formed microporous or tripolitic chert and described the original fabric to contain various amounts of sponge spicules deposited along ramp margins. Although Mazzullo et al. (2009) did not refer to their porous bedded spiculite facies as tripolitic chert, they did interpret significant diagenetic alteration including silicification and dissolution, with the majority of porosity formation resulting from meteoric dissolution.

Variable Chert Breccia

The variable chert breccia has two textures, which are based on matrix and clast types. The first texture (texture 1) is characterized by angular to round clasts of tripolitic chert, sponge-spicule-rich packstone, echinoderm-rich bioclastic wacke-packstone, and dolomitic wackestone; all are silicified in this facies. Clasts are mostly in grain support with dark shale matrix (Fig. 6). This texture is found below but stratigraphically close to (no more than 35 feet (11 m) below) the Mississippian-Pennsylvanian boundary and is also found below subaerial exposure surfaces in genetic unit 2. Proximal to the Mississippian-Pennsylvanian boundary the breccia is monomictic with a fitted fabric, vugs, and dissolutional truncation along some clast margins. Dark clay

matrix has an infill fabric and appears similar to Pennsylvanian shale when found proximal to the Mississippian-Pennsylvanian boundary.

Dissolution from meteoric water is a well-known process that can form solution-collapse breccias (Kerans, 1989; 1990). Although other authors (Abegg, 1992; Bartberger, et al., 2001) have documented solution-collapse breccias in the Mississippian of Kansas resulting from dissolution of evaporites, I found no evidence of evaporites in the study (including any relict textures in preserved chert such as chicken-wire texture, relict laths, or length-slow chalcedony). Therefore, I favor formation of texture 1 breccia from influx of meteoric water associated with the subaerial unconformities, followed by collapse of cavities. Also, some of the breccias show closely spaced, compacted clasts, which may indicate compaction and rebrecciation during burial (Fig. 6C&D; Loucks and Handford, 1992).

The second texture (texture 2) is characterized by angular to subangular clasts of silicified argillaceous wackestone or brecciated chert nodules in clast support, with argillaceous soft-sediment-deformed wackestone matrix. Fractures in chert nodules are filled with argillaceous wackestone, indicating that chert formation and compactional fracturing of chert occurred before lithification of argillaceous wackestone (Fig. 6B). This breccia texture is not observed proximal to subaerial unconformities. These characteristics are indications of early differential compaction; the timing of which will be discussed in the Diagenesis section. Franseen (2001) noted similar features in Mississippian strata and used this for evidence of early silicification.

Ooid Packstone

This facies occurs as a single, 1-2 foot thick interval in the study area. It is characterized by disarticulated and somewhat abraded skeletal fragments in addition to abundant ooids and carbonate mud. This facies generally lacks sedimentary structures but there are rare burrow mottles.

Modern ooids are generally deposited in high-energy environments in water depths less than 32 feet (10 m; Newell et al., 1960; Purdy, 1961; Ball, 1967; Harris, 1979). If there was a shallow water environment of deposition for oolitic facies in the southeast Kansas study area, the facies would be expected to have tabular or trough cross stratification, fenestral fabrics, hardgrounds, rhizoliths, or alternating coarse and less coarse laminations all of which indicate deposition in shallow-water, high-energy, or beach foreshore environments (Newell et al., 1960; Purdy, 1961; Ball, 1967; Harris, 1979). As such structures are absent, it is likely that grains were generated elsewhere and transported into deeper, lower energy waters.

As physical sedimentary structures are absent it is likely that they were destroyed by bioturbation after sediment was transported into lower energy deeper waters. The one oolite layer in the study area is envisioned to be the down-dip equivalent of the Short Creek Oolite Member of the Keokuk Limestone (Thompson, 1986). Some updip exposures of the Short Creek Oolite were interpreted as beach foreshore and shoreface deposits (Ritter 2004). Ritter (2004) interpreted that a bioturbate oolitic facies was deposited downdip of the shallow-water site of ooid generation.

Dark Shale

Dark shale facies is most prevalent in dissolution cavities, fractures, and breccia matrix directly above and up to 25 feet (8 m) below the Mississippian-Pennsylvanian boundary. It appears that dissolution and fracture features associated with subaerial exposure were infilled by Pennsylvanian shale during deposition of the Pennsylvanian Cherokee Group. Previous studies trace this shale up to the Riverton interval of the Krebs Formation (Pennsylvanian Desmoinesian Series, Cherokee Group), which immediately overlies the Mississippian-Pennsylvanian unconformity in this region (Saueracker, 1966; Lange, 2003). The Riverton interval consists of phosphatic black shale, pyritic black shale, and coal and has been described to represent deposition in a marsh, swamp, and brackish-marginal-marine environments (Saueracker, 1966; Lange, 2003). Below the Mississippian-Pennsylvanian unconformity, the shale equivalent observed here is deposited as a stratigraphic leak in caves.

Dark shale is also found with another occurrence, farther down from the Mississippian-Pennsylvanian unconformity, as layered intervals (1-5 mm thick) interstratified with Mississippian strata. The shale contains parallel laminations and lacks any evidence of burrowing. The dark grey to black coloration is probably the result of high organic content preserved by deposition in dysoxic to anoxic conditions (Heckel, 1977). The dark shale also contains minor amounts of pyrite and contains no macrofauna, which is consistent with an anoxic environment. All of the features are consistent with deposition by low-energy, off-shore, deep-water environment below storm-wave base (Hardie and Ginsburg, 1977; Heckel, 1977). A shallow-water lagoonal environment is ruled out based on lack of biota, lack of laterally

equivalent shallow water deposits, and lack of shallow water deposits stratigraphically above or below (Ramsbottom, 1978; Inden and Moore, 1983).

This facies is interpreted as the deepest marine facies described in the study area. Mazzullo et al. (2009) interpreted dark-gray shale with burrows and lenses of packstone to have been deposited in a low-energy suboxic to anoxic environment. Watney et al. (2001) recognized shale lithofacies as an end member of autoclastic chert with clay infill facies but did not consider it a bed in their chat cycles. They recognized the shale lithofacies as evidence of flooding events.

Lithofacies Name	Characteristic Skeletal Constituents	Sedimentary Structures	Key Features	Porosity Type	Depositional Environment
Echinoderm-rich bioclastic wacke-packstone (Fig. 4A, B)	Echinoderms (60%, 500 μm), bryozoans (commonly fenestrate bryozoans, 15%, 250 μm), gastropods (15%, 100 μm), foraminifera (5%, 400 μm), sponge-spicules (5%, 50 μm)	Mostly massively bedded and mottled with bioturbation, contains cm-scale skeletal-rich and skeletal-poor layering with grain sorting into fine-grained layers and coarse-grained layers; overly close packing in packstone fabrics	Grains are highly disarticulated but not abraded; cm-scale beds and nodules of silicified fossil grains and matrix when replaced by silica; grain textures may be preserved or are molds filled with silica	Inter- and intra-particle, moldic	Subtidal-normal-marine environment below fair-weather wave base that was subjected to times of higher energy likely related to storms or prevalent currents
Sponge-spicule-rich packstone (Fig. 4C, D)	Siliceous sponge spicules (dominantly monaxon, 60%, 20 μm) and their molds, echinoderms (15%, 300 μm), bryozoans (10%, 300 μm), gastropods (10%, 300 μm), foraminifera (5%, 100 μm)	Mostly massively bedded with common mottled texture from bioturbation; mm-scale wispy laminations	Bioclasts are highly disarticulated but not abraded; matrix contains dense chert, highly porous chert, and micrite	Moldic, fracture, intraparticle, intercrystalline	Subtidal-normal-marine environment below fair-weather wave base along breaks in slope to allow for elevated nutrients and silica sourced by oceanic upwelling

Dolomitic bioclastic wackestone (Fig. 5A, B)	Bioclasts in mud support; echinoderms (50% of total bioclasts, 500 μm), brachiopods (25%, 500 μm), bryozoans (25%, 500 μm)	Mm-scale undulose to wispy laminations imparted by clay and horsetail stylolites; grains are unsorted; burrows and bioturbation are present but not abundant	Crystalline (50-70 μm) subhedral dolomite; bioclasts are either preserved as molds or remain calcitic; generally disarticulated but not highly abraded	Intercrystalline, moldic	Quiet-water subtidal normal marine environment below fair weather wave base
Argillaceous wackestone (Fig. 5C, D)	Identifiable grains are rare constituting 10-20% of bulk volume; dolomitic matrix constitutes 80-90% of bulk volume; dolomite rhombohedra are commonly encapsulated in argillaceous material	Mottled texture from cm-scale dark colored sub-circular burrows; mm-scale wispy laminations	Mm-scale beds and cm-scale nodules of complexly silicified material; compaction results in local brittle brecciation of chert beds and soft sediment deformation and stylolitization of wackestone fabrics	Typically tight with low intercrystalline porosity, fracture	Quiet-water deep subtidal open-marine environment below storm wave base

Tripolitic chert (Fig. 5E, F)	Sponge spicules (dominantly monaxon, 60%, 20 μm), echinoderms (15%, 300 μm), bryozoans (10%, 300 μm), gastropods (10%, 300 μm), foraminifera (5%, 100 μm)	Mottled with cm-scale subround elongate burrows, mm-scale wispy laminations	Bioclasts are highly disarticulated but not abraded; most likely precursor was sponge-spicule-rich packstone that has undergone silicification, brecciation, and dissolution	Microporous, moldic	Subtidal-normal marine-environment below fair-weather wave base along slope to allow for elevated nutrients and silica sourced by oceanic upwelling; with diagenetic overprint of autoclastic fabric, silicification, and microporosity
Variable chert breccias (Fig. 6)	Clasts composition: tripolitic chert, sponge-spicule-rich packstone, echinoderm-rich bioclastic wacke-packstone, and dolomitic wackestone; all are silicified in this facies	Clasts of variable size, greatly variable shape, poorly sorted, in clast support, common fracturing	Infilling matrix is commonly dark brown-gray clay rich material when found proximal to the M-P boundary; other occurrences: infilling matrix composed of argillaceous wackestone	Fracture	Solution collapse and differential compaction
Ooid Packstone	Ooids (90%, 300 μm), echinoderms (5%, 500 μm), bryozoans (5%, 500 μm)	Rare mottled bioturbation	Bioclasts are disarticulated and slightly abraded	Tight	Transported downdip of shallow water ooid generation

Dark Shale	No grains identified	Fine mm-scale parallel laminations	Most prevalent in karst features; minor amounts of pyrite	Tight	Stratigraphic leak in caves and low-energy off-shore deep-water environment below storm wave base
------------	----------------------	------------------------------------	---	-------	---

Table 1. Characteristics of lithofacies described in Lower Mississippian Osagean-Meramecian strata. Millimeter (mm) scale and centimeter (cm) scale are abbreviated.

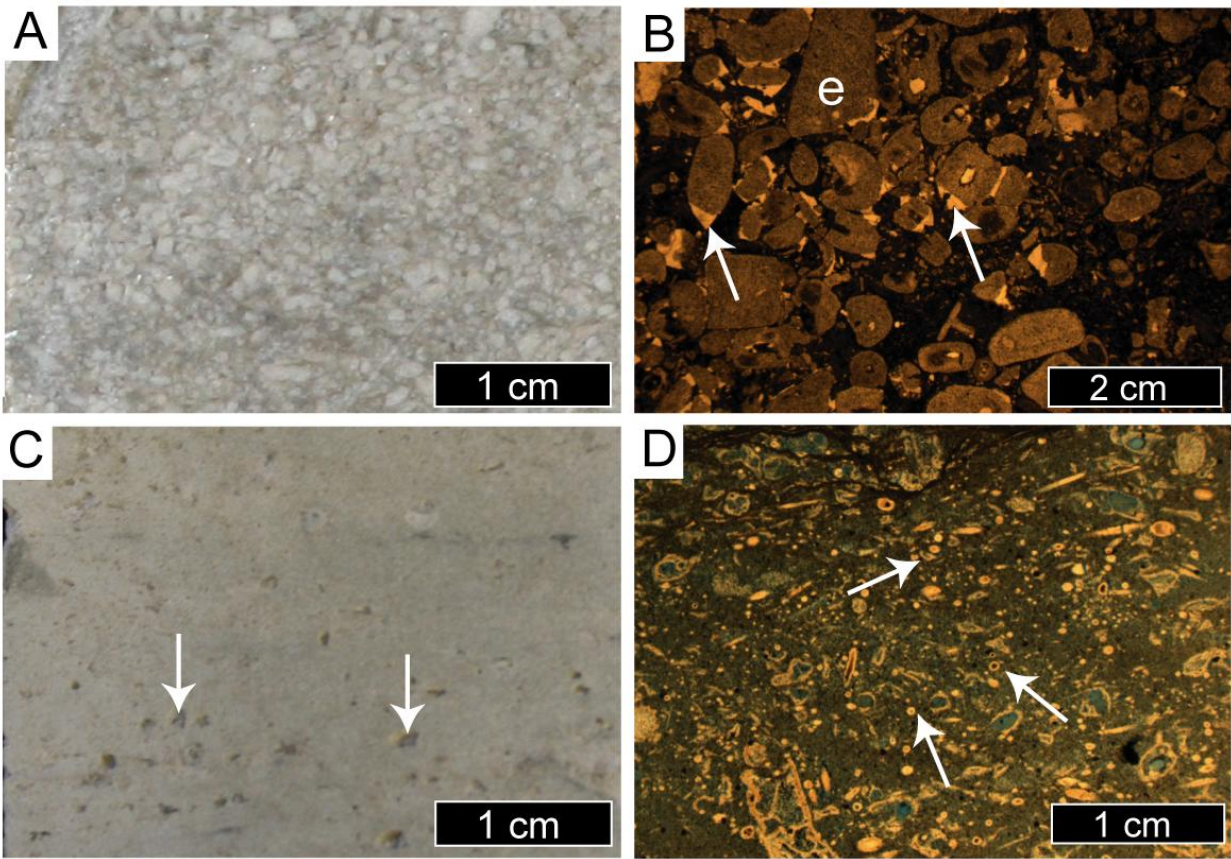


Figure 4. **A)** Core photograph of echinoderm-rich bioclastic wacke-packstone (PM-12; 533). Packstone texture mostly composed of echinoderm fragments. **B)** Photomicrograph of echinoderm-rich bioclastic wacke-packstone taken in plain polarized light (PM-12; 504). Echinoderms (e) are overgrown with calcite (arrow). **C)** Core photograph of sponge-spicule-rich packstone (PM-12; 625'). Arrows point to molds on core surface. **D)** Photomicrograph of sponge-spicule-rich packstone impregnated with blue epoxy and taken in plain polarized light (PM-12; 623'). Notice the abundance of sponge-spicules and their molds (arrows).

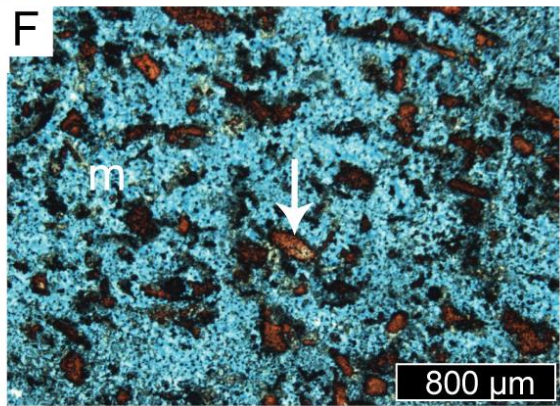
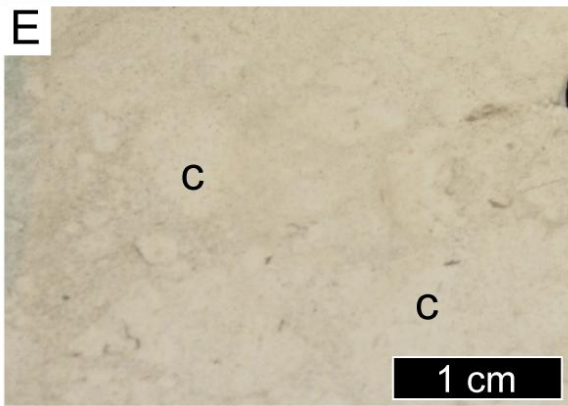
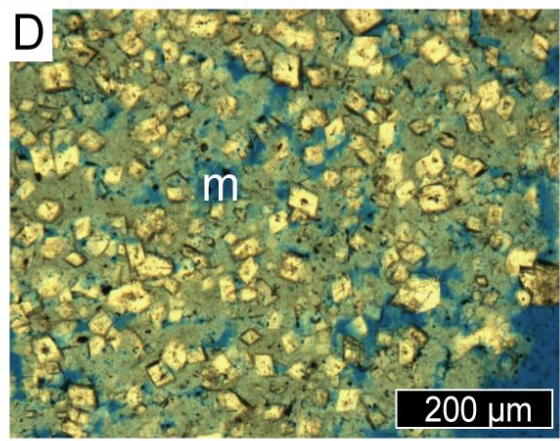
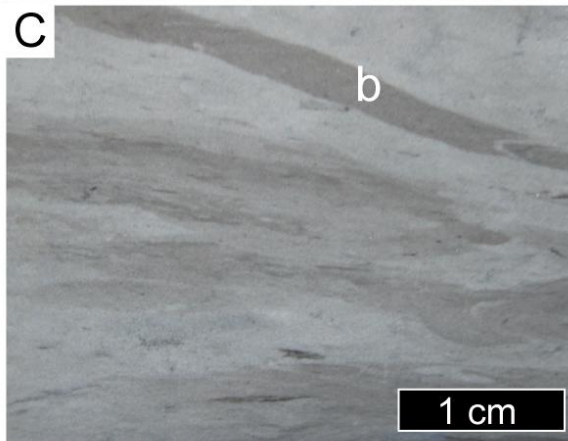
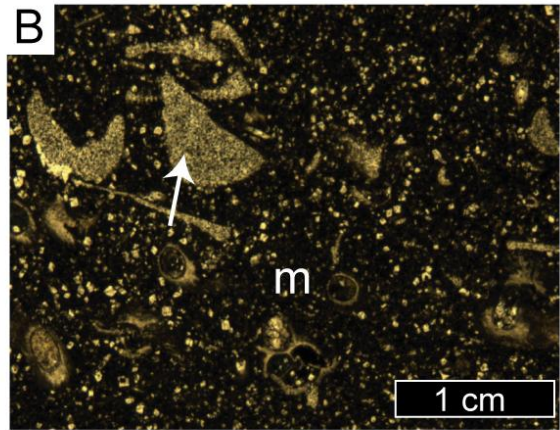
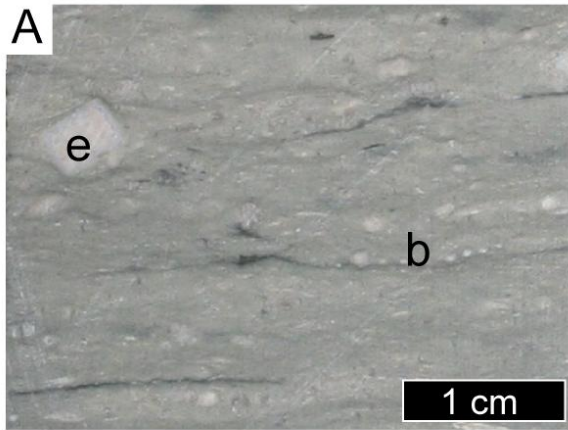


Figure 5. **A)** Core photograph of dolomitic bioclastic wackestone with bryozoans (b) and echinoderms (e; PM-12; 691'). **B)** Photomicrograph of dolomitic bioclastic wackestone taken in plain polarized light (PM-12; 705'). Fossil fragments (arrow) are surrounded by argillaceous dolomitic matrix (m). **C)** Core photograph of argillaceous wackestone facies with burrowed (b) texture (PM-12; 605'). **D)** Photomicrograph of argillaceous wackestone facies impregnated with blue epoxy and taken in plain polarized light (PM-12; 616'). Dolomite rhombohedra are surrounded by microporous matrix (m). **E)** Core photograph of tripolitic chert (PM-12; 513'). Notice clasts (c) and surrounding matrix are composed of nearly the same material. **F)** Photomicrograph of tripolitic chert impregnated with blue epoxy, stained with alizarin red S and potassium ferricyanide, and taken in plain polarized light (PM-12; 512'). Fossil fragments remain calcitic (arrow) surrounded by microporous chert matrix (m).

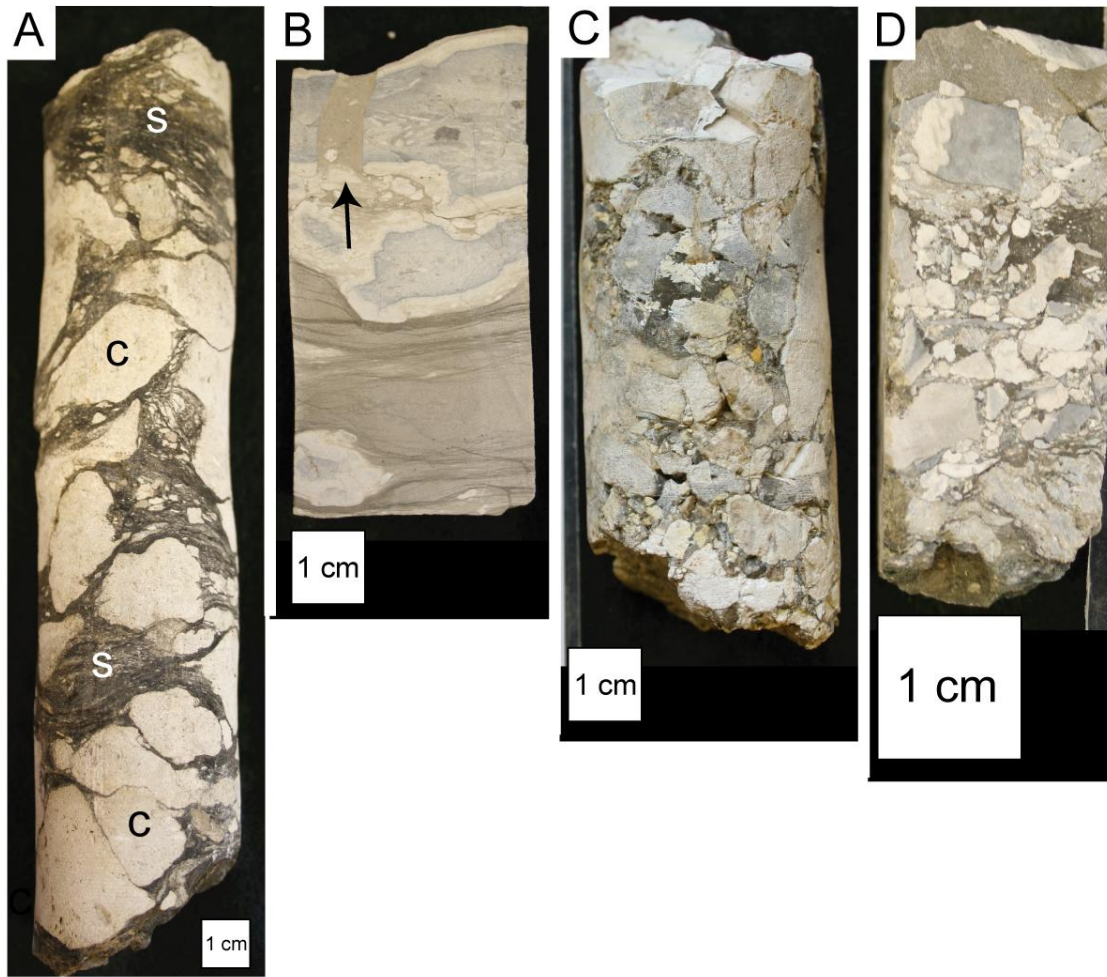


Figure 6. Core photographs of variable chert breccias, white boxes are 1x1 cm. **A)** Angular to round chert clasts (c) in dark shale matrix (s) proximal to the Mississippian-Pennsylvanian boundary. Breccia is the result of solution-collapse and weathering during subaerial exposure (PM-12; 439'). **B)** Argillaceous wackestone with nodular chert replacement. Breccia is the result of differential compaction during burial (PM-12; 472'). Note that fracture (arrow) cuts across white-colored microporous rim of chert nodule, indicating that the porous rim formed before burial compaction. The intrusion of argillaceous wackestone into the fracture indicates that chert formation, chert weathering to create the white-colored rim, and compactional fracture, all occurred early, before lithification of the argillaceous wackestone. **C)** Angular polymictic chert clasts. Breccia is the result of reworking of insoluble residue during subaerial exposure (PM-12; 552'). **D)** Angular polymictic chert clasts. Breccia is the result of reworking of insoluble residue during subaerial exposure (PM-12; 478').

GENETIC STRATIGRAPHY

Previous studies have described Osagean-Meramecian strata across much of the mid-continent. Handford and Manger (1993) conducted a regional sequence stratigraphic study on outcrops in northern Arkansas and southwestern Missouri. Their interpretations of systems tracts are labeled on the cross-section and include transitions from a transgressive systems tract to a highstand systems tract, followed by a lowstand systems tract (Fig. 8). In Osagean strata of Iowa, a high to mid-ramp position, Witzke and Bunker (1996) interpreted three high-frequency transgressive-regressive cycles. These cycles consisted of lithofacies interpreted as shallowing-upward successions with complex stratal architecture. Watney et al. (2001) interpreted subsurface strata in south-central Kansas to contain four stacked, shallowing-upward cycles, indicating regional transgressive-regressive cycles. Mazzullo et al. (2009) interpreted the subsurface Cowley depositional sequence in south-central Kansas to represent onlapping, upward deepening strata in basal beds, and shallowing-upward, progradational clinofolds in upper beds; representing a transgressive systems tract and offlapping highstand systems tract.

I identified three genetic units bounded by flooding surfaces or sequence boundaries in the study area. Sequence boundaries are identified on the basis of evidence for relative falls in sea level. Stratigraphic distribution of lithofacies is presented below and correlations are illustrated in the cross section (Fig. 8).

Unit 1

Unit 1 comprises four lithologies: argillaceous wackestone, dolomitic bioclastic wackestone, echinoderm-rich bioclastic wacke-packstone, and sponge-spicule-rich packstone.

The base of Unit 1 is composed of argillaceous wackestone that grades upward into dolomitic bioclastic wackestone. This transition is repeated above but is capped by echinoderm-rich bioclastic wacke-packstone. The transition upward from argillaceous wackestone to dolomitic bioclastic wackestone to echinoderm-rich bioclastic wacke-packstone is repeated eight times in Unit 1, representing shallowing followed by a deepening event, but is not always complete (Fig. 9). Vertical transitions within each of these eight shallowing to deepening units are gradational, with boundaries marked by sharp flooding surfaces; these are characteristic features of parasequences (e.g. Van Wagoner et al., 1990). However, as discussed in the Lithofacies section, I interpret the depths of deposition between the argillaceous wackestone and echinoderm-rich bioclastic wacke-packstone to be likely greater than 131 feet (40 m). When compared with thickness of each unit (average of approximately 15 feet (3 m), even if decompacted by 50%, the thickness does not account for interpreted variations in water depth between facies. Therefore, I believe there is a component of relative fall in sea level, and I interpret these eight units to represent sequences reflecting fluctuations (including falls) in relative sea level, rather than parasequences (Fig. 9; U1S1-8). Sequences 2, 4, and 7 are complete with all three facies whereas sequences 1, 3, 5, 6, and 8, are only partial successions containing two of the facies mentioned above (Fig. 9). On the basis of lithofacies, the sequences represent shallowing upward from quiet-water, low-energy, subtidal environment below fair-weather wavebase to shallow subtidal, fair-weather wave base with storm-influenced settings marked by intermittent high energy. These environments most likely represent a depositional range from an outer ramp environment shallowing upward to middle and marginal ramp

environments (Witzke, 1990; Johnson and Budd, 1994; Rogers et al., 1995; Montgomery et al., 1998; Watney et al., 2001; Franseen, 2006; Mazzullo et al., 2009).

At the base of U1S3 (Fig. 9) there is a noticeably thicker shale bed compared to other flooding surfaces in Unit 1. This is interpreted to represent a greater increase in relative sea level to allow accumulation of offshore deposits. Within U1S4-5 (Fig. 9) there are three sharp based beds of bioclastic grainstone that are normally graded with muddy-infiltration fabrics. These are interpreted to represent density flows transported downslope by storms or prevailing currents (Heckel, 1972).

Unit 1 is 140 feet (43 m) thick in the southwestern core (PM-17) and thins or is not sampled by core to the northeast (PM-12). Echinoderm-rich bioclastic wacke-packstone is only observed in the southwestern most core and is interpreted to be the shallowest water facies in Unit 1. Thus, the core immediately to the northeast of PM-17 (PM-12) represents deeper water conditions than PM-17 during Unit 1 deposition.

An accumulation of sponge-spicule-rich packstone is observed at the top of Unit 1 in the PM-12 Core (Fig. 9, location A). Watney et al. (2001) interpreted sponge-spicule accumulations to occur along ramp margin locations in proximity to upwelling currents. The sponge-spicule accumulations near the top of Unit 1 likely indicate the start of upwelling or development of a nearby slope.

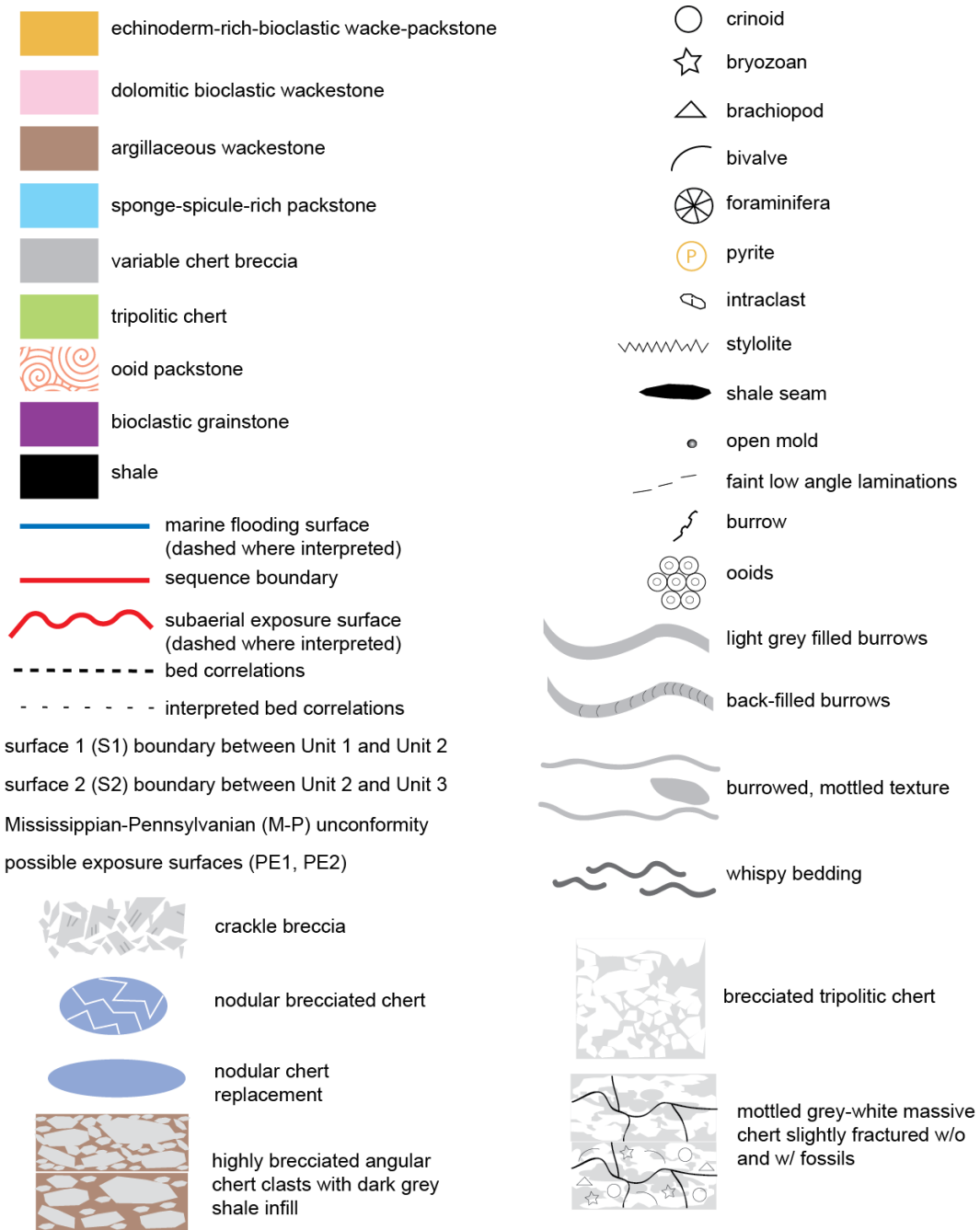


Figure 7. Legend for core description and cross section used for Figures 8, 9, 10, and 11.

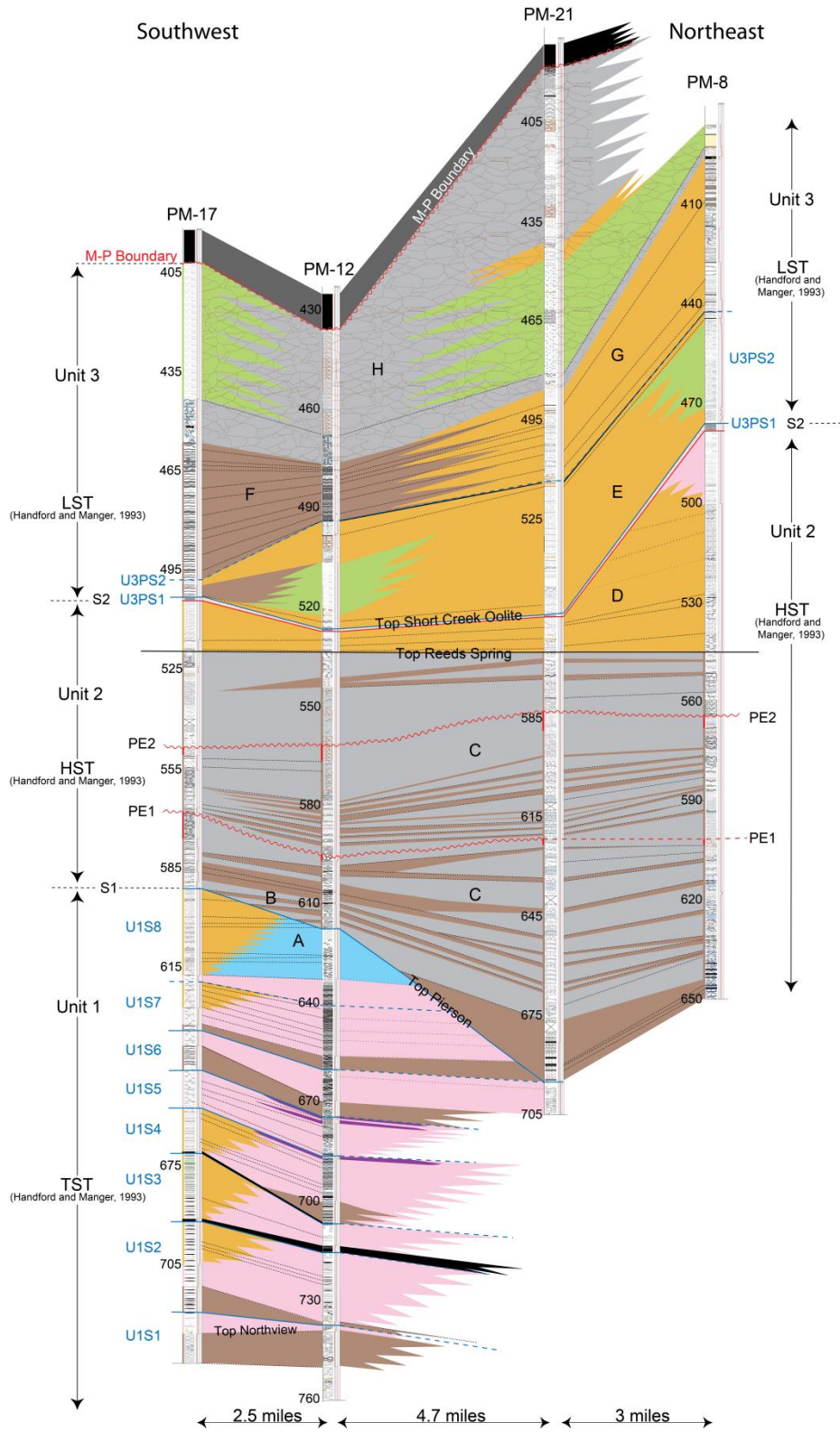


Figure 8. Core descriptions and southwest-northeast trending stratigraphic cross section for the four cores from northwest Cherokee County (see Fig. 1 for locations and line of cross section). Datum is the top of the Reeds Spring Limestone member equivalent. Detailed diagram of each genetic unit is shown in Figures 9, 10, and 11. Letters represent observation localities referred to in the text but are also explained on individual genetic unit diagrams. Horizontal scale is shown in miles along bottom of cross section. Vertical scale is in feet below the surface labeled along each individual core description. Figure 7 is the legend for this cross section.

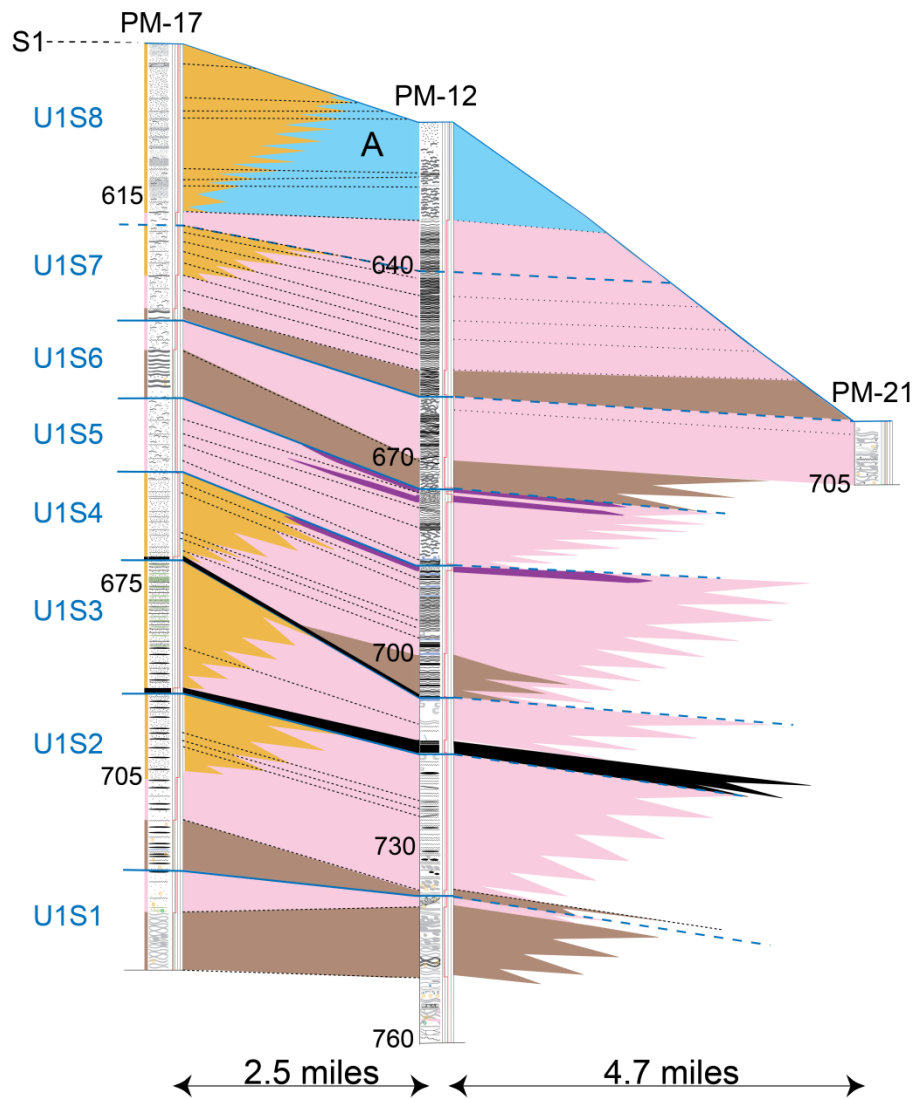


Figure 9. Genetic Unit 1 contains eight shallowing-upward high-frequency sequences (U1S1-8). Accumulations of sponge-spicule-rich packstone are at locality (A). Vertical numbers along margins of cores represent depth in feet below the surface. Horizontal scale is represented in miles. Figure 7 is the legend for this cross section.

The top of Unit 1 is marked by a significant surface (S1), with chert-free grain supported limestone and dolomite below, and argillaceous, micritic, cherty dolomites above (Fig. 8). On the basis of the deeper water environment interpreted for the argillaceous wackestone above the surface, the transition to Unit 2 may represent a flooding event. Interpreted geometries above the surface suggest toes of clinoforms that converge or downlap onto the surface (Fig. 8, location B), indicating that S1 may represent a maximum flooding surface. Facies distribution in Unit 1 indicates shallower water to the southwest and geometries in Unit 2 indicate shallower water to the northeast. Paleogeographic maps indicate the shallowest water toward the north and deeper water toward the south (Fig. 3). The change in slope from Unit 1 to 2 could be due to either Unit 1 being a localized build-up forming downslope of the main ramp, shallow water carbonate sourcing from both the northeast and the northwest, or tectonic deformation during deposition of Unit 1.

Internal correlations in Unit 1 suggest erosional truncation of units below S1 (Fig. 8). In the nearby outcrop belt to the east, erosional truncation and angular discordance is recognized at the top of the Pierson Formation (Missouri Highway 71, north of Jane, MO; Thompson, 1986), which likely correlates to this surface. Boardman et al. (2010) interpreted this as an angular unconformity. North-south compression in the Osagean was thought to generate east-west trending folds within the Pierson Formation. They observed no evidence of subaerial exposure along the unconformity, and proposed that erosion was submarine. The interpretation of submarine erosion and angular discordance is consistent with the observations in the cores in southeast Kansas.

The origin of Genetic Unit 1 is deposition during low relative sea level, punctuated by high-frequency relative sea-level changes. Unit 1 geometries indicate shallow water deposition to the southwest which is different than the overlying units. Unit 1 does not contain chert whereas units 2 and 3 have abundant chert and porous chert.

Unit 2

The basal succession of Unit 2 is the interval between S1 and the datum (top of the Reeds Spring Limestone; Fig. 8). The top of the Reeds Spring is used as the datum in this cross section and has been used as a datum in other studies (Watney et al., 2008). I believe it allows the closest possible reconstruction of actual depositional topography. Strata in the basal succession of Unit 2 consist of interbedded argillaceous wackestone and brecciated chert facies. Thickness is 80 feet (24 m) in the southwest and 120 feet (37 m) in the northeast. Beds of argillaceous wackestone and brecciated chert thin, pinch-out, and downlap to the southwest (Fig. 10, location B). In the northeast, there are more interbeds, thicker beds, and an overall higher percentage of argillaceous wackestone than in the southwest. On the basis of the argillaceous wackestone lithology, the basal succession of Unit 2 is interpreted as a subtidal, deep-water, outer ramp environment.

The basal succession contains two possible subaerial exposure surfaces characterized by dissolution features in core, possibly from meteoric water, which created microkarst with silty infill material, in-situ breccias, and partially dissolved and reworked clasts (Fig. 10, PE1&2). Subaerial exposure associated with these surfaces created some enhanced porosity in limestone facies, consisting of partially dissolved limestone clasts, microkarst, and minor collapse breccia

porosity. Limited duration of subaerial exposure is inferred from absence of larger paleokarst solution cavities (D'Argenio et al., 1997). Mazzullo et al. (2009) also recognized subaerial exposure surfaces in medial-ramp deposits and interpreted them to reflect periods of relative or eustatic sea-level fall during deposition.

This upper succession of Unit 2 is the interval between the datum and S2 (Fig. 8). It is 15 feet (5 m) thick in the southwest locations and thickens to 70 feet (21m) to the northeast. There is a gradational contact between argillaceous wackestone facies below the datum and echinoderm-rich bioclastic wacke-packstone facies above. Internally, units thicken to the northeast producing a wedge-like geometry on a southward facing ramp (Fig. 10, location D). The wedge-shaped geometry is most likely caused by the erosive nature of the upper surface (Fig. 10, S2) and depositional thinning to the southwest. The general vertical transition from wackestone and cherty-dolomites into grainy packstone is interpreted to represent an overall shoaling in association with a relative sea-level fall or depositional shallowing.

In the northeastern most core (PM-8), the echinoderm-rich-bioclastic wacke-packstone (Fig. 10, location D) is overlain by a bed of dolomitic bioclastic wackestone. This particular bed of dolomitic bioclastic wackestone is an isolated occurrence and is not observed in other cores at this stratigraphic interval. The overlying surface (Fig. 10, S2) is interpreted to be erosive based on tracing of internal units within Unit 2; the truncation is interpreted to have been caused by submarine erosion because there is no evidence of subaerial exposure. Therefore, the top of this interval has most likely been removed. In general, the dolomitic bioclastic wackestone facies is

interpreted to represent deposition in a normal-marine, quiet-water subtidal environment, below fair-weather wave base; it most likely reflects deepening at this stratigraphic position.

On the basis of lithofacies, the upper succession of Unit 2 (datum to S2) is interpreted to represent moderate to high energy, shallow-water ramp deposits. This succession of coarse-grained bioclastic wacke-packstones may be equivalent to the Burlington-Keokuk Limestone on the basis of lithology and stratigraphic position (Lane, 1978; Thompson, 1986).

Surface 2 (Fig. 8, S2) is the boundary between Units 2 and 3. On the basis of tracing of internal units within Unit 2, the surface appears to be an erosional truncation surface. The truncation is interpreted to have been caused by submarine erosion because there is no evidence of subaerial exposure. The overlying oolite deposits (Unit 3) are supportive of increased energy.

The origin of Genetic Unit 2 is deposition after a major deepening event. There is a record of two shallowing events, each capped by possible subaerial exposure surfaces in the lower succession. The upper succession represents shallowing followed by a poorly preserved deepening event. Unit 2 geometries indicate shallow-water deposition to the northeast. Overall wedge-shaped geometry is controlled by topography on erosion surfaces above and below the unit, and depositional thinning and downlap to the southwest. Compared to Unit 1, Unit 2 contains copious amounts of chert and porous chert with the majority of porous chert located in the southwest.

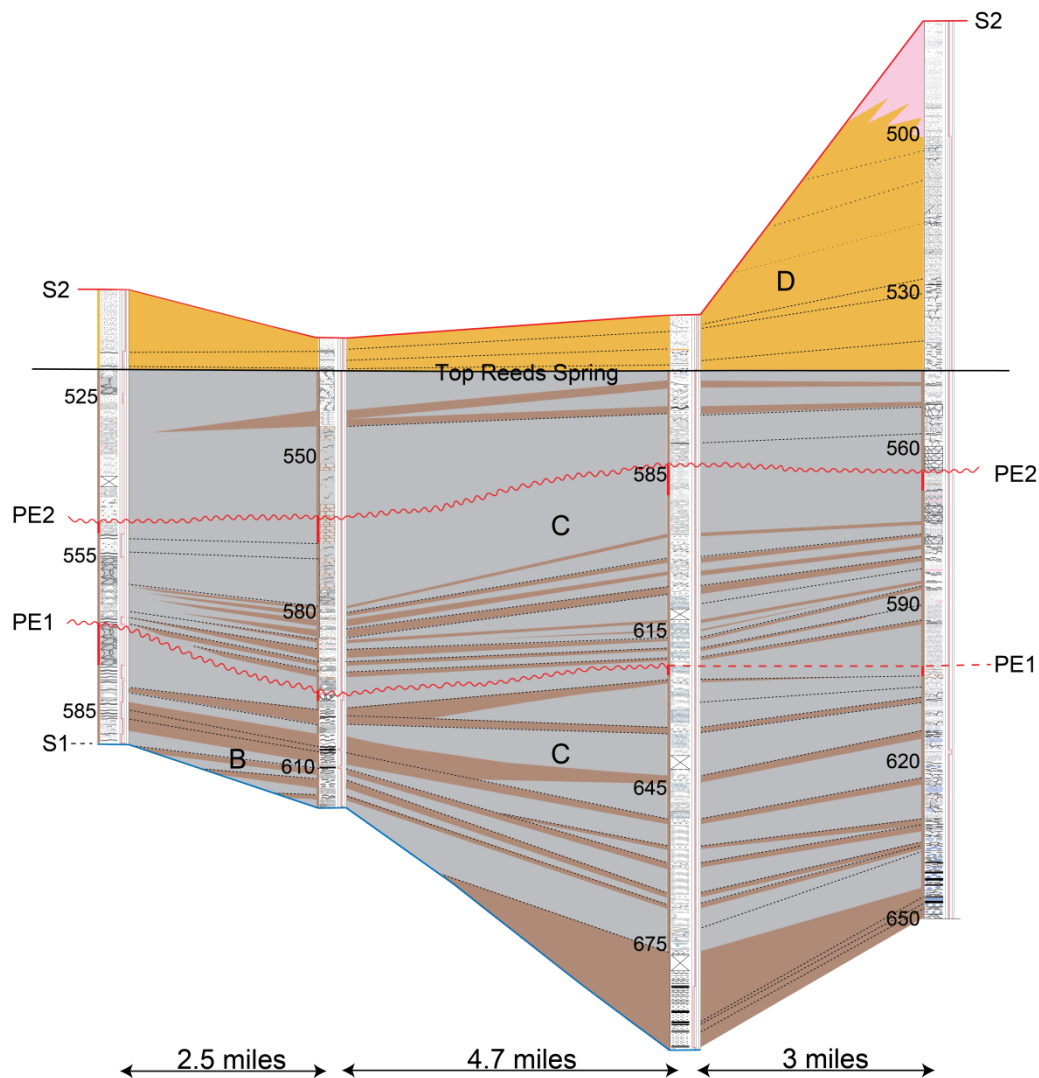


Figure 10. Genetic Unit 2 is deposited after a major deepening event. The lower succession consists of complexly interbedded argillaceous wackestone and brecciated chert facies (C). Clinoform toes (B) converge or downlap onto S1 and there is a record of two shallowing events each capped by a subaerial exposure surface (PE1&PE2). At the contact between the lower and upper succession (top of Reeds Spring), argillaceous wackestone grades upward into echinoderm-rich-bioclastic wacke-packstone. The upper succession thickens to the northeast producing a wedge-like geometry (D) overlain by dolomitic wackestone. Internally, strata appear to thin or downlap to the southwest. Horizontal scale is shown in miles along bottom of cross section. Vertical scale is in feet below the surface labeled along each individual core description. Figure 7 is the legend for this cross section.

Unit 3

Unit 3 is up to 170 feet (52 m) thick in northeast locations and thins to 90 feet (27 m) thick to the southwest. The base of Unit 3 consists of a laterally continuous interval of ooid packstone. This ooid packstone is interpreted to be equivalent to the Short Creek Oolite on the basis of lithology and stratigraphic position (Thompson, 1986). Regional studies (Ritter, 2004), indicated that the Short Creek Oolite was deposited in association with a relative sea-level lowstand.

Ritter (2004) described a structureless (bioturbated) oolite facies that was deposited in > 2 m (6.5 ft) water depth. It was interpreted to form in shallower water than a bioclastic grainstone facies, which he showed to form in 10-50 m water depth (33-164 ft). As Ritter's (2004) structureless oolite facies is similar to the ooid packstone facies of this study, it is likely that both were deposited in a similarly shallow environment. In contrast, the dolomite wackestone and echinoderm-rich wackestone-packstone facies at the top of Unit 2 have been interpreted, in my study, to form at depths greater than those interpreted for the oolite. Thus, in considering the regional evidence, the interpreted submarine erosion surface (S2) at the base of Unit 3, and the interpreted water depths for facies, the transition from the top of Unit 2 to the oolite at the base of Unit 3 likely represents a relative sea-level fall.

The echinoderm-rich bioclastic wackestone-packstone facies immediately overlying the oolite facies is interpreted to form in deeper water, suggesting a relative sea-level rise after oolite deposition. This is consistent with regional evidence that the Short Creek Oolite represents

deposition in association with a lowstand and overlying strata form during relative sea level rise (Ritter, 2004).

In U3PS2, the echinoderm-rich-bioclastic wacke-packstone in PM-8 and 12 passes upward to tripolitic chert (Fig. 11, location E). In PM-21, the interval is all echinoderm-rich bioclastic wacke-packstone. To the southwest, in PM-17, the base of the interval is argillaceous wackestone. In PM-17 and PM-12, the top of the interval is echinoderm rich bioclastic wacke-packstone. The argillaceous wackestone facies to the southwest indicates the position of deeper-water, outer-ramp environment. Intervals of tripolitic chert facies represent sponge-spicule accumulations in areas of upwelling.

In PM-17 and 12 echinoderm-rich bioclastic wacke-packstone at the top of U3PS2 is overlain by argillaceous wackestone, indicating a marine flooding surface (Fig. 11). To the northeast, the correlative flooding surface has been extrapolated updip, even though strong evidence of a flooding surface is lacking. Above this flooding surface echinoderm-rich bioclastic wacke-packstone in the two northeastern cores indicates shallower water to the northeast (Fig. 11, location G). Argillaceous wackestone in the southwestern cores indicates deeper water to the southwest (Fig. 11, location F).

Above the stratigraphic interval defined by location G and location F (Fig. 11), the overlying succession to the Mississippian-Pennsylvanian unconformity is a series of chert breccias and tripolitic chert with minor echinoderm-rich bioclastic wacke-packstone (Fig. 11, location H). Although chert is observed throughout this genetic unit, the majority of porous chert occurs in southwest locations. The diagenetic overprint on the original fabric of these

rocks is so severe that recognition of depositional environment and relative sea-level history is very difficult. In large part, the original facies is unknown. The result of the diagenetic overprint is a section dominated by breccias and tripolitic chert in the 35-75 feet (11-23 m) underlying the Mississippian-Pennsylvanian unconformity.

The relative sea-level fall along the Mississippian-Pennsylvanian boundary resulted in an extensive period of subaerial exposure lasting approximately 10 million years (Merriam, 1963; Ross and Ross, 1988; Montgomery et al, 1998; Watney et al., 2001; Franseen, 2006). Effects of this major subaerial exposure event (sequence boundary) will be discussed further in the Diagenesis section.

The origin of Genetic Unit 3 is deposition during a relative sea-level lowstand. There is a record of two deepening events, preserved by flooding surfaces, representing parasequences. Overall unit geometries indicate shallow-water deposition to the northeast. Unit 3 terminates at the Mississippian-Pennsylvanian unconformity.

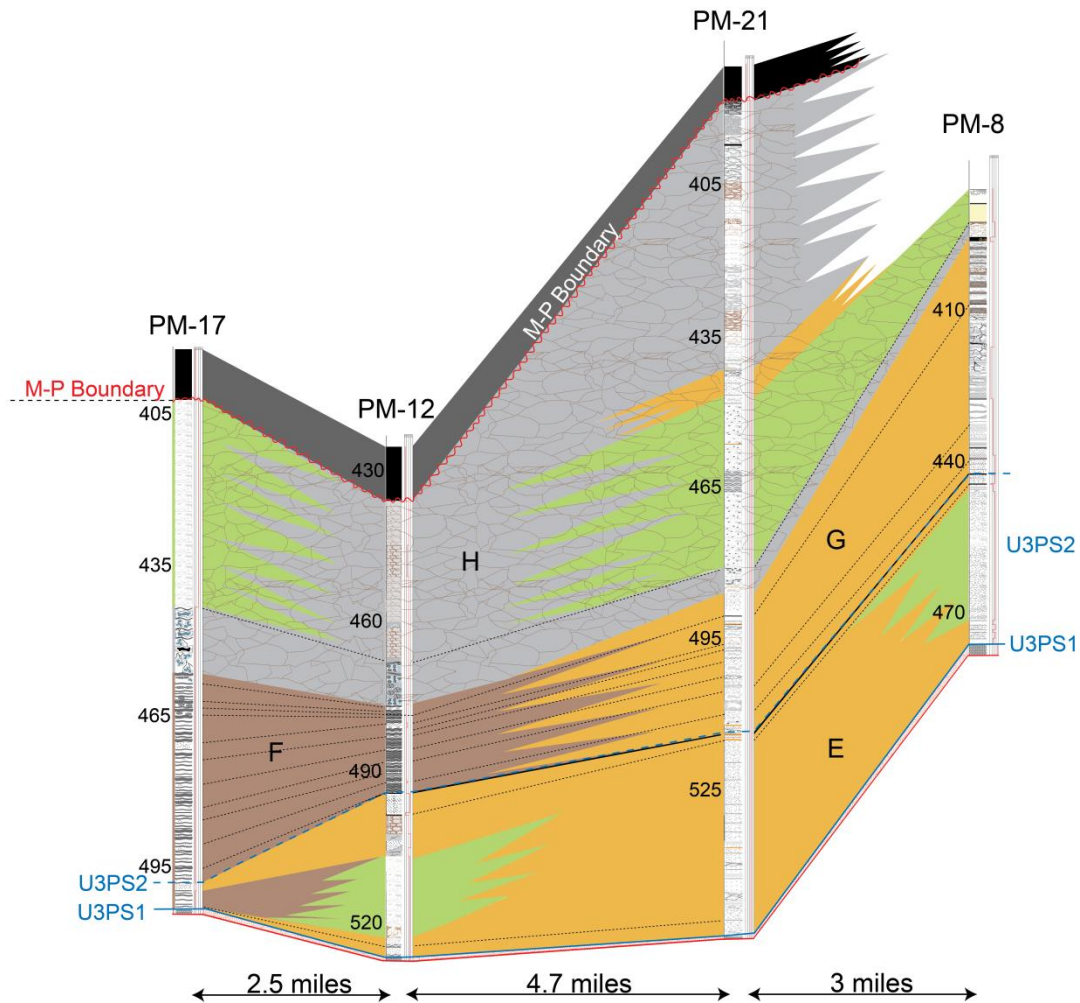


Figure 11. Genetic Unit 3 starts during a lowstand in relative sea level and two parasequences (U3PS1, U3PS2), represent deepening during relative sea-level rise. Genetic Unit 3 terminates at the Mississippian-Pennsylvanian (M-P) unconformity. Shallow water deposits (E, G) are dominant to the northeast in the lower and upper parasequence. Deeper water argillaceous wackestone accumulates downdip to the southwest (F). Chert breccias and tripolitic chert (H), which are significantly altered during subaerial exposure, make up the upper part of the unit. Horizontal scale is shown in miles along bottom of cross section. Vertical scale is in feet below the surface labeled along each individual core description. Figure 7 is the legend for this cross section.

DIAGENESIS

The paragenetic sequence consists of 22 major stages. The relative timing of each stage and influence on porosity evolution is summarized in Figure 12. This chronologic sequence was established by petrographic cross-cutting and superpositional relationships. The paragenetic stages are grouped into Mississippian, subaerial exposure, burial, and late hydrothermal time intervals. The Mississippian interval (stages 1-5) formed before subaerial exposure and meteoric diagenesis associated with the Mississippian-Pennsylvanian unconformity. It includes all fabrics cross-cut by fractures and brecciation (associated with the Mississippian-Pennsylvanian subaerial exposure event) that are infilled with Pennsylvanian shale. The subaerial exposure interval comprises stages 6-9 and consists of those stages formed during Mississippian-Pennsylvanian karst and infilled with Pennsylvanian shale. The burial interval comprises stages 10-15, which consist of compaction features, including grain-to-grain pressure solution, fracturing, stylolitization, and calcite cementation that cut across all previous stages. The late hydrothermal interval comprises stages 16-22 and post dates compaction features. It is characterized by fracturing, quartz and calcite dissolution, megaquartz, pyrite, and baroque dolomite precipitation.

Stage 1- Deposition. Observed depositional fabrics are discussed in detail in the Lithofacies section. Although depositional fabrics have been obscured by dolomitization and silicification, wackestone and packstone fabrics tend to be most prevalent whereas grainstone and mudstone fabrics are rare.

Stage 2- Micritization. Micrite envelopes are commonly observed along the margins of calcitic and silicified bioclasts. Micrite envelopes developed early as evidenced by micrite

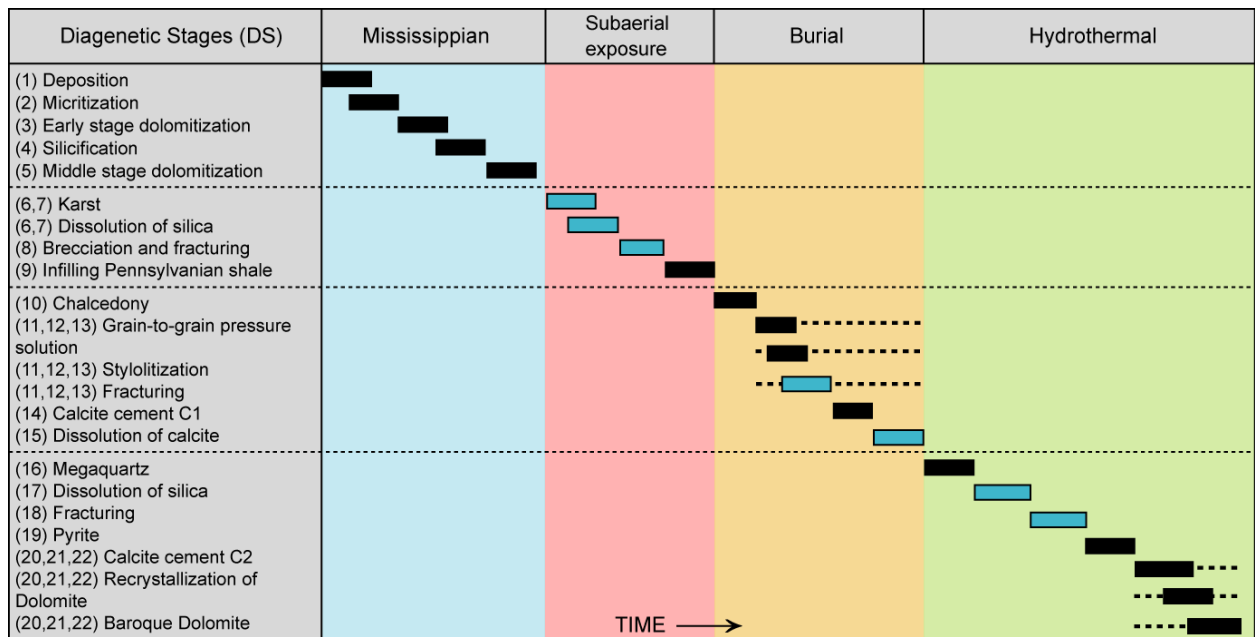


Figure 12. Paragenetic sequence. Blue boxes represent stages related to porosity formation. Dashed lines indicate relative timing is ambiguous. Length of boxes is not considered to be a quantitative representation of duration.

envelopes that are encapsulated by dolomite and diagenetic quartz. Micritization is an early process thought to occur during or soon after the time of deposition (Bathurst, 1975).

Stage 3- Early Stage Dolomitization. Partial dolomitization of depositional wackestone and packstone occurred pre-silicification (stage 4). Dolomite included in chert lacks the late growth zones present outside of the chert. Inside the chert, there are fewer rhombohedra that are more widely spread than outside of the chert (Fig. 13C, D). Dolomite shows patchy luminescence under cathodoluminescence (CL). Dolomite texture is crystalline (20-60 μm) planar-s to planar-e (Sibley and Gregg, 1987) and does not typically take a stain in alizarin red-s and potassium ferricyanide solution, indicating that it is non-ferroan (Dickson, 1966).

Stage 4- Silicification. Microcrystalline and cryptocrystalline quartz replaces matrix and fossil fragments and produces dense chert beds and nodules. Although non-dolomitized material was selectively silicified, some early dolomite growth zones of stage 3 are locally engulfed in silica. Silicified areas preserve fabrics indicating silicification before compaction (Fig. 13B, C, D); whereas the areas without silicification show compaction fabrics (stage 11, 12, or 13; Fig. 14A). This indicates the early dolomite (stage 3) was before compaction and silicification, and silicification was before compaction.

Stage 5- Middle Stage Dolomitization. Dolomite in non-silicified areas contains late growth zones not present in stage 3 dolomitization, indicating additional dolomitization occurred after silicification (Fig. 13C, D). Dolomite rhombohedra show patchy luminescence under CL. Dolomite texture is crystalline (20-60 μm) planar-s to planar-e (Sibley and Gregg, 1987). The

dolomite does not typically take a stain in alizarin red-s and potassium ferricyanide solution, indicating that it is non-ferroan (Dickson, 1966).

Stage 6 or 7- Karst. Before Pennsylvanian deposition, the Mississippian system was exposed to meteoric conditions (Duren, 1960; Euwer, 1965; Thomas, 1982; Rogers et al., 1995; Montgomery et al., 1998; Watney et al., 2001; Mazzullo et al., 2009). During this time dissolution of carbonate material occurred, which created vugs, caves, and microkarst (Fig. 6). Some of the dissolution features are filled with Pennsylvanian shale. Stage 6 or 7 karst features cross-cut all previous stages.

Stage 6 or 7- Dissolution of Silica. Early dissolution of silica can be observed by a porous rim around chert nodules, cross-cut by fractures. The fractures are filled with marine carbonate sediment soon after their formation prior to lithification. This relationship indicates early dissolution of silica followed by compactional fracturing, and then squeezing in of unlithified sediment (Fig. 6B). Stage 6 or 7 dissolution of silica is concentrated in the stratigraphic interval from the Mississippian-Pennsylvanian unconformity to 75 feet (23 m) below, although evidence of this dissolution stage occurs up to 100 feet (30 m) below the unconformity.

Stage 8- Brecciation and Fracturing. During stage 6 or 7 karst, dissolution, interpreted to be from meteoric water, resulted in cavities, which later resulted in formation of solution-collapse breccias (Fig 6A, C, D).

Stage 9- Infilling Pennsylvanian Shale. Some of the fracture and breccia porosity that remained open was filled by Pennsylvanian shale during initial phases of deposition of overlying Pennsylvanian formations (Fig. 6A and Fig. 13A).

Stage 10- Chalcedony Precipitation. The timing of chalcedony precipitation is tentatively placed after subaerial exposure events and before burial events because it is cross-cut by vertical fractures associated with stylolitization (stage 11, 12, 13). Also, chalcedony forms an isopachous cement in interparticle pore space and fractures associated with karsting (stage 8; Fig. 14C and Fig. 15A), and it occupies interparticle pore space directly next to calcitic bioclast molds (stage 15). If precipitation occurred after dissolution of calcitic bioclasts then I would expect to see chalcedony in those molds. Therefore, chalcedony is interpreted to have precipitated after fracturing associated with karst, but before burial compaction and dissolution of calcite.

Stage 11 or 12 or 13- Grain-to-grain Pressure Solution. Overly close packing of grains and pressure solution seams between grains are prevalent in grain-supported fabrics where silicification is not pervasive (Fig. 14A). Grain-to-grain contacts are sutured; portions of each grain may be missing, with no primary interparticle pore space preserved between grains. This is interpreted to form as a result of burial compaction.

Stage 11 or 12 or 13- Stylolitization. Pressure solution seams between grain boundaries (stage 11, 12, 13) are cross-cut by stylolites. Stylolites are prevalent in argillaceous zones. Stylolites likely progressed during the onset of burial compaction and continued to develop during further burial.

Stage 11 or 12 or 13- Fracturing. Vertically oriented fractures occur along and perpendicular to the trace of horizontal stylolites (Fig. 13B). These vertical fractures are interpreted to be a direct result of stresses associated with stylolitization. Stages 11, 12, and 13 are interpreted to occur at about the same time due to burial compaction, so relative timing is inconclusive.

Stage 14- Calcite Cement (C1). The vertical fractures associated with stylolitization (stage 11, 12, 13) are commonly filled with calcite cement C1 (Fig. 13B). C1 takes a pink stain in alizarin red-s and potassium ferricyanide solution, indicating that it is non-ferroan (Dickson, 1966). C1 appears dull under cathodoluminescence and exhibits no compositional zoning.

Stage 15- Dissolution of Calcite. Calcitic bioclasts underwent dissolution leaving moldic pores (Fig. 14D). The margins of some molds exhibit a dogtooth geometry (Fig. 14D) as if there were calcite overgrowths on the bioclasts that had been dissolved. Note that as these inferred overgrowths are not preserved, their precipitation has not been placed in the paragenesis. Megaquartz occurs in some of these bioclast molds and the molds of interpreted calcite overgrowths, but there is no chalcedony in these molds. Therefore, I interpret the dissolution of calcitic bioclasts to have taken place after the precipitation of chalcedony (stage 10), but before precipitation of megaquartz (stage 16).

Stage 16- Megaquartz Precipitation. Megaquartz occupies molds of calcitic bioclasts (stage 15) and interparticle porosity following precipitation of chalcedony (stage 10; Fig. 15A). As will be discussed below, megaquartz has high homogenization temperatures; therefore it is interpreted to signify the onset of hydrothermal fluid migration (see Fluid Inclusion

Microthermometry). It is unknown, if Stage 14 and 15 formed during or before hydrothermal fluid migration. These stages have been placed in the burial interval because the first positive evidence for hydrothermal fluid migration is Stage 16 megaquartz precipitation.

Stage 17- Dissolution of Silica. Dissolution of microcrystalline and cryptocrystalline quartz and chalcedony is interpreted to occur after precipitation of megaquartz (stage 16), because no megaquartz occupies pores created by stage 17 dissolution (Fig. 14B, C and Fig. 15A). Stage 17 dissolution of silica is concentrated in PM-17 from 440-400 ft, PM-12 from 505-525 ft, PM-21 from 450-480 ft, and in PM-8 from 385-392 ft and 445-470 ft (Fig. 8). Stage 17 dissolution of silica is found up to 120 feet (36 m) below the Mississippian-Pennsylvanian unconformity (stage 6 or 7). The combined effects of stage 6-7 and stage 17 dissolution resulted in the following distributions. PM-17 and PM-12 contain 37% chert (by thickness) and of that, 32% is porous. PM-21 and PM-8 contain 55% chert (by thickness) and of that, 25% is porous.

Stage 18- Fracturing. Fractures cross-cut megaquartz (stage 16) but not pyrite (stage 19) or calcite cement 2 (stage 20 or 21 or 22; Fig. 15C).

Stage 19- Pyrite Precipitation. Aggregates of coarse cubic crystals (3-25 mm) of pyrite are precipitated in interparticle and fracture porosity (stage 18; Fig. 15B, C) following megaquartz precipitation (stage 16).

Stage 20 or 21 or 22 - Calcite cement C2. Calcite is precipitated in pores lined with megaquartz (stage 16) and pyrite (stage 19) but is not cross-cut by the late fractures (stage 18; Fig. 15C). Therefore, it is interpreted to precipitate after pyrite. No relationship has been found to determine timing of calcite cement C2 in relation to baroque dolomite. C2 takes a pink stain

in alizarin red-s and potassium ferricyanide solution, indicating that it is non-ferroan (Dickson, 1966). C2 appears dull under cathodoluminescence and exhibits no compositional zoning.

Stage 20 or 21 or 22- Recrystallization of Dolomite. Patchy cathodoluminescence and corrosion surfaces in dolomite rhombohedra indicate recrystallization (Fig. 15D). Rhombohedra are overgrown by baroque dolomite (stage 20 or 21 or 22) with similar luminescence, indicating recrystallization during precipitation of baroque dolomite.

Stages 20 or 21 or 22- Baroque Dolomite Precipitation. Baroque dolomite occurs as overgrowths on dolomite rhombohedra that have undergone recrystallization (stage 20 or 21 or 22). Baroque dolomite also occurs as cement in interparticle pore space and is not cross-cut by any of the previous stages (Fig. 15D). Baroque dolomite is growth zoned under CL, with dull and moderate luminescent zones (Fig. 15D). It does not take a stain in alizarin red-s and potassium ferricyanide solution, indicating that it is non-ferroan (Dickson, 1966). As will be shown below, baroque dolomite shows high homogenization temperatures; therefore it is interpreted to signify hydrothermal fluid migration.

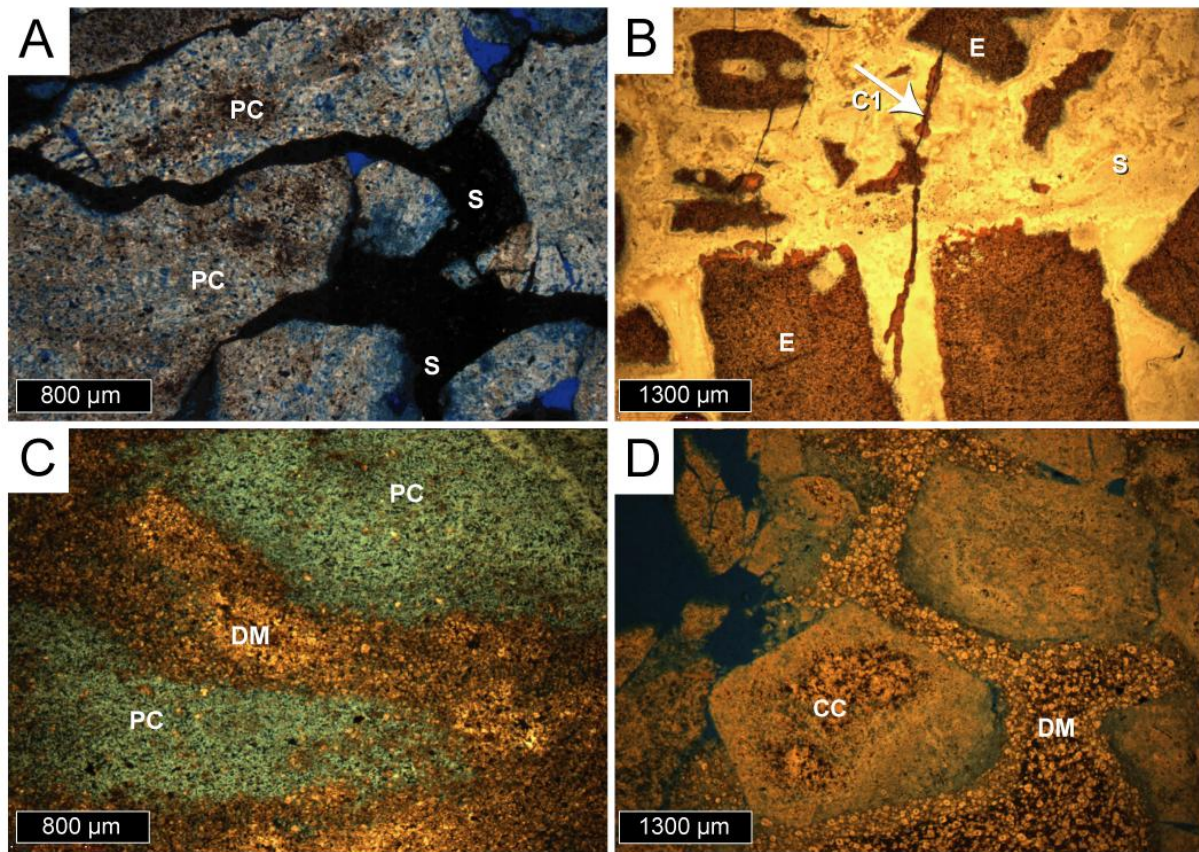


Figure 13. Photomicrographs illustrating characteristics leading to interpretation of diagenetic stages 1-14 (DS). **A)** Deposition of spicule-rich carbonate (DS-1) followed by silicification (DS-4) and dissolution of silica resulting in porous chert clasts (PC; DS-6, 7). Pennsylvanian shale occurs as fill (S; DS-9) between brecciated chert clasts (DS-8). Thin section was impregnated with blue epoxy and photomicrograph has been taken in plain polarized light (PM-12; 459'). **B)** Silicified matrix (S; DS-4) preserves fabric and engulfs and partially silicifies echinoderm grains (E). Fractures associated with stylolitization (DS-11, 12, 13) are filled with calcite cement C1 (DS-14). Thin section is stained with alizarin red S and potassium ferricyanide and photomicrograph has been taken in plain polarized light (PM-17; 691'). **C)** Compared to non-silicified areas (DM; DS-5), silicified areas contain only early stage dolomitization (DS-3) with fewer and more spread out rhombohedra and only early growth zones (PC; DS-4). The silicified areas have undergone dissolution (DS-6, 7) leaving porous areas (PC) and tight dolomitic matrix (DM). Thin section was impregnated with blue epoxy and photomicrograph has been taken in plain polarized light (PM-21; 571'). **D)** Similar to photomicrograph C except chert clasts (CC) have not been affected by dissolution. Chert clasts (CC) contain few dolomite rhombohedra with early growth zones (DS-3) in silica (DS-4) whereas matrix is tight dolomite with later growth zones (DS-5). Thin section was impregnated with blue epoxy and photomicrograph has been taken in plain polarized light (PM-12- 616').

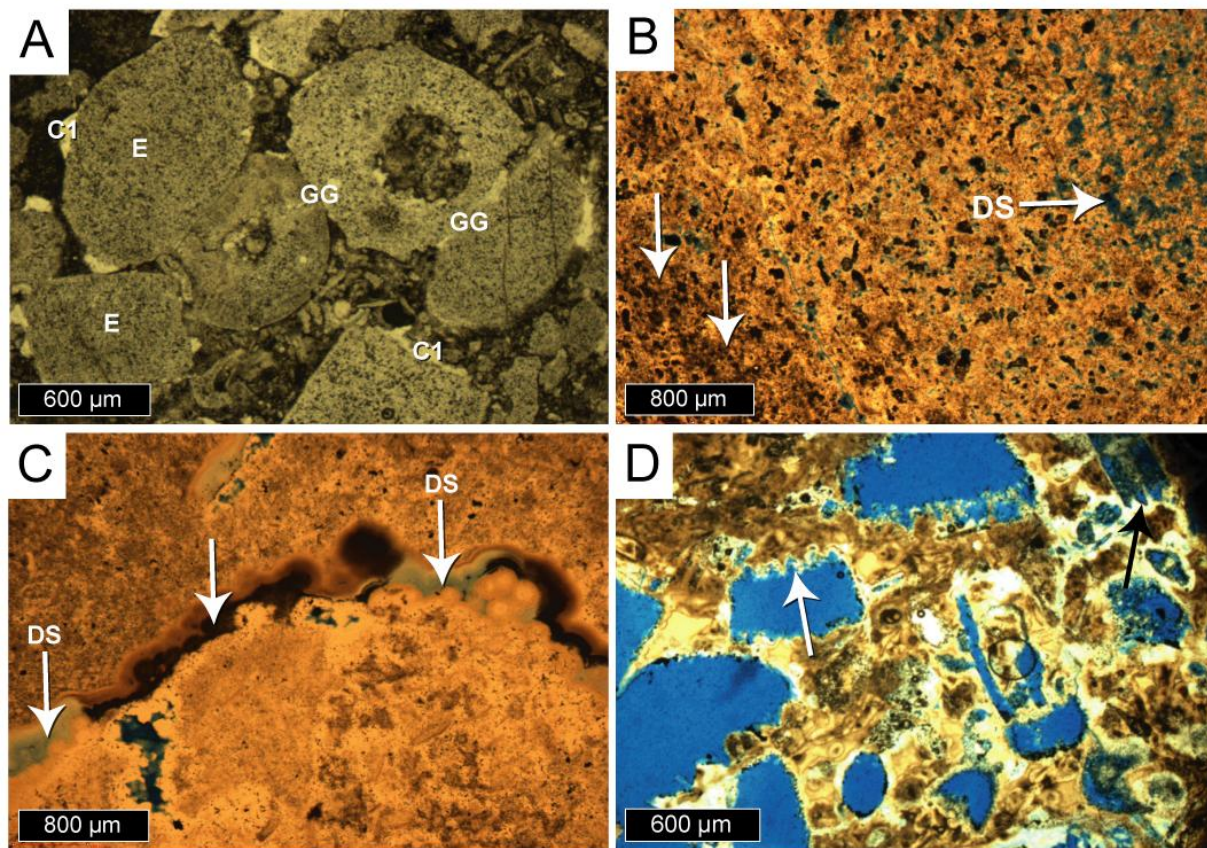


Figure 14. Photomicrographs illustrating characteristics leading to interpretation of diagenetic stages 14-17 (DS). **A)** Where silicification is not pervasive, grainy fabrics, especially echinoderm fragments (E), experienced compaction-related grain-to-grain pressure solution (GG). Calcite cement 1 (C1; DS-14) forms as overgrowths on echinoderm fragments after pressure solution. Photomicrograph is taken in plain polarized light (PM-12; 504'). **B)** Pore space is created by dissolution of microcrystalline and cryptocrystalline silica (DS; DS-17). Arrows point to areas where silica has not dissolved. Thin section was impregnated with blue epoxy and photomicrograph has been taken in plain polarized light (PM-12; 571'). **C)** Similar to photomicrograph **B** except pore space is created by dissolution of finely crystalline chalcedony (DS; DS-17). Arrows point to areas where chalcedony has not dissolved. Thin section was impregnated with blue epoxy and photomicrograph has been taken in plain polarized light (PM-12; 553'). **D)** Calcitic bioclasts underwent dissolution (DS-15) leaving moldic pores (blue epoxy areas). The margins of some molds exhibit a dogtooth geometry (arrows) as if there were calcite overgrowths on the bioclasts that had been dissolved out. Thin section was impregnated with blue epoxy and photomicrograph has been taken in plain polarized light (PM-12; 539').

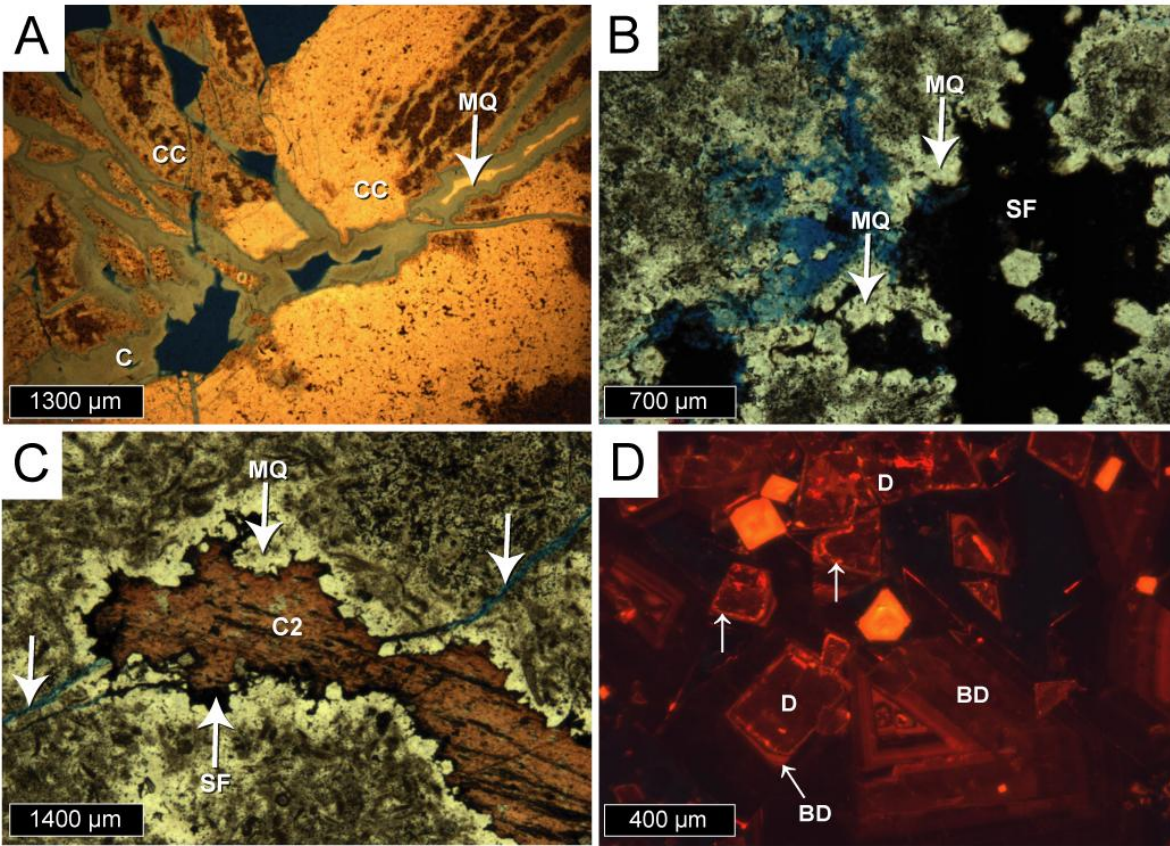


Figure 15. Photomicrographs illustrating characteristics leading to interpretation of diagenetic stages 10-22 (DS). **A**) Brecciated chert clasts (CC) with porous chalcedony (C; DS-10, 17) filling in fractures and megaquartz (MQ; DS-16) precipitates in pore space following precipitation of chalcedony. Thin section was impregnated with blue epoxy and photomicrograph has been taken in plain polarized light (PM-12; 616'). **B**) Pyrite precipitation (SF; DS-19) partially filled open pore space after precipitation of megaquartz (MQ; DS-16). Thin section was impregnated with blue epoxy and photomicrograph has been taken in plain polarized light (PM-12; 538'). **C**) Pore space lined with megaquartz (MQ; DS-16), followed by pyrite precipitation (SF; DS-19), and then precipitation of calcite cement 2 (C2; DS-20, 21, 22). Open fracture (arrow) cross-cuts MQ but not SF or C2. Thin section is stained with alizarin red S and potassium ferricyanide and photomicrograph has been taken in plain polarized light (PM-12; 538'). **D**) Rhombohedral dolomite (D) is overgrown by baroque dolomite (BD; DS-20, 21, 22). Rhombohedral dolomite shows patchy luminescence and a corrosion surface (arrows), with luminescence indicating recrystallization during precipitation of baroque dolomite (DS-20, 21, 22). Photomicrograph is taken under cathodoluminescence (PM-12; 619').

FLUID INCLUSIONS

Fluid inclusion microthermometry was used to characterize temperature and fluid composition encapsulated in inclusions during diagenesis. The following section uses the methodology and terminology for fluid inclusion analysis proposed by Goldstein and Reynolds (1994). Fluid inclusion assemblages (FIAs) were defined as all fluid inclusions along the most finely divisible concentric growth zones. This section describes fluid inclusion data from megaquartz (stage 16) and baroque dolomite (stage 20 or 21 or 22). Fluid inclusion data are presented in Figures 17, 18, and 19.

Megaquartz

Fluid Inclusion Data- Fluid inclusions in megaquartz are common, giving it a cloudy appearance under transmitted light. These inclusions have variable shapes and sizes. Primary FIAs are identified in growth zones and contain fluid inclusions oriented in the direction of crystal growth and parallel to growth direction. Most FIAs of primary fluid inclusions contain two-phase aqueous fluid inclusions with liquid and a gas bubble exhibiting consistent vapor to liquid ratios. Others contain two-phase aqueous fluid inclusions but each inclusion seems to have a different vapor to liquid ratio; many of these fluid inclusions were dominated by the gas phase. The gas-rich inclusions were not petrographically paired with gas-poor inclusions, and thus, they have not been altered by necking down after a phase change (e.g. Goldstein, 2003). These inclusions represent heterogeneous entrapment during conditions of gas-liquid immiscibility. Still other FIAs contain all-liquid fluid inclusions at room temperature. These inclusions likely represent entrapment at temperatures below about 50°C (Goldstein, 1993).

Secondary inclusions are present along healed fractures that cross-cut growth zones. No secondary inclusions were measured in this study.

Megaquartz is divided into three phases of mineral growth based on transmitted light petrography (Fig. 16A and B). Quartz phase one (Q1) is concentrated in the cloudy cores of quartz crystals and is considered the first phase of megaquartz precipitation. Quartz phase two (Q2) is concentrated in the middle growth zones of quartz crystals and is considered the second phase of quartz precipitation. Q2 contains several concentric growth zones alternating between cloudy inclusion-rich zones and clear zones, which represent multiple FIAs. Quartz phase three (Q3) is concentrated in fibrous re-entrants on the margins of quartz crystals and is considered the last phase of quartz precipitation on the basis of superpositional relationships on Q2. It also consists of alternating cloudy and clear growth zones. All-liquid fluid inclusions observed in Q3 and are thought to represent the latest phase of quartz precipitation. Temperatures of homogenization (T_h) were only measured for fluid inclusions in FIAs containing two-phase aqueous fluid inclusions with liquid and a gas bubble exhibiting consistent vapor to liquid ratios.

T_h in Q1 inclusions range from 71 to 125°C with a mode between 91 to 105°C. T_h measurements of FIAs in Q1 show repeated rises and falls in the direction of crystal growth (Fig. 18). Seven FIAs were measured in Q1. Five of these FIAs have consistent homogenization temperatures (over 90% of the FIA fall within 10-15°C interval). The presence of consistent T_h in FIAs suggests that there has been little thermal reequilibration. Final melting temperatures ($T_{m_{ice}}$) are from -3.3 to -3.6°C indicating fluids with a salinity of 5.4 to 5.9 wt% NaCl equivalent

(Bodnar, 1992). First melt temperatures (T_e) between -19 and -21°C indicate the presence of a NaCl-rich fluid (Goldstein and Reynolds, 1994).

T_h for Q2 inclusions range from 99.4 to 135.8°C with a mode between 120 to 130°C. T_h measurements of FIAs in Q2 show repeated rises and falls in the direction of crystal growth (Fig. 18). Four FIAs were measured in Q2. Two of these FIAs have consistent homogenization temperatures, one with a strong mode at 100°C and the other at 120°C. The presence of consistent T_h in FIAs suggests that there has been little thermal reequilibration. Final melting temperatures ($T_{m_{ice}}$) are from -2.8 to -8.7°C indicating fluids with a salinity of 4.7 to 12.5 wt% NaCl equivalent (Bodnar, 1992). First melt temperatures (T_e) around -35°C provides only ambiguous evidence of fluid composition (Goldstein and Reynolds, 1994).

T_h for Q3 inclusions range from 150.5 to 156.8°C. One consistent FIA was measured in Q3. Some FIAs consist of all-liquid fluid inclusions at room temperature. Final melting temperatures ($T_{m_{ice}}$) are from -13.9 to -21.7°C indicating fluids with a salinity of 17.7 to 23.5 wt% NaCl equivalent (Bodnar, 1992). First melt temperatures (T_e) around -50°C indicate the presence of a Na-Ca-rich fluid (Goldstein and Reynolds, 1994).

Baroque Dolomite

Fluid Inclusion Data- Fluid inclusions in baroque dolomite (BD) are common, giving it a cloudy appearance under transmitted light. Two-phase aqueous fluid inclusions containing liquid and a gas bubble are present at room temperature. These inclusions are of variable shapes and sizes with consistent vapor to liquid ratios. There is no evidence for necking down after a phase change or heterogeneous entrapment. Primary inclusions are concentrated in growth zones

and are oriented in the direction of crystal growth and parallel to growth direction (Fig. 16C and D).

T_h for BD inclusions range from 102 to 157.7°C with a strong mode between 130 and 150°C. Final melting temperatures ($T_{m_{ice}}$) are from -16.5 to -18.9°C indicating fluids with a salinity of 19.8 to 21.6 wt% NaCl equivalent (Bodner, 1992). Four FIAs were measured in baroque dolomite (BD). Two of these FIAs yield consistent homogenization temperatures. The presence of consistent FIAs suggests that there has been little thermal reequilibration. First melt temperatures (T_e) around -50°C indicate the presence of a Na-Ca-rich fluid (Goldstein and Reynolds, 1994).

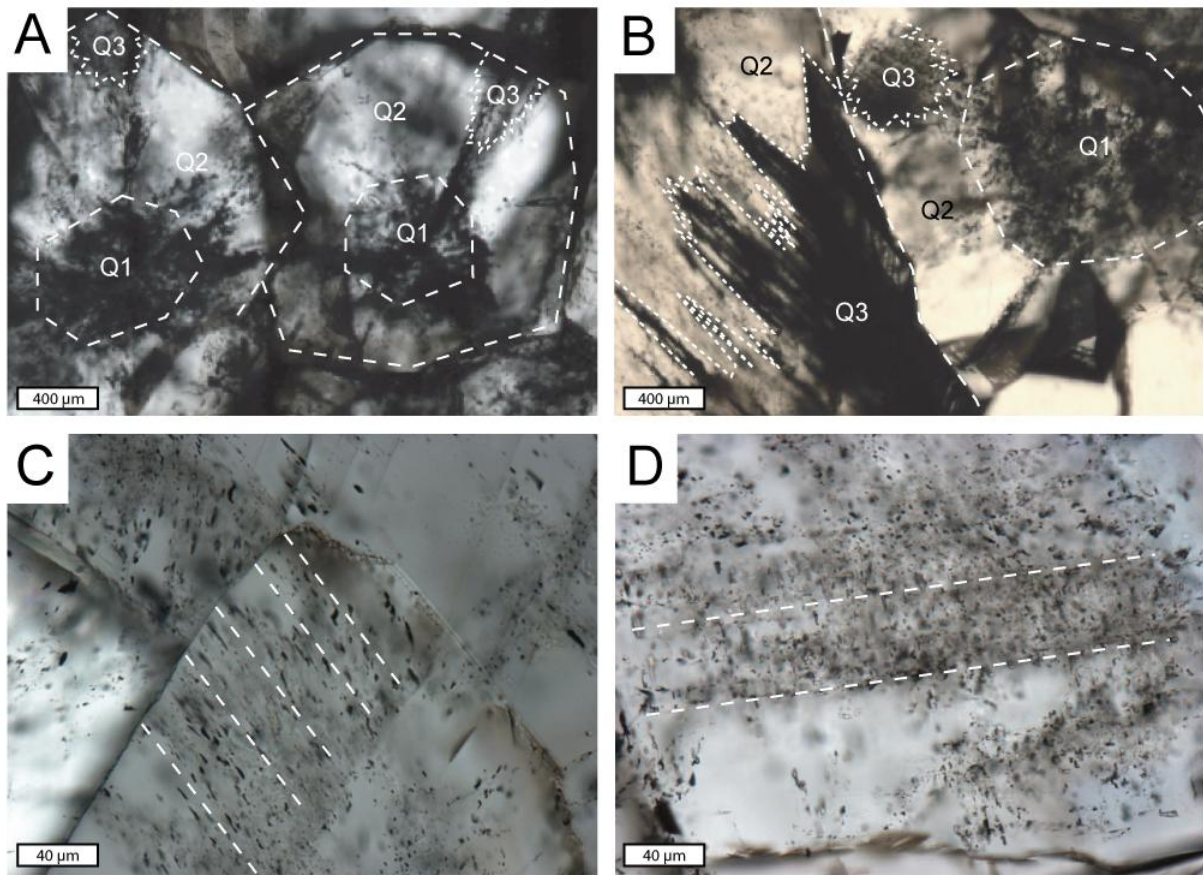


Figure 16. **A)** and **B)** Photomicrographs of three phases of mineral growth in megaquartz. Quartz phase one (Q1) is concentrated in the cores of quartz crystals and is considered the first phase of quartz precipitation. Quartz phase two (Q2) is concentrated in the middle growth zones of quartz crystals and is considered the second phase of quartz precipitation. Quartz phase three (Q3) is concentrated in fibrous re-entrants on the margins of quartz crystals and is considered the last phase of quartz precipitation. **C)** Photomicrographs of primary fluid inclusions in baroque dolomite (BD). Primary fluid inclusions are concentrated in growth zones and are oriented in the direction of crystal growth and parallel to growth direction (dashed lines). **D)** Photomicrograph of fluid inclusions in BD. Photomicrograph shows primary fluid inclusions oriented in the direction of crystal growth and parallel to growth direction (dashed lines). Secondary inclusions are present along healed fractures that cross-cut growth zones. No secondary inclusions were measured in this study.

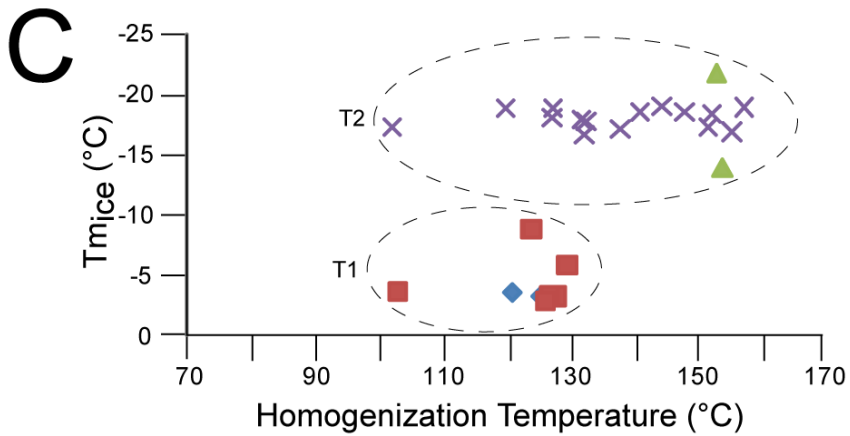
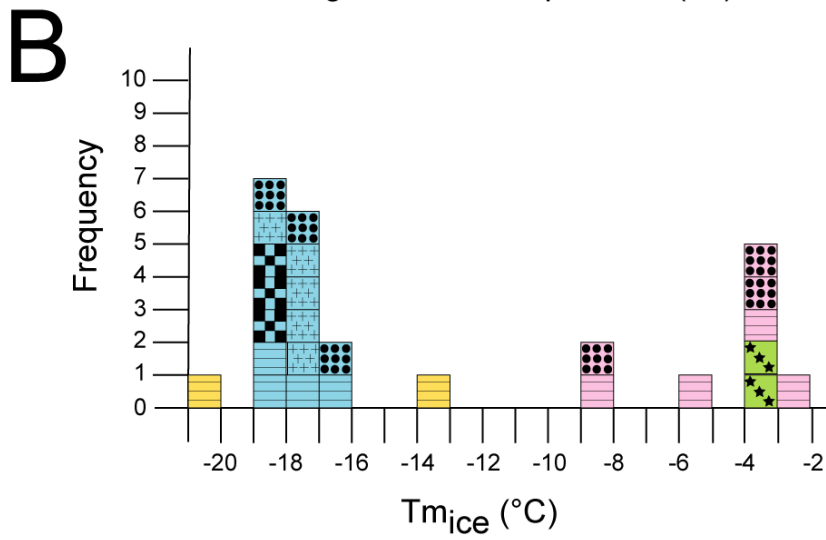
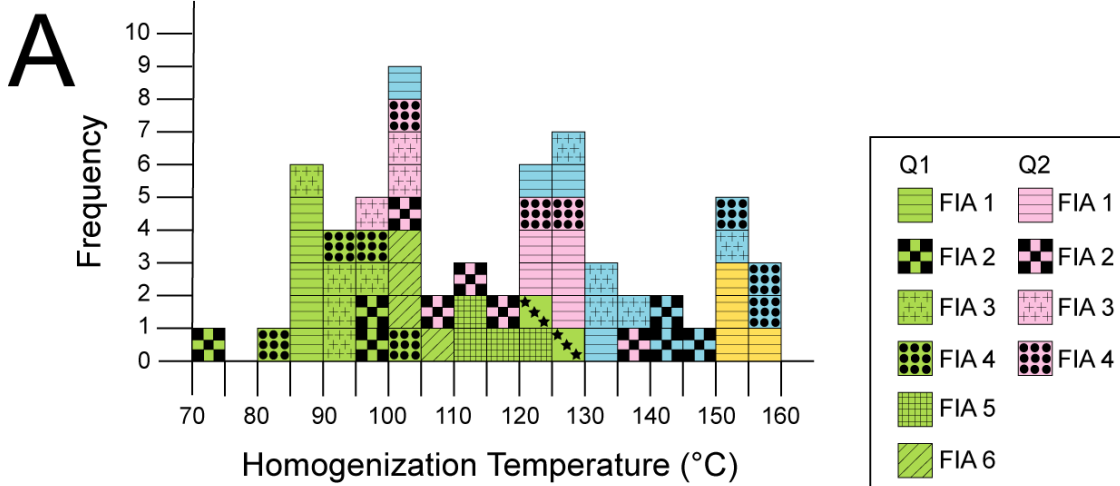


Figure 17. Fluid inclusion data. **A)** Histogram of homogenization temperatures (T_h) from all FIAs measured in megaquartz (Q1, Q2, Q3) and baroque dolomite (BD). Note that all-liquid fluid inclusions in Q3 are not shown on histogram. **B)** Histogram of final melting temperatures of ice ($T_{m_{ice}}$) from all FIAs measured in megaquartz (Q1, Q2, Q3) and baroque dolomite (BD). **C)** Crossplot of T_h vs. $T_{m_{ice}}$ for all fluid inclusions in megaquartz and baroque dolomite. Plot shows the distribution defining two clusters of data. One cluster (T1) has a T_h below 130°C and a $T_{m_{ice}}$ below -10°C in Q1 and Q2. The other cluster (T2) has a T_h range around 130 to 150°C and a $T_{m_{ice}}$ between -15 and -20°C in Q3 and BD.

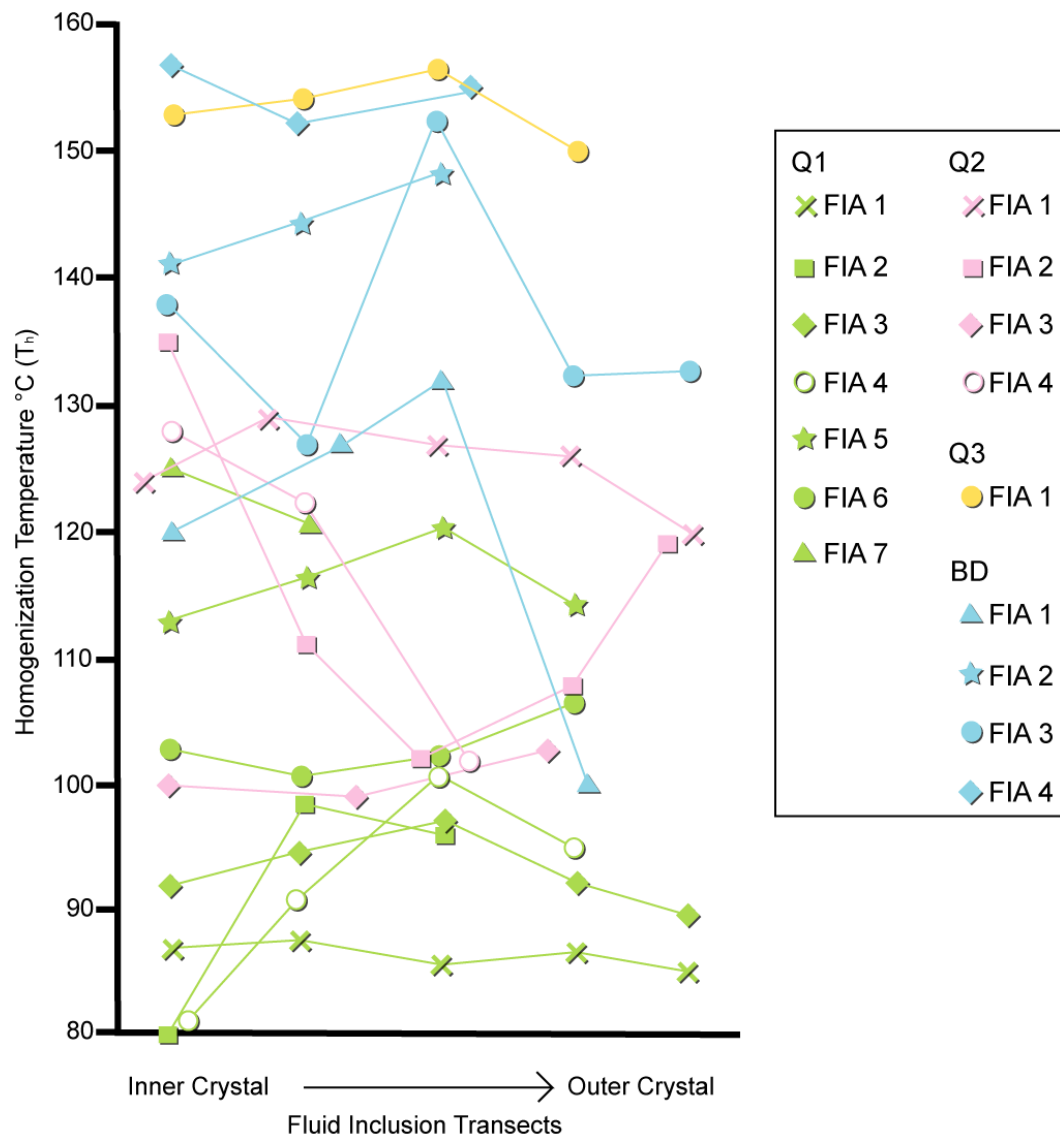


Figure 18. FIA transects of fluid inclusion homogenization temperature from inner growth zones to outer growth zones. Graph shows temperature increase and decrease through time.

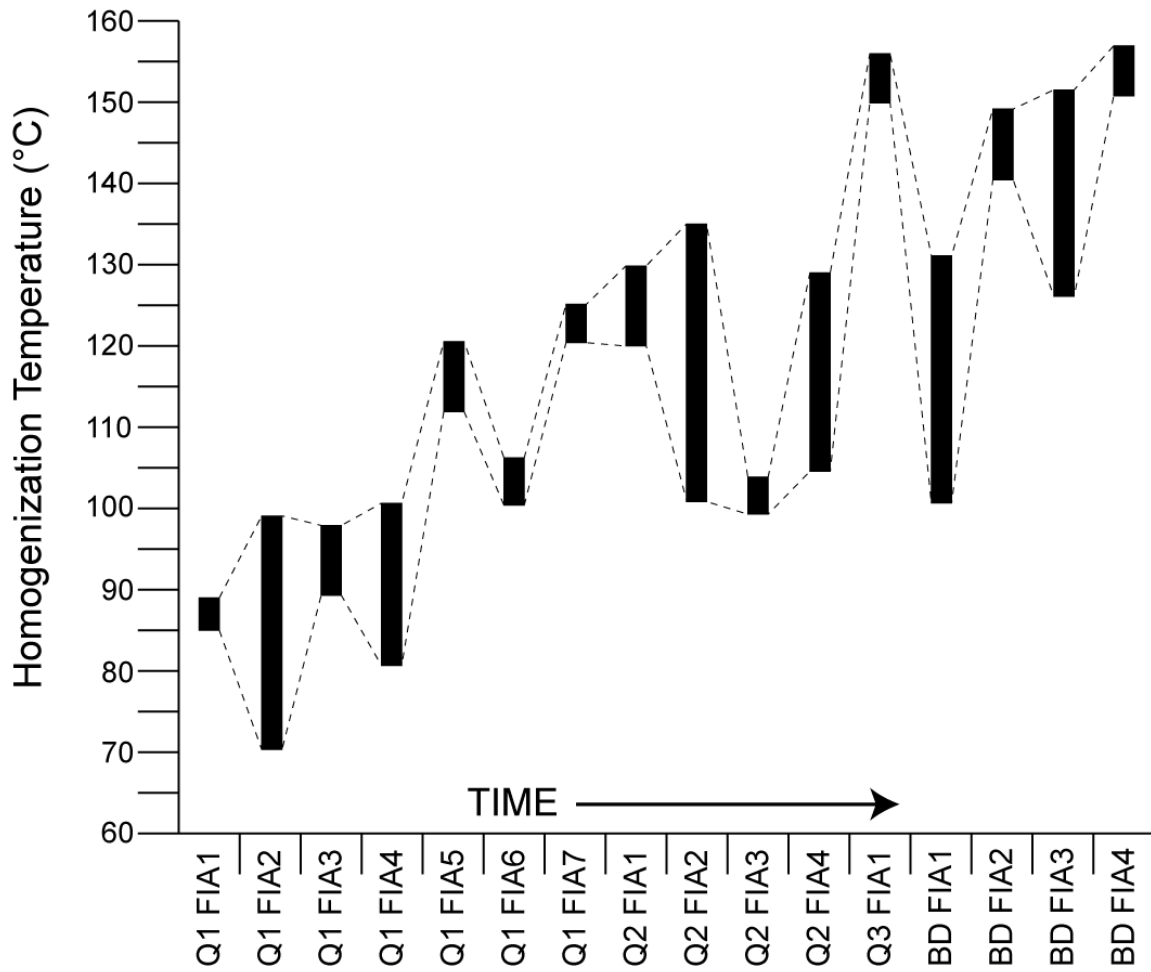


Figure 19. Diagrammatic representation of fluid inclusion homogenization temperatures through time. Black boxes represent FIAs. Dashed lines connect data from FIAs to one another. Diagram shows overall increasing temperature through time with interspersed fluctuations. Although FIAs in Q3 show all-liquid fluid inclusions, this diagram does not represent drops to less than 50°C, because timing of entrapment of these fluid inclusions is petrographically difficult to determine.

DISCUSSION

Hydrothermal System

Petrographic observations indicate that megaquartz and baroque dolomite precipitated late in the paragenetic sequence (stages 16 and 20 or 21 or 22). Megaquartz precipitated after all subaerial exposure related stages (stages 6-9) and after burial stages (stages 10-15). Baroque dolomite precipitated after megaquartz and pyrite precipitation (stages 16 and 19).

The presence of all-liquid fluid inclusions in megaquartz most likely indicates low entrapment temperatures in some FIAs in Q3, late in the paragenesis. According to Goldstein (1993), large all-liquid inclusions indicate entrapment below about 50°C. Thus, at least some of the quartz likely precipitated at low temperature, perhaps less than 50°C, but relative timing of formation of these FIAs has been difficult to determine.

The identification of two-phase inclusions in FIAs with inconsistent vapor to liquid ratios is most likely due to heterogeneous entrapment, because necking down after a phase change has been discounted on the basis of the lack of petrographic pairing and a high percentage of gas in some areas. Other FIAs with consistent T_h suggest there has been little thermal reequilibration. Heterogeneous entrapment of an immiscible gas phase and liquid aqueous phase indicates that at times, the fluid system was saturated with gas. Thus, no pressure correction should be applied to homogenization temperatures and T_h should approximate temperature of entrapment (Goldstein and Reynolds, 1994).

The T_h data for Q1 indicate entrapment temperatures between 71 and 125°C, Q2 temperatures indicate entrapment between 99.4 and 135°C, Q3 temperatures indicate entrapment

between 150 and 156.8°C as well as below 50°C, and BD temperatures indicate entrapment between 102-157.7°C. Measured T_h data indicate the lowest temperature (71°C) during precipitation of Q1, although all-liquid fluid inclusions indicate the lowest temperature (50°C) during precipitation of Q3. The highest temperature of entrapment was recorded during precipitation of BD (157.7°C). Overall the T_h data increase through time with repeated rises and falls (Fig. 19). Measured $T_{m_{ice}}$ data indicate the lowest salinity fluid inclusions recorded during precipitation of Q2 (4.7 wt% NaCl equivalent) and the highest salinity fluid inclusions recorded during precipitation of Q3 (23.5 wt% NaCl equivalent). The bivariate plot of T_h versus $T_{m_{ice}}$ of all measured fluid inclusions indicates two clusters of data (Fig. 17C). One cluster (T1) has a T_h below 130°C and a $T_{m_{ice}}$ below -10°C and only contains data from Q1 and Q2. The other cluster (T2) has a T_h range around 130 to 150°C and a $T_{m_{ice}}$ between -15 and -20°C and only contains data from Q3 and BD.

The occurrences of MVT deposits, gangue minerals, epigenetic metal sulfides, and some petroleum throughout the midcontinent have been explained by hydrothermal fluids migrating out of the Arkoma Basin (Leach and Rowan, 1986; Sverjensky, 1986; Gregg and Shelton, 1989; Coveney, 1992; Wojcik et al., 1992; Byrnes and Lawson, 1999). Wojcik et al., (1992) estimated the maximum burial temperature expected for Mississippian and Pennsylvanian strata in the Cherokee Basin to be no more than 95°C, but found data indicative of higher temperatures. Present formation temperature at maximum depth of cores in this study (760 ft; 232 m) is ~21°C, assuming a mean annual surface temperature of 13°C (Barker et al., 1992). Given the current geothermal gradient of ~35°C/km (Kinney, 1976; Stavnes and Steeples, 1982) and additional peak burial of ~6,000 feet (1829 m; Merriam, 1963), normal maximum burial temperature was

more likely about 77°C. Some of the homogenization temperatures measured in this study exceed the maximum possible value for normal burial conditions. Therefore, either an elevated geothermal gradient or hydrothermal fluid must be invoked. The T_h data show repeated rises and falls in homogenization temperature, and this cannot be explained by elevated geothermal gradient. An elevated geothermal gradient would produce stagnant or steadily rising or falling temperature; therefore pulsed injection of hydrothermal fluid is the only reasonable explanation for elevated homogenization temperatures.

There are three possible scenarios to consider for explaining the fluid inclusion data. These scenarios must explain the overall range and temporal variability of T_h data, with repeated rises and fall of temperature, the lack of a correlation between T_h and $T_{m_{ice}}$, increasing temperature and increasing salinity through time, and the known stratigraphic and tectonic history of the area.

One possible explanation is the simplest one, that of a single event of injection of a hydrothermal fluid into the Mississippian section. This would lead to two-component mixing between a low temperature connate fluid (likely at low salinity and burial temperature of 77°C) and a high temperature hydrothermal fluid (likely at high salinity and temperature of at least 157.7°C, the highest T_h measured). Given, this scenario, T_h and $T_{m_{ice}}$ should be correlated. As such a correlation is lacking (Fig. 17C), this scenario is unlikely. In addition, this simple scenario would lead to progressive increase in temperature over time, rather than repeated rises and falls in T_h (Figs. 18, 19). Therefore, a simple two-component mixing model is disproven. Multiple times of mixing of multiple fluids of different temperatures and salinities still remains a

possibility. The repeated rises and falls in T_h indicate pulsed events of fluid flow. The configuration of the aquifer was likely complex and changed through time as the system fractured, leading to multiple sites of fluid mixing and multiple events of fluid injection.

The second scenario involves fluids discharged from the Arkoma basin at multiple times. First, connate basin fluids were discharged before Permian reflux, and then saline basin fluids discharged after Permian reflux (Fig. 20A). Before Permian reflux, the stratigraphic section in the pre-Permian Arkoma basin was buried to as much as 30,000-40,000 feet (9,144-12,192 m; Byrnes and Lawyer, 1999). Thus, there should be ample burial depth to provide a source for hot fluids. As most deep fluids were likely connate at this time, the source of fluids was likely lower in salinity than those that postdate Permian reflux, easily explaining the early phase of migration of low salinity (12.5 wt% NaCl equivalent), high temperature (130°C) hydrothermal fluids into the study area along migration pathways such as faults, the M-P unconformity, and the basal Cambrian sandstone (Fig. 20A1). During Permian time, cold saline brines generated through evaporative concentration at the surface could sink into the basin (Fig. 20A2), charging the deep part of the basin with higher salinity fluids. Evidence of Permian reflux in the Midcontinent supports the idea of charging of the basin with highly saline fluids (Anderson, 1989; Musgrove and Banner, 1993; Wojcik et al., 1993). It is possible that after the basin was charged with brines, they could be discharged northward during changes in hydrologic regime (Fig. 20A3), giving rise to the observed high salinity, high temperature hydrothermal fluids observed during the later phases of quartz cementation and during baroque dolomite precipitation (Fig. 17C; Fig. 18). On the basis of observed radiometric dates in the area (251 Ma, 165 Ma, 137 Ma, 67 Ma, 65 Ma, and 39 Ma; Brannon et al., 1996; Coveney et al., 2000; Blackburn et al., 2008), end Permian

events associated with the Alleghenian-Ouachita orogeny, Jurassic extension associated with formation of the Gulf of Mexico, Cretaceous-Tertiary Laramide orogeny, and later events remain possible.

The third scenario also involves fluids ejected from the Arkoma basin at multiple times, but from increasing depths as structures penetrated more deeply into the basin through time (Fig. 20B). Evidence for pulses of fluid flow, close association to fracturing, and regional evidence of Pennsylvanian-Permian timing for hydrothermal fluids (Gregg, 1985; Leach & Rowan, 1986; Shelton et al., 1986; Brannon et al., 1996) all support an idea that fluid flow could be tectonically valved during deformation of the Ouachita foreland (Arkoma basin). Consider that the stratigraphic section in the Pennsylvanian-Permian Arkoma basin was buried to as much as 30,000-40,000 feet (9,144-12,192 m; Byrnes and Lawyer, 1999) deep, allowing for basinal temperature to easily reach 130°C. As is observed in many basins (e.g. Dickey, 1969; Appold and Nunn, 2005), salinity of aqueous fluids tends to increase with depth. Structural deformation in the shallow section could form migration pathways allowing the lower temperature, lower salinity fluids to migrate northward (Fig. 20B1). Structural deformation of the deep section could form migration pathways allowing the higher temperature, higher salinity fluids to migrate northward (Fig. 20B2). Migration pathways northward could be along fracture zones, the altered strata near the top of the Mississippian section, altered strata near the top of the Arbuckle Group, or the basal Cambrian sandstone. If the Arkoma basin changed from earlier thin-skinned deformation to later thick-skinned deformation as it thickened and evolved structurally during the Pennsylvanian to Permian (e.g. Lawton, 1986) or if the basin evolved from syndepositional growth faults during Atokan time to later post-Desmoinesian regional folding and high angle

faulting (e.g. Byrnes and Lawyer, 1999), hydrothermal fluids would show an overall increase in temperature and salinity over time. As the system would be tectonically valved, one would expect evidence for rises and falls in temperature through time. This idea is consistent with increases in T_h and salinity observed in the hydrothermal system from the study area, and may indicate an overall tectonic driver for the fluid flow history.

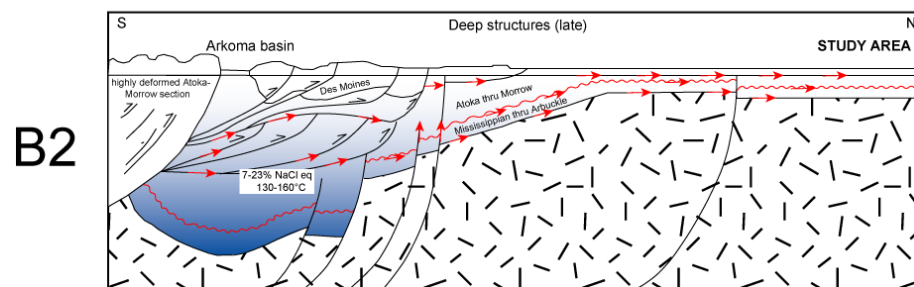
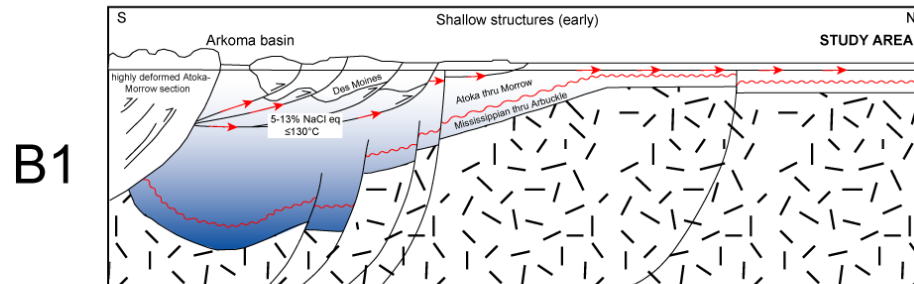
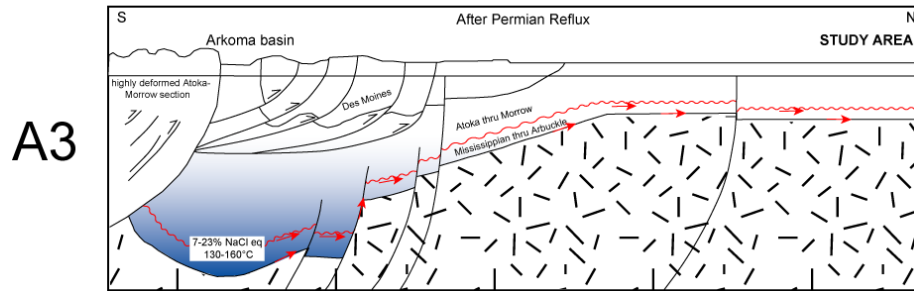
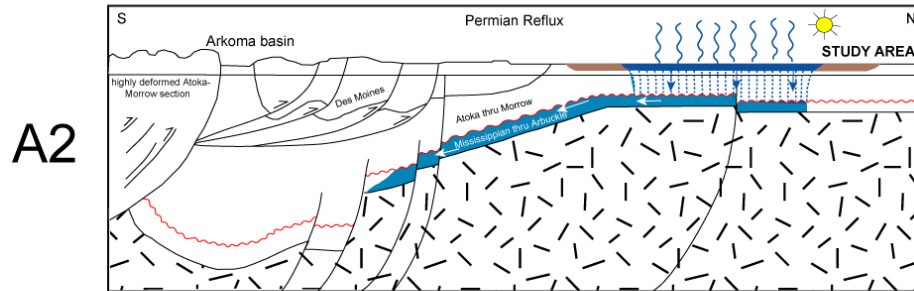
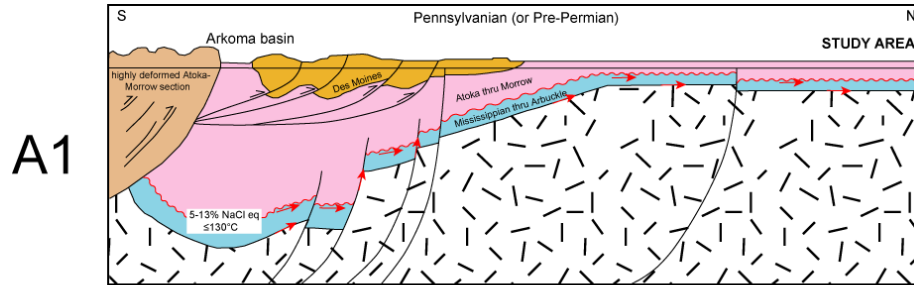


Figure 20. Schematic diagrams illustrating scenario two and three to explain homogenization and salinity data recorded in fluid inclusions. **A1)** Represents Pennsylvanian (or pre-Permian) time when connate subsurface brines were discharged out the Arkoma basin. Fluids (red arrows) migrate along conduits including faults, the M-P unconformity, and the base of the sedimentary section. This time period is represented by fluid inclusions recorded during T1 (Fig. 17C). **A2)** Represents Permian time when sea water was evaporating and charged the basin with evaporitic brines. The basin was experiencing subsequent burial and thickness of the sedimentary package was increasing. **A3)** Represents time after Permian reflux when the salinity stratified basin experienced subsequent burial and evaporitic brines residing in the deep basin were remobilized. This time period is represented by fluid inclusions recorded during T2 (Fig. 17C). **B1)** Represents time in the early stages of tectonism when thrust sheets penetrated the upper section of the Paleozoic strata. Thrust sheets provided conduits for connate subsurface brines to migrate out of the salinity stratified basin. This time period is represented by fluid inclusions recorded during T1 (Fig. 17C). **B2)** Represents time during later stages of tectonism when thrust sheets penetrated deeper into the Paleozoic strata. This allowed discharge of hotter and more saline brines from the deep basin northward onto the platform. This time period is represented by fluid inclusion recorded during T2 (Fig. 17C). Basin configuration is modified from Branan (1987).

Subaerial Versus Hydrothermal Porosity Enhancement in Chert

It has been suggested that the enhancement of porosity and permeability in Mississippian siliceous facies in the mid-continent, especially in ramp margin locations where the accumulations are thick, is due to subaerial exposure and weathering under meteoric diagenetic conditions associated with unconformities, especially the Mississippian-Pennsylvanian unconformity (Duren, 1960; Euwer, 1965; Thomas, 1982; Rogers et al., 1995; Montgomery et al., 1998; Watney et al., 2001; Mazzullo et al., 2009). When assessing the timing of silica dissolution and its close association with precipitation of megaquartz and baroque dolomite (Fig. 12) it is difficult to consider subaerial exposure, weathering, and karsting as the only origin for enhanced porosity. The observations summarized in the Diagenesis section show that subaerial exposure must be a contributor. There is a close association between microporosity in chert facies immediately below the Mississippian-Pennsylvanian unconformity. In the cores studied, the most porous chert facies (tripolitic chert) is found in the stratigraphic interval from the Mississippian-Pennsylvanian unconformity to no more than 75 feet (23 m) below it. However, other porous chert facies extend more deeply. The two possible subaerial exposure surfaces identified in Genetic Unit 2 appear to have had little effect on the formation of porosity in chert, as porosity in chert is not enhanced immediately below them. Subaerial exposure associated with these unconformities did create some enhanced porosity in limestone facies, however, with some dissolved material in limestone clasts, microkarst, and minor collapse breccia porosity.

Tripolitic chert is concentrated in sponge-spicule packstone facies. The skeleton of a living siliceous sponge is opal-A, an amorphous and hydrated silica phase (Simpson, 1984). Studies have shown that the opal-A in siliceous sponges is unstable, can be quickly dissolved,

and the silica redistributed to other sediment, even in full marine conditions (Land, 1976; Knauth, 1979; Hein and Parrish, 1987; Jones and Murchey, 1986). Studies of chert occurrences in the Paleozoic have documented an early diagenetic stage of silica cementation and replacement from dissolution of siliceous sponges (e.g. Bissell, 1959; Carlson, 1994; Cavoroc and Ferm, 1968; Meyers, 1977; Geeslin and Chafetz, 1982; Maliva and Siever, 1989; Ruppel and Hovorka, 1995), including studies of Mississippian rocks in Kansas (Franseen, 2006; Montgomery et al., 2000; Watney et al., 2001). Results of my study also show an early diagenetic event of dissolution of sponge spicules (thereby leaving molds) and redistribution of silica as evidenced by silicification of original lime-mud material and calcitic fossils.

Cross-cutting relationships show that much of the porosity in tripolitic chert and other porous chert facies is early, in that it predates compaction and subaerial exposure (e.g., Fig. 6B). This is observed by porous rims around chert nodules cross-cut by fractures where the fractures were filled with marine-carbonate sediment. This is evidence that the porous rims must have formed before burial-related compactional fracturing and before lithification of some carbonate sediment (Fig. 6B). Subsequent dissolution through subaerial exposure and/or hydrothermal processes are important for modifying porosity and creating tripolitic chert. My study indicates that hydrothermal processes are important, in addition to subaerial exposure processes. Understanding the vertical and lateral distribution of tripolitic chert in relation to subaerial exposure surfaces, faults, fractures, other structural elements, can aid in distinguishing between the processes and may result in better predictive capabilities.

Early porosity enhancement extends below the tripolitic chert (upper 75 feet (23 m), and can be found as much as 100 feet (30 m) below the Mississippian-Pennsylvanian unconformity. The most likely explanation for early formation of porosity in chert, and distribution of the most porous chert facies immediately below the Mississippian-Pennsylvanian unconformity, indicates that subaerial weathering during formation of the Mississippian-Pennsylvanian unconformity was important in localizing porosity in chert. Although its effects were concentrated in the uppermost 75 feet (23 m), alteration extended to 100 feet (30 m) below the unconformity.

My study also reveals that there is a late dissolution stage that further enhances porosity in silica (Fig. 12). Dissolution of cryptocrystalline silica, sponge-spicules, and remaining calcitic bioclasts is closely associated with the influx of hydrothermal fluids. The later dissolution occurs in stage 17 (Fig. 12). Thus it is after burial and after the precipitation of megaquartz, which generated T_h data indicative of hydrothermal fluid flow. Late porosity enhancement in chert is concentrated in PM-17 from 440-400 ft, PM-12 from 505-525 ft, PM-21 from 450-480 ft, and in PM-8 from 385-392 ft and 445-470 ft (Fig. 8). Evidence for late porosity enhancement is found up to 120 feet (36 m) below the Mississippian-Pennsylvanian unconformity, and thus, is unlikely to be related to weathering. Although evidence of late silica dissolution is observed directly underlying the Mississippian-Pennsylvanian unconformity, late dissolution associated with hydrothermal fluids is found up to 120 feet (37 m) below the unconformity.

There is no quantitative measure of how much porosity is created by silica dissolution during subaerial exposure or hydrothermal fluid flow, as they are difficult to distinguish from one another in some areas. The porosity enhancement created during subaerial exposure and hydrothermal fluid flow overlap a sizeable amount of the stratigraphic interval covered in the

study area. However, it appears that hydrothermal fluid flow, focused by late faulting and fractures, may have exerted a major control on the porous cherts. For example, the two cores to the northeast contain 55% chert (by thickness) and the two cores to the southwest have only 37% chert. As discussed earlier, the abundance of chert is likely controlled by depositional environment, and in this case, the more updip cores in a location of upwelling contain the most chert. If porosity in cherts were solely related to duration and intensity of subaerial weathering along unconformities, one would predict that the updip (northeast) cores would preserve the highest amounts of porous as opposed to tight chert. On the contrary, although chert is less abundant in the southwest locations, the percent of that chert that is porous is higher to the southwest (32%) and lower (25%) to the northeast (Fig. 8). This supports the idea that much of the porosity in the cherts is not related to subaerial weathering, and thus, is related to late processes during hydrothermal fluid flow. A fault mapped in Precambrian rocks, immediately below the southwest cores could provide an explanation for why the southwest cores developed better porosity in cherts during hydrothermal fluid flow. If the mapped fault provided a zone of weakness that led to post Mississippian fracturing and faulting this could have created a preferred conduit for hydrothermal fluids that enhanced porosity (e.g. Blair et al., 1992).

Evidence of deformation within the Arkoma basin has been documented for several time periods; mid-Desmoinesian (Dane et al., 1938), Permian (Melton, 1930), Mississippian and Morrowan (Houseknecht, 1981), and Atokan (Underwood and Viele, 1985). Some studies recognize contemporaneous structural deformation with spicule-rich deposition, creating favorable bottom topography for spicule accumulation (Watney et al., 2001; Watney et al., 2008; Boardman et al., 2010), so the first structural creation of conduits for fluid flow may have began

during the Osagean-Meramecian. It is likely that faults and fractures provided the opportunity for cross-formational flow. Complex vitrinite reflectance versus depth profiles have been explained by a model involving hydrothermal fluid migration up faults and away from the Ouachita orogenic belt along diverse flow paths directed by permeability orientations of different facies (Houseknecht et al., 1992). Among the stratigraphic units that are likely pathways for lateral fluid migration are the Regan/Lamotte sandstone, altered and karsted zones in the Arbuckle Group, Simpson Group sands, and the altered zone immediately below the Mississippian-Pennsylvanian unconformity. Alteration below unconformities provides, directly or indirectly, porous and permeable plumbing systems for circulation of fluids (Mills and Eyrich, 1966), which would have allowed for the migration of hydrothermal fluid. In the tri-state area, MVT mineralization is concentrated along the top of the Mississippian section (Wojcik et al., 1992; Wojcik et al., 1994; Wojcik et al., 1997; Watney et al., 2008). The Pennsylvanian section is relatively shale-rich, and therefore more of an aquitard. In such a scenario, upward migration of hot, hydrothermal fluids would preferentially flow along the top of the Mississippian section. Stratigraphic variation in vitrinite reflectance values from Pennsylvanian strata of southeastern Kansas show that anomalously high vitrinite values are located in close stratigraphic proximity to the sub-Pennsylvanian unconformity. As the sub-Pennsylvanian unconformity is a regional paleokarst, it acted as a regional stratigraphic conduit for hydrothermal fluid flow. The Pennsylvanian section, however, acted as a leaky confining unit (Barker et al. 1992; Walton et al. 1995).

Localization of Best Reservoir Facies

Localization of the optimal reservoir porosity requires a depositional environment conducive to deposition of spicules and formation of chert. As has been discussed, the setting is on the proximal slope or break in slope of a distally steepened ramp, where upwelling has occurred. Chert forms best in genetic units where relative sea level is high, and not where it is relatively low in relation to upwelling that is most active during transgression (Lane and DeKeyser, 1980; Gutschick and Sandberg, 1983; Lumsden, 1988; Wright, 1991; Lasemi et al., 1998, 2003; Franseen, 2006; Mazzullo et al., 2009). A combination of both subaerial exposure and hydrothermal fluid migration may be the best explanation for enhancing the porosity in chert. Thus, the system must be high enough on the ramp to have experienced subaerial exposure along the sub-Pennsylvanian unconformity. A more basinward position would result in a lower duration of subaerial exposure, and thus, less porosity in chert. Subaerial exposure surfaces are well-known in effecting porosity and permeability in carbonate systems (Read and Horbury, 1993; Saller et al., 1994; Budd et al., 1995; Wagner et al., 1995). With this model in mind, there should be a relatively narrow, distally steepened ramp margin to slope, where reservoirs of this sort are possible. The very best reservoirs are predicted to lie in this narrow setting, but specifically in areas where fractures and faults led to preferred hydrothermal fluid flow into the Mississippian section.

CONCLUSIONS

Lithofacies described in this study include echinoderm-rich-bioclastic wacke-packstone, sponge-spicule-rich packstone, dolomitic bioclastic wackestone, argillaceous wackestone, tripolitic chert, variable chert breccias, ooid packstone, and dark shale. Lithofacies represent a

depositional range from quiet-water, low energy, subtidal environment below fair weather wave base to shallow subtidal, fair weather wave base with storm-influenced settings marked by intermittent high energy. These environments likely represent deposition along inner, middle, marginal, and outer portions of ramp environments.

Facies associated with chert-reservoir rocks in this area contain various amounts of sponge-spicules and bioclasts in packstone fabrics. Sponge-spicule accumulations are attributed to upwelling nutrient-rich waters in a distal-ramp setting, leading to localization of chert accumulations.

Three genetic units are represented in the four cores of the study area. Genetic Unit 1 contains eight high-frequency sequences reflecting relative fluctuations (including falls) in sea level. On the basis of lithofacies, each sequence represents shallowing upward from a quiet-water, low-energy, subtidal environment below fair-weather wave base to shallow subtidal, fair-weather wave base settings (influenced by storms). These environments most likely represent a depositional range from an outer ramp environment shallowing upward to middle and marginal ramp environments. Unit 1 geometries indicate shallow water deposition to the southwest which is different than the overlying units.

Genetic Unit 2 is deposited after a major deepening event and consists of interbedded argillaceous wackestone and brecciated chert facies that thin, pinch-out, and downlap to the southwest. The interbedded argillaceous wackestone and brecciated chert facies are interpreted as a subtidal, deep-water, outer-ramp environment. There are two possible subaerial exposure surfaces in Unit 2 as seen by dissolution features, microkarst, in-situ breccia, partially dissolved

and reworked clasts likely indicating relative sea-level falls. Argillaceous wackestone grades upward into echinoderm-rich bioclastic wacke-packstone and is interpreted to represent an overall shoaling in association with a relative sea-level fall or depositional shallowing. The upper succession of Unit 2 is interpreted to represent moderate to high energy, shallow-water ramp deposits.

The base of Genetic Unit 3 is a laterally continuous interval of ooid packstone, interpreted to be the equivalent to the Short Creek Oolite, which indicates deposition during a relative sea-level lowstand as indicated by regional studies. It is overlain by echinoderm-rich bioclastic wacke-packstone interpreted to represent deepening. The echinoderm-rich bioclastic wacke-packstone is overlain by argillaceous wackestone in the southwest locations indicating a marine-flooding surface. The southwest locations are thought to represent the deeper-water, outer-ramp environment and shallower water to the northeast. The stratigraphic interval proximal to the Mississippian-Pennsylvanian unconformity is a series of chert breccias and tripolitic chert with minor amounts of echinoderm-rich bioclastic wacke-packstone facies. Effects of this major subaerial exposure event are seen by the extensive diagenetic overprint proximal to this surface.

The paragenetic sequence consists of 22 major stages. Dissolution of silica occurs in stage 6 or 7 and stage 17 which are most pertinent for porosity development in chert. Petrography reveals early silicification (stage 4) and chalcedony (stage 10) filling primary intergranular pore space that predates compaction. Karsting under subaerial conditions created vugs and cave structures resulting in a series of solution collapse breccias. There is a stage of

post-burial dissolution of calcitic fossil fragments (stage 15), which also affected the chert facies. Of the two silica dissolution events, the later event is closely associated with precipitation of megaquartz and baroque dolomite and the earlier one is related to subaerial weathering along the sub-Pennsylvanian unconformity. Fluid inclusion microthermometry conducted on diagenetic megaquartz and baroque dolomite reveals homogenization temperatures between 70-160°C, which exceed the value for normal burial conditions. Salinity increased over time. Fluid inclusions assist the interpretation that hydrothermal fluids migrated through these rocks in preferred conduits for fluid flow, such as fractures in association with faults and immediately below unconformity surfaces. There are three scenarios to explain hydrothermal fluid migration as recorded by fluid inclusions; the first model is two-component mixing, the second model is discharge of connate fluids followed by Permian reflux and then hydrothermal discharge, and the third model invokes shallow structures tapping shallow fluids followed by deep structures tapping deep fluids. In addition to karstification and weathering along the Mississippian-Pennsylvanian unconformity, hydrothermal fluids are responsible for porosity enhancement.

Understanding structural and stratigraphic controls on fluid flow can assist in exploitation of chert reservoirs. The best reservoirs require a depositional environment conducive to deposition of spicules and formation of chert, and a combination of both subaerial exposure and hydrothermal fluid migration for enhancing the porosity in chert in areas where fractures and faults led to preferred hydrothermal fluid flow.

REFERENCES CITED

- Abegg, F.E., 1992, Lithostratigraphy, depositional environments, and sequence stratigraphy of the St. Louis and Ste. Genevieve Limestones (Upper Mississippian), southwestern Kansas: Ph.D. Dissertation, The University of Kansas, Lawrence, Kansas.
- Anderson, J.E., 1989, Diagenesis of the Lansing and Kansas City Groups (Upper Pennsylvanian), northwestern Kansas and southwestern Nebraska: Master's thesis, The University of Kansas, Lawrence, Kansas.
- Appold, M.S., and J.A. Nunn, 2005, Hydrology of the western Arkoma basin and Ozark platform during the Ouachita orogeny: implications for Mississippi Valley-type ore formation in the Tri-State Zn-Pb district: *Geofluids*, v. 5, p.308-325.
- Baars, D.L., and W.L. Watney, 1991, Paleotectonic control on reservoir facies, *in* E.K. Franseen, W.L. Watney, C.G.St.C. Kendall, and W. Ross, eds., *Sedimentary modeling-computer simulations and methods for improved parameter definition*: Kansas Geological Survey, Bulletin 233, p. 253-262.
- Ball, M.M., 1967, Carbonate Sand Bodies of Florida and the Bahamas: *Journal of Sedimentary Petrology*, v. 37, p. 556-571.
- Banner, J.L., G.N. Hanson, and W.J. Meyers, 1988a, Rare earth element and Nd isotopic variations in regionally extensive dolomites from the Burlington-Keokuk Formation (Mississippian): Implications for REE mobility during carbonate diagenesis: *Journal of Sedimentary Petrology*, v. 58, no. 3, p. 415-432.
- Banner, J.L., G.N. Hanson, and W.J. Meyers, 1988b, Determination of initial Sr isotopic compositions of dolostones from the Burlington-Keokuk Formation (Mississippian): Constraints from cathodoluminescence, glauconite paragenesis and analytical methods: *Journal of Sedimentary Petrology*, v. 58, no. 4, p. 673-687.
- Barker, C.E., R.H. Goldstein, J.R. Hatch, A.W. Walton, and K.M. Wojcik, 1992, Burial history and thermal maturation of Pennsylvanian rocks, Cherokee basin, southeastern Kansas, *in* K.S. Johnson and B.J. Cardott, eds., *Source Rocks in the Southern Midcontinent, 1990 Symposium*: Oklahoma Geological Survey Circular 93, p. 133-143.
- Bartberger, C.E., T.S. Dyman, and S.A. Cook, 2001, Solution-subsidence origin, architecture, and hydrocarbon-trapping mechanisms of basal-Pennsylvanian Morrow fluvial valleys, southwest Kansas: AAPG National Meeting, Denver, CO.
- Bathurst, R.G.C., 1975, Carbonate sediments and their diagenesis: *Developments in Sedimentology 12*: New York, Elsevier, 658 p.

- Bissell, H.J., 1959, Silica in sediments of the upper Paleozoic of the Cordilleran area, *in* H.A. Iredland, ed., *Silica in sediments: Society of Economic Paleontologists and Mineralogists Special Publication 7*, p. 150-185.
- Blackburn, T.J., D.F. Stockli, R.W. Carlson, and P. Berendsen, 2008, (U-Th)/He dating of kimberlites- A case study from north-eastern Kansas: *Earth and Planetary Science Letters*, v. 275, p. 111-120.
- Blair, K.P., P. Berendsen, and C.M. Seeger, 1992, Structure-contour maps on the top of the Mississippian carbonates and on the top of the Upper Cambrian and Lower Ordovician Arbuckle Group, Joplin 1° X 2° Quadrangle, Kansas and Missouri: *Kansas Geological Survey and Missouri Department of Natural Resources, Division of Geology and Land Survey, Miscellaneous Field Study Map MF-2125-C*, scale 1:250,000.
- Boardman, D.R., S.J. Mazzullo, and B.W. Wilhite, 2010, Lithostratigraphy and conodont biostratigraphy of the Kinderhookian to Osagean Series in SW Missouri, NW Arkansas, and NE Oklahoma: *Geological Society of America Field Guide for Joint North-Central and South-Central Meeting, Branson, MO*.
- Bodnar, R.J., 1992, Revised equation and table for freezing point depressions of H₂O-salt fluid inclusions (Abstract): *PACROFI IV, Fourth Biennial Pan-American Conference on Research on Fluid Inclusions, Program and Abstracts, Lake Arrowhead, CA*, v. 14, p. 15.
- Branan, C.B.Jr., 1987, Natural gas in Arkoma basin of Oklahoma and Arkansas: *AAPG Memoir 9*, v. 2, p. 1616-1635.
- Brannon, J.C., S.C. Cole, F.A. Podosek, V.M. Ragan, R.M. Jr. Coveney, M.W. Wallace, and A.J. Bradley, 1996, Th-Pb and U-Pb dating of ore-stage calcite and Paleozoic fluid flow: *Science*, v. 271, p. 491-493.
- Budd, D.A., A.H. Saller, and P.M. Harris, 1995, Unconformities and porosity in carbonate strata: *AAPG Memoir 63*, 313 p.
- Byrnes, A., and G. Lawyer, 1999, Burial, maturation, and petroleum generation history of the Arkoma Basin and Ouachita Foldbelt, Oklahoma and Arkansas: *Natural Resources Research*, v. 8, no. 1, p. 3-26.
- Carlson, E.H., 1994, Paleoshoreline patterns in the transgressive-regressive sequences of Pennsylvanian rocks in the northern Appalachian basin, U.S.A.: *Sedimentary Geology*, v. 93, p. 209- 222.
- Cavoroc, V. V., Jr., and Ferm, J. C., 1968, Siliceous spiculites as shoreline indicators in deltaic sequences: *Geological Society of America, Bulletin*, v. 79, p. 263-272.

- Choquette, P.W., A. Cox, and W.J. Meyers, 1992, Characteristics, distribution and origin of porosity in shelf dolostones: Burlington-Keokuk Formation (Mississippian), U.S. Midcontinent: *Journal of Sedimentary Petrology*, v. 62, no. 2, p.167-189.
- Colleary, W.M., E.D. Dolly, M.W. Longman, and J.C. Mullarkey, 1997, Hydrocarbon production from low resistivity chert and carbonate reservoirs in the Mississippian of Kansas: AAPG, Rocky Mountain Section Meeting, Program Book and Expanded Abstracts Volume, p. 47-51.
- Coveney, R.M.Jr., 1992, Evidence for expulsion of hydrothermal fluids and hydrocarbons in the Midcontinent during the Pennsylvanian, *in* K.S. Johnson and B.J. Cardott, eds., *Source Rocks in the Southern Midcontinent, 1990 Symposium: Oklahoma Geological Survey Circular 93*, p. 133-143.
- Coveney, R.M.Jr., 1999, Contributions from migrating oil-field brines to Carboniferous beds in the U.S. Midwest, *in* D.F. Merriam ed., *Geoscience for the 21st Century: AAPG Midcontinent Section Meeting*, p. 29-34.
- Coveney, R.M.Jr., V.M. Ragan, and J.C. Brannon, 2000, Temporal benchmarks for modeling Phanerozoic flow of basinal brines and hydrocarbons in the southern Midcontinent based on radiometrically dated calcite: *Geology*, v. 28, no. 9, p. 795-798.
- D'Argenio, B., V. Ferreri, S. Amodio, and N. Pelosi, 1997, Hierarchy of high-frequency orbital cycles in Cretaceous carbonate platform strata: *Sedimentary Geology*, v. 113, p. 169-193.
- Dane, C.H., H.E. Rothrock, and J.S. Williams, 1938, Geology and fuel resources of the southern part of the Oklahoma coal field, Part 3: Quinto-Scipro district: *USGS Bulletin*, 871-C, p. 151-253.
- Dickey, P.A., 1969, Increasing concentration of subsurface brines with depth: *Chemical Geology*, v. 4, no. 1-2, p. 361-370.
- Dickson, J.A.D., 1966, Carbonate identification and genesis as revealed by staining: *Journal of Sedimentary Petrology*, v. 36, no.2, p. 491-505.
- Dunham, R.J., 1962, Classification of carbonate rocks according to depositional texture, *in* W.E. Ham, ed., *Classification of carbonate rocks- A Symposium: AAPG Memoir 1*, p. 108-121.
- Duren, J.D., 1960, Some petrophysical aspects of the Mississippian "chat", Glick field, Kiowa County, Kansas: *Shale Shaker*, v. 11, p. 2-8.

- Elrick, M. and J.F. Read, 1991, Cyclic ramp-to-basin carbonate deposits, lower Mississippian, Wyoming and Montana: A combined field and computer modeling study: *Journal of Sedimentary Petrology*, v. 61, no. 7, p. 1194-1224.
- Euwer, R. M., 1965, Glick field, *in* P. M. Gerlach and T. Hansen, eds., *Kansas oil and gas fields: Wichita*, Kansas Geological Society, v. 4, p. 88-94.
- Franseen, E.K., 1999, Controls on Osagean-Meramecian (Mississippian) ramp development in central Kansas: Implications for Paleogeography and Paleooceanography: *Kansas Geological Survey, Open-File Report 99-50*.
- Franseen, E.K., 2006, Mississippian (Osagean) Shallow-water, mid-latitude siliceous sponge spicule and heterozoan carbonate facies: An example from Kansas with implications for regional controls and distribution of potential reservoir facies: *Current Research in Earth Sciences Bulletin 252*, part 1.
- Gammon, P.R., N.P. James, and A. Pisera, 2000, Eocene spiculites and spongolites in southwestern Australia-Not deep, not polar, but shallow and warm: *Geology*, v. 28, p. 855-858.
- Geeslin, J.H., and H.S. Chafetz, 1982, Ordovician Aleman ribbon cherts; An example of silicification prior to carbonate lithification: *Journal of Sedimentary Petrology*, v. 52, p. 1,283-1,293.
- Goldstein, R.H., 1993, Fluid inclusions as microfibrils: a petrographic method to determine diagenetic history, *in* R. Rezak and D. Lavoie, eds., *Carbonate Microfibrils, Frontiers in Sedimentary Geology*: New York, Springer-Verlag, p. 279-290.
- Goldstein, R.H., and T.J. Reynolds, 1994, Systematics of fluid inclusions in diagenetic minerals: *SEPM Short Course 31*, SEPM, Tulsa, OK.
- Goldstein, R.H., 2003, Ch. 2: Petrographic analysis of fluid inclusions, *in* I. Samson, A. Anderson, and D. Marshall, eds., *Fluid Inclusions: Analysis and Interpretation*, Mineralogical Association of Canada Short Course 32, p. 9-53.
- Gordon, M. Jr., 1964, Carboniferous Cephalopods of Arkansas: *U.S. Geological Survey Professional Paper 460*, p. 322.
- Gregg, J.M., 1985, Regional epigenetic dolomitization in the Bonnetterre Dolomite (Cambrian), southeastern Missouri: *Geology*, vol. 13, p. 503-506.
- Gregg, J.M. and K.L. Shelton, 1989, Geochemical and petrographic evidence for fluid sources and pathways during dolomitization and lead-zinc mineralization in southeast Missouri: A review: *Carbonates and Evaporites*, vol. 4, p. 153-175.

- Gutschick, R.C., and C.A. Sandberg, 1983, Mississippian continental margins of the conterminous United States, *in* D.J. Stanley and G.T. Moore, eds., *The shelfbreak: Critical interface on continental margins*: SEPM Special Publication 33, p. 79–96.
- Handford, C.R., and W.L Manger, 1993, Sequence stratigraphy of a Mississippian carbonate ramp, north Arkansas and southwestern Missouri: AAPG Field Guide for 1993 Annual Convention.
- Hardie, L.A., and R.N. Ginsburg, 1977, Layering: the origin and environmental significance of lamination and thin bedding, *in* L.A. Hardie, ed., *Sedimentation on the modern carbonate tidal flats of Northwest Andros Island, Bahamas*: John Hopkins University Press, Baltimore, p. 50-123.
- Harris, P.M., 1979, Facies anatomy and diagenesis of a Bahamian ooid shoal, *in* R.N. Ginsburg, ed., *Sedimenta VII: The Comparative Sedimentology Laboratory*, Division of Marine Geology and Geophysics, University of Miami, Rosenstiel School of Marine & Atmospheric Science, Miami, Florida, 163 p.
- Heckel, P.H., 1972, Recognition of ancient shallow water marine environments, *in* J.K. Rigby, and W.K. Hamblin, eds., *Recognition of Ancient Sedimentary Environments*: Society of Economic Paleontologists and Mineralogists, Special Publication, No. 16, p. 226-286.
- Heckel, P.H., 1977, Origin of phosphatic black shale facies in Pennsylvanian cyclothems of mid-continent North America: AAPG Bulletin, v. 61, no. 7, p. 1045-1068.
- Hein J.R., and J.T. Parrish, 1987, Distribution of siliceous deposits in space and time, *in* J.R. Hein ed., *Siliceous sedimentary rock-hosted ores and petroleum*: New York, Van Nostrand Reinhold Co., p. 10– 57.
- Houseknecht, D.W., 1981, Tectonic influence on foreland basin sedimentation: The Hartshorne Formation of the Arkoma Basin: Geological Society of America Abstracts with Programs, 13, p. 476.
- Houseknecht, D.W., L.A. Hathon, and T.A. McGilvery, 1992, Thermal maturity and Paleozoic strata in the Arkoma Basin: Oklahoma Geological Survey Circular 93, p. 122-132.
- Inden, R.F. and C.H. Moore, 1983, Ch. 5: Beach Environment, *in* P.A. Scholle, D.G. Bebout, and C.H. Moore, eds., *Carbonate Depositional Environments*, AAPG Memoir 33, p. 212-264.
- James, N.P., 1997, The cool-water carbonate depositional realm, *in* N.P. James and J.A.D. Clarke, eds., *Cool-Water Carbonates*, SEPM Special Publication 56, p. 1-22.
- Jones, D.L., and B. Murchey, 1986, Geologic significance of Paleozoic and Mesozoic radiolarian chert: Annual Review of Earth and Planetary Sciences, v. 14, p. 455-492.

- Johnson, R.A., and D.A. Budd, 1994, The utility of continual reservoir description—An example from Bindley field, western Kansas: AAPG Bulletin, v. 78, p.722-743.
- Katz, A., and A. Matthews, 1977, The dolomitization of CaCO₃; an experimental study at 252-295°C: *Geochimica et Cosmochimica Acta*, v. 41, p. 297-308.
- Kerans, Charles, 1989, Karst-controlled reservoir heterogeneity and an example from the Ellenburger Group (Lower Ordovician) of West Texas: The University of Texas at Austin, Bureau of Economic Geology Report of Investigations No. 186, 40 p.
- Kerans, Charles, 1990, Depositional systems and karst geology of the Ellenburger Group (Lower Ordovician), subsurface West Texas: The University of Texas at Austin, Bureau of Economic Geology Report of Investigations No. 193, 63 p.
- Kinney, D.M., 1976, Geothermal gradient map of North America: AAPG and U.S. Geological Survey, scale 1:5,000,000.
- Knauth, L.P., 1979, A model for the origin of chert in limestone: *Geology*, v. 7, p. 274-277.
- Land, L.S., 1976, Early dissolution of sponge spicules from reef sediments, North Jamaica: *Journal of Sedimentary Petrology*, v. 46, p. 967-969.
- Lane, H.R., 1978, The Burlington shelf (Mississippian, north-central United States): *Geologica et Paleontologica*, v. 12, p. 165-176.
- Lane, H.R., and T.L. De Keyser, 1980, Paleogeography of the late Early Mississippian (Tournaisian 3) in the central and south-western United States, *in* T.D. Fouch and E.R. Magathan, eds., *Paleozoic Paleogeography of west-central United States: Rocky Mountain Section SEPM*, p. 149-159.
- Lange, J.P., 2003, Stratigraphy, depositional environments and coalbed methane resources of Cherokee Group coals (Middle Pennsylvanian)-Southeastern Kansas: Kansas Geological Survey, Open-File Report, 2003-82.
- Lasemi, Z., R.D. Norby, and J.D. Treworgy, 1998, Depositional facies and sequence stratigraphy of a Lower Carboniferous bryozoan-crinoidal carbonate ramp in the Illinois Basin, midcontinent U.S.A., *in* V. P. Wright and T. P. Burchette, eds., *Carbonate ramps: Geological Society Special Publication 149*, p. 369–395.
- Lawton, T.F., 1986, Fluvial systems of the Upper Cretaceous Mesaverde Group and Paleocene North Horn Formation, Central Utah: A record of transition from thin-skinned to thick-skinned deformation in the foreland region: Part III. Middle Rocky Mountains, AAPG Special Publication Paleotectonics and Sedimentation in the Rocky Mountain Region, United States, vol. M41, p. 423-442

- Leach, D.L. and E.L. Rowan, 1986, Genetic link between Ouachita foldbelt tectonism and the Mississippi valley-type lead-zinc deposits of the Ozarks: *Geology*, v. 14, no. 11, p. 931-935.
- Loucks, R.G., Handford C.R., 1992, Origin and recognition of fractures, breccias and sediment fills in paleocave-reservoir networks, *in* M.P. Candelaria and C.L. Reed, eds., Paleokarst, karst related diagenesis and reservoir development: examples from Ordovician-Devonian age strata of west Texas and the mid-continent Permian Basin Section, SEPM Publication 92-33, p. 31-44.
- Luebking, G.A., M.W. Longman, and W.J. Carlisle, 2001, Unconformity-related chert/dolomite production in the Pennsylvanian Amsden Formation, Wolf Springs fields, Bull Mountains basin of central Montana: *AAPG Bulletin*, v. 85, no.1, p. 131-148.
- Lumsden, D.N., 1988, Origin of the Fort Payne Formation (Lower Mississippian), Tennessee: *Southeastern Geology*, v. 28, p. 167-180.
- Maliva, R.G., and R. Siever, 1989, Nodular chert formation in carbonate rocks: *Journal of Geology*, v. 97, p. 421-433.
- Maples, C.G., 1994, Revision of Mississippian stratigraphic nomenclature in Kansas, *in* D.L. Baars, ed., Revision of stratigraphic nomenclature in Kansas: Kansas Geological Survey Bulletin 230, p. 67-74.
- Mazzullo, S.J., B.W. Wilhite, and I.W. Woolsey, 2009, Petroleum reservoirs within a spiculite-dominated depositional sequence: Cowley Formation (Mississippian: Lower Carboniferous), south-central Kansas: *AAPG Bulletin*, v. 93, no.12, p.1649-1689.
- Melton, F.A., 1930, Age of the Ouachita orogeny and its tectonic effects: *AAPG Bulletin*, v.14, p. 57-72.
- Merriam, D.F., 1963, The Geologic History of Kansas, Kansas Geological Survey Bulletin 162, p. 135-144 &165-169.
- Meyers, W.J., 1974, Carbonate cement stratigraphy of the Lake Valley Formation (Mississippian) Sacramento Mountains, New Mexico: *Journal of Sedimentary Petrology*, v. 44, p. 837-861.
- Meyers, W.J., 1977, Chertification in the Mississippian Lake Valley Formation, Sacramento Mountains, New Mexico: *Sedimentology*, v. 24, p. 75-105.
- Mills, J.W., and H.T. Eyrich, 1966, The role of unconformities in the localization of epigenetic mineral deposits in the United States and Canada: *Economic Geology*, vol. 61, p. 1232-1257.

























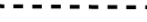











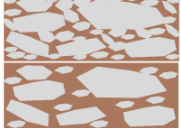
- Montgomery, S.L., J.C. Mullarkey, M.W. Longman, W.M. Colleary, and J.P. Rogers, 1998, Mississippian “chat” reservoirs, south Kansas-Low-resistivity pay in a complex chert reservoir: AAPG Bulletin, v. 82, p. 187-205.
- Musgrove, M.L., and J.L. Banner, 1993, Regional ground-water mixing and the origin of saline fluids: Midcontinent, United States: Science, vol. 259, no. 5103, p. 1877-1882.
- Newell, N.D., E.G. Purdy, and J. Imbrie, 1960, Bahamian oolitic sand: Journal of Geology, v. 68, p. 481-497.
- Packard, J.J., I. Al-Asam, I. Samson, Z. Berger, and J. Davies, 2001, A Devonian hydrothermal chert reservoir: the 225 bcf Parkland field, British Columbia, Canada: AAPG Bulletin, v. 85, no.1, p. 51-81.
- Peeler, J.A., 1985, Reservoir characterization of the Mississippian “chat”, Hardtner field, southern Barber County, Kansas: Master’s thesis, Wichita State University, Wichita, Kansas, p. 132.
- Pettijohn, F.J., 1975, Sedimentary Rocks (3rd edition); Harper & Row, New York, 628 p.
- Purdy, E.G., 1961, Bahamian oolite shoals, *in* J.A. Peterson and J.C. Osmond, eds., Geometry of sandstone bodies: AAPG, Tulsa, OK, p. 53-62.
- Purser, B.H. and E. Seibold, 1973, The principal environmental factors influencing Holocene sedimentation and diagenesis in the Persian Gulf, *in* B.H. Purser, ed., The Persian Gulf: New York, Springer-Verlag, p. 1-10.
- Ramsbottom, W.H.C., 1978, Carboniferous, *in* W.S. McKerrow, ed., The Ecology of Fossils: Cambridge, Massachusetts, MIT Press, p. 146-183.
- Read, J.F. and A.D. Horbury, 1993, Eustatic and tectonic controls on porosity evolution beneath sequence-bounding unconformities and parasequence disconformities on carbonate platforms, *in* A.D. Horbury and A.G. Robinson, eds., Diagenesis and basin development- Studies in Geology 36: Tulsa, OK, p. 155-197.
- Ritter, M.E., 2004, Diagenetic and sea-level controls on porosity evolution for oolitic and crinoidal carbonates of the Mississippian Keokuk Limestone and Warsaw Formation: Master’s thesis, The University of Kansas, Lawrence, Kansas, p. 50.
- Rogers, J.P., M.W. Longman, and R.M. Lloyd, 1995, Spiculitic chert reservoir in Glick field, south-central Kansas: The Mountain Geologist, v. 32, p.1-22.
- Rogers, J.P., and M.W. Longman, 2001, An introduction to chert reservoirs of North America, 2001, AAPG Bulletin, v. 85, no.1, p. 1-5.
- Rogers, S.M., 2001, Deposition and diagenesis of Mississippian chat reservoirs, north-central Oklahoma, AAPG Bulletin, v. 85, no.1, p. 115-129.

- Ross, C.A., and J.R.P. Ross, 1988, Late Paleozoic transgressive-regressive deposition, *in* C.W. Wilgus, H.W. Posamentier, C.A. Ross, and C.G. Kendall, eds., *Sea-Level Changes-An Integrated Approach: SEPM Special Publication 42*, p. 227-247.
- Ruppel, S.C., and S.D. Hovorka, 1995, Controls on reservoir development in Devonian chert: Permian Basin, Texas: *AAPG Bulletin*, v. 79, p. 1757-1785.
- Ruppel, S.C., and R.J. Barnaby, 2001, Contrasting styles of reservoir development in proximal and distal chert facies: Devonian Thirtyone Formation, Texas: *AAPG Bulletin*, v. 85, no.1, p. 7-33.
- Rygel, M.C., C.R. Fielding, T.D. Frank, and L.P. Birgenheier, 2008, The magnitude of late Paleozoic glacioeustatic fluctuations: A synthesis: *Journal of Sedimentary Research*, v. 78, no. 8, p. 500-511
- Saller, A.H., D.A. Budd, P.M. Harris, 1994, Unconformities and porosity development in carbonate strata- Ideas from a Hedberg Conference: *AAPG Bulletin*, v. 78, p. 857-871.
- Saueracker, P.R., 1966, Solution features in southeast Kansas: *The Compass*, v. 43, no. 2, p. 109-128.
- Saunders, W.B., W.L. Manger, and M.Jr. Gordon, 1977, Upper Mississippian and Lower and Middle Pennsylvanian ammonoid biostratigraphy of northern Arkansas, *in* P.K. Sutherland and W.L. Manger, eds., *Upper Chesterian-Morrowan Stratigraphy and the Mississippian Pennsylvanian Boundary in Northeastern Oklahoma and Northwestern Arkansas: Oklahoma Geological Survey, Guidebook 18*, p. 117-137.
- Scotese, C.R., 1999, Paleomap Project Web site: <<http://www.scotese.com/>>.
- Shelton, K.L., J.M. Reader, L.M. Ross, G.W. Viele, and D.E. Seidemann, 1986, Ba-rich adularia from the Ouachita Mountains, Arkansas: Implications for a postcollisional hydrothermal system: *American Mineralogist*, vol. 71, p.916-923.
- Sibley, D.F., and T.R. Bartlett, 1987, Nucleation as a rate limiting step in dolomitization, *in* R. Rodriguez-Clemente and Y. Tardy, eds., *Proceedings, geochemistry and mineral formation in the Earth surface: Madrid, Consejo Superior de Investigaciones Cientificas*, p. 733-741.
- Sibley, D.F., R.E. Dedoes, and T.R. Bartlett, 1987, Kinetics of dolomitization: *Geology*, v. 15, p. 112-114.
- Sibley, D.F., and J.M. Gregg, 1987, Classification of dolomite rock textures: *Journal of Sedimentary Petrology*, vol. 57, no. 6, p. 967-975.
- Stavnes, S.A., and D.W. Steeples, 1982, Relationships between geology and geothermal gradients in Kansas, *in* C.A. Ruscetta, ed., *Proceedings, geothermal direct heat program*

- roundup technical conference: Earth Science Laboratory, University of Utah Research Institute, Publication ESL-98, v. 1, p. 88-104.
- Sverjensky, D.A., 1986, Genesis of Mississippi valley-type lead-zinc deposits: Annual Review of Earth and Planetary Sciences, vol. 14, p. 177-199.
- Tarr, W.A., 1938, Terminology of the chemical siliceous sediments: National Research Council, Division of Geology and Geography, Annual Report for 1937, p. 8-27.
- Thomas, M.A., 1982, Petrology and diagenesis of the Lower Mississippian, Osagean Series, western Sedgwick basin, Kansas: Master's thesis, University of Missouri-Columbia, p. 87.
- Thompson, T.L., 1972, Conodont Biostratigraphy of Chesterian Strata in Southwestern Missouri: Missouri Geological Survey, Report of Investigations 50, p. 1.
- Thompson, T.L., 1986, Paleozoic succession in Missouri, Part 4, Mississippian System: Missouri Geological Survey, Report of Investigations No. 70, p. 76-96.
- Thompson, T.L., and L.D. Fellows, 1970, Stratigraphy and conodont biostratigraphy of Kinderhookian and Osagean rocks of southwestern Missouri and adjacent areas: Missouri Geological Survey and Water Resources, Report of Investigations 45, p. 263.
- Underwood, M.B., and G.W. Viele, 1985, Early Pennsylvanian tectonic transition within the frontal Ouachitas of Arkansas: Geological Society of America Abstracts with Programs, v. 17, p. 195.
- Vail, P.R., R.M. Mitchum, R.G. Todd, J.M. Widmier, S. Thompson, J.B. Sangree, J.N. Bubb, W.G. Hatlelid, 1977, Seismic stratigraphy and global changes of sea level, *in* C.E. Payton, ed., Seismic Stratigraphy-Applications to hydrocarbon exploration: AAPG Memoir 26, p. 49-212.
- Van Wagoner, J.C., R.M. Mitchum, K.M. Campion, and V.D. Rahmanian, 1990, Siliclastic sequence stratigraphy in well logs, cores, and outcrops: Concepts for high resolution correlation of time and facies: AAPG Methods in Exploration Series, No. 7, 55 p.
- Wagner, C.W. and C. van der Togt, 1973, Holocene sediment types and their distribution in the southern Persian Gulf, *in* B.H. Purser, ed., The Persian Gulf: New York, Springer-Verlag, p. 123-156.
- Wagner, P.D., D.R. Tasker, and G.P. Wahlman, 1995, Reservoir degradation and compartmentalization below subaerial unconformities- limestone examples from West Texas, China, and Oman, *in* D.A. Budd, A.H. Saller, and P.M. Harris, eds, Unconformities in carbonate strata- their recognition and the significance of associated porosity: AAPG Memoir 63, p. 177-195.





- Walton, A.W., K.M. Wojcik, R.H. Goldstein, and C.E. Barker, 1995, Diagenesis of Upper Carboniferous rocks in the Ouachita foreland shelf in mid-continent USA--An overview of widespread effects of a Variscan-equivalent orogeny: *Geologische Rundschau*, v. 84, p. 535-551.
- Watney, W.L., W.J. Guy, and A.P. Byrnes, 2001, Characterization of the Mississippian chat in south-central Kansas: *AAPG Bulletin*, v. 85, no.1, p. 85-113.
- Watney, W.L., E.K. Franseen, J.H. Doveton, T.L. Thompson, D.R. Boardman, E.T. Rasbury, K.D. Newell, J. Victorine, N.H. Suneson, and E. Starbuck, 2008, High-resolution sequence stratigraphic and chronostratigraphic investigations of the lower shelf and basal lithofacies of the Mississippian subsystem in the southern Midcontinent U.S.A.: AAPG National Meeting, San Antonio, TX.
- Witzke, B.J., 1990, Paleoclimatic constraints for Paleozoic paleolatitudes of Laurentia and Euramerica, *in* W.S. McKerrow and C.R. Scotese, eds., *Paleozoic paleogeography and biogeography*: London, Geological Society Memoir 12, p. 57-73.
- Witzke, B.J., and B.J. Bunker, 1996, Relative sea-level changes during Middle Ordovician through Mississippian deposition in the Iowa area, North American craton, *in* B.J. Witzke, G.A. Ludvigson, and J. Day, eds., *Paleozoic sequence stratigraphy: views from the North American craton*: Geological Society of America Special Paper 306, p. 307-330.
- Wojcik, K.M., M.E. McKibben, R.H. Goldstein, and A.W. Walton, 1992, Diagenesis, thermal history, and fluid migration, Middle and Upper Pennsylvanian rocks, southeastern Kansas: *Oklahoma Geological Survey Circular*, v. 93, p. 144-159.
- Wojcik, K.M., M.E. McKibben, R.H. Goldstein, and A.W. Walton, 1994, History of diagenetic fluids in a distant foreland area, Middle and Upper Pennsylvanian, Cherokee basin, Kansas, USA: Fluid inclusion evidence: *Geochimica et Cosmochimica Acta*, v. 58, p. 1175-1191.
- Wojcik, K.M., R.H. Goldstein, and A.W. Walton, 1997, Regional and local controls of diagenesis driven by basin-wide flow system: Pennsylvanian sandstones and limestones, Cherokee basin, southeastern Kansas, *in* I.P. Montanez, J.M. Gregg, and K.L. Shelton, eds., *Basin-wide diagenetic patterns; integrated petrologic, geochemical, and hydrologic considerations*: SEPM Special Publication No. 57, p. 235-252.
- Wright, V.P., 1991, Paleokarsts: types, recognition, controls, and associations, *in* V.P. Wright, ed., *Paleokarst and paleokarstic reservoirs*: Postgraduate Research Institute for Sedimentology, Occasional Publication Series 2, p. 56-88.
- Ziegler, P.A., 1989, *Evolution of Laurussia: a study in Late Paleozoic plate tectonics*: Kluwer Academic Publishing, Dordrecht, The Netherlands, 102 p.

Appendix 1
Core Descriptions

	echinoderm-rich-bioclastic wacke-packstone		crinoid
	dolomitic bioclastic wackestone		bryozoan
	argillaceous wackestone		brachiopod
	sponge-spicule-rich packstone		bivalve
	variable chert breccia		foraminifera
	tripolitic chert		pyrite
	oid packstone		intraclast
	bioclastic grainstone		stylolite
	shale		shale seam
	marine flooding surface (dashed where interpreted)		open mold
	sequence boundary		faint low angle laminations
	subaerial exposure surface (dashed where interpreted)		burrow
	bed correlations		ooids
	interpreted bed correlations		light grey filled burrows
surface 1 (S1) boundary between Unit 1 and Unit 2			back-filled burrows
surface 2 (S2) boundary between Unit 2 and Unit 3			burrowed, mottled texture
Mississippian-Pennsylvanian (M-P) unconformity			whispy bedding
possible exposure surfaces (PE1, PE2)			crackle breccia
	nodular brecciated chert		brecciated tripolitic chert
	nodular chert replacement		mottled grey-white massive chert slightly fractured w/o and w/ fossils
	highly brecciated angular chert clasts with brown-black infill		

Legend for core description sheets

Gulf Oil Corporation
Pittsburg-Midway
PM-17
Cherokee, Co., KS
T32S-R21E-Sec.36

Depth	Gulf Oil Corporation Pittsburg-Midway PM-17 Cherokee, Co., KS T32S-R21E-Sec.36 Depth:393-411	Texture				Sedimentary Structures	Fossils	Abrasion			Visual Porosity	Comments (color, grains, etc.)
		M	W	P	G			N	M	A		
393	Top of Core									tight	black shale	
395										tight	black shale	
397										tight	black shale	
399										tight	black shale	
401										tight	black shale	
403					mottled white fine brecciation					fracture, microporous	white mottled microporous chert, finely brecciated, microporous, not porous enough to be tripolitic, oil stains, iron-poor calcite	
405					mottled white fine brecciation					fracture, microporous	white mottled microporous chert, finely brecciated, microporous, not porous enough to be tripolitic, oil stains, iron-poor calcite	
407					mottled white fine brecciation					fracture, microporous	white mottled microporous chert, finely brecciated, microporous, not porous enough to be tripolitic, oil stains, iron-poor calcite	
409					mottled white fine brecciation					fracture, microporous	white mottled microporous chert, finely brecciated, microporous, not porous enough to be tripolitic, oil stains, iron-poor calcite	
411												

Depth	Gulf Oil Corporation Pittsburg-Midway PM-17 Cherokee, Co., KS T32S-R21E-Sec.36 Depth: 411-429	Texture				Sedimentary Structures	Fossils	Abrasion			Visual Porosity	Comments (color, grains, etc.)
		M	W	P	G			N	M	A		
411						mottled white fine brecciation				fracture, microporous	white mottled microporous chert, finely brecciated, microporous, not porous enough to be tripolitic, oil stains, iron-poor calcite	
413						mottled white fine brecciation				fracture, microporous	white mottled microporous chert, finely brecciated, microporous, not porous enough to be tripolitic, oil stains, iron-poor calcite	
415						mottled white fine brecciation				fracture, microporous	white mottled microporous chert, finely brecciated, microporous, not porous enough to be tripolitic, oil stains, iron-poor calcite	
417						mottled white fine brecciation				fracture, microporous	white mottled microporous chert, finely brecciated, microporous, not porous enough to be tripolitic, oil stains, iron-poor calcite	
419						mottled white fine brecciation				fracture, microporous	white mottled microporous chert, finely brecciated, microporous, not porous enough to be tripolitic, oil stains, iron-poor calcite	
421						mottled white fine brecciation				fracture, microporous	white mottled microporous chert, finely brecciated, microporous, not porous enough to be tripolitic, oil stains, iron-poor calcite	
423						mottled white fine brecciation				fracture, microporous	white mottled microporous chert, finely brecciated, microporous, not porous enough to be tripolitic, oil stains, iron-poor calcite	
425						mottled white fine brecciation				fracture, microporous	white mottled microporous chert, finely brecciated, microporous, not porous enough to be tripolitic, iron-poor calcite	
427						mottled white fine brecciation				fracture, microporous	white mottled microporous chert, finely brecciated, microporous, not porous enough to be tripolitic, iron-poor calcite	
429						mottled white fine brecciation				fracture, microporous	white mottled microporous chert, finely brecciated, microporous, not porous enough to be tripolitic, iron-poor calcite	

Depth	Gulf Oil Corporation Pittsburg-Midway PM-17 Cherokee, Co., KS T32S-R21E-Sec.36 Depth: 429-447	Texture				Sedimentary Structures	Fossils	Abrasion			Visual Porosity	Comments (color, grains, etc.)
		M	W	P	G			N	M	A		
429						mottled white fine brecciation				fracture, microporous	white mottled microporous chert, finely brecciated, microporous, not porous enough to be tripolitic, iron-poor calcite	
431						mottled white fine brecciation				fracture, microporous	white mottled microporous chert, finely brecciated, microporous, not porous enough to be tripolitic, iron-poor calcite	
433						mottled white fine brecciation				fracture, microporous	white mottled microporous chert, finely brecciated, microporous, not porous enough to be tripolitic, iron-poor calcite	
435						mottled white fine brecciation				fracture, microporous	white mottled microporous chert, finely brecciated, microporous, not porous enough to be tripolitic, iron-poor calcite	
437						mottled white fine brecciation				fracture, microporous	white mottled microporous chert, finely brecciated, microporous, not porous enough to be tripolitic, iron-poor calcite	
439						mottled white fine brecciation				fracture, microporous	white mottled microporous chert, finely brecciated, microporous, not porous enough to be tripolitic, iron-poor calcite	
441						mottled white fine brecciation				fracture, microporous	white mottled microporous chert, finely brecciated, microporous, not porous enough to be tripolitic, iron-poor calcite	
443						nodular blue- grey-white chert replacement				tight	light grey silty mudstone with nodular blue-grey-white chert replacement, few thin shale seams, iron-poor calcite	
445						nodular blue- grey-white chert replacement				tight	light grey silty mudstone with nodular blue-grey-white chert replacement, few thin shale seams, iron-poor calcite	
447												

Depth	Gulf Oil Corporation Pittsburg-Midway PM-17 Cherokee, Co., KS T32S-R21E-Sec.36 Depth: 447-465	Texture				Sedimentary Structures	Fossils	Abrasion			Visual Porosity	Comments (color, grains, etc.)
		M	W	P	G			N	M	A		
447						nodular blue-grey-white chert replacement fractured					fracture	light grey silty mudstone with nodular blue-grey-white chert replacement, few thin shale seams, iron-poor calcite
449						nodular blue-grey-white chert replacement fractured					fracture	light grey silty mudstone with nodular blue-grey-white chert replacement, few thin shale seams, iron-poor calcite
451						nodular blue-grey-white chert replacement fractured					fracture	light grey silty mudstone with nodular blue-grey-white chert replacement, fractures, few thin shale seams, iron-poor calcite
453						nodular blue-grey-white chert replacement fractured					fracture	light grey silty mudstone with nodular blue-grey-white chert replacement, fractures, few thin shale seams, iron-poor calcite
455						nodular blue-grey-white chert replacement fractured increased silt					fracture	light grey silty mudstone with nodular blue-grey-white chert replacement, fractures, few thin shale seams, iron-poor calcite
457						shale seams nodular black chert whispy laminations					tight	light grey silty mudstone with whispy laminations and shale seams, nodular black-grey mottled chert replacement, blue-grey nodular chert, iron-poor calcite
459						shale seams nodular black chert whispy laminations					tight	dark grey-black mudstone with whispy laminations and shale seams, nodular black-grey mottled chert replacement, iron-poor calcite
461						shale seams nodular black chert whispy laminations					tight	dark grey-black mudstone with whispy laminations and shale seams, nodular black-grey mottled chert replacement, iron-poor calcite
463						shale seams nodular black chert whispy laminations scattered crinoids					tight	dark grey-black mudstone with whispy laminations and shale seams, 1-3 mm scattered crinoids, nodular black-grey mottled chert replacement, iron-poor calcite
465						shale seams nodular black chert whispy laminations scattered crinoids					tight	dark grey-black mudstone with whispy laminations and shale seams, 1-3 mm scattered crinoids, nodular black-grey mottled chert replacement, iron-poor calcite

Depth	Gulf Oil Corporation Pittsburg-Midway PM-17 Cherokee, Co., KS T32S-R21E-Sec.36 Depth: 465-483	Texture				Sedimentary Structures	Fossils	Abrasion			Visual Porosity	Comments (color, grains, etc.)
		M	W	P	G			N	M	A		
465						shale seams whispy lamina- tions				tight	dark grey-black mudstone with whispy laminations and shale seams, interrupted by crinoid concentrations made up of 1-7 mm size crinoids, iron-poor calcite	
467						shale seams whispy lamina- tions				tight	dark grey-black mudstone with whispy laminations and shale seams, interrupted by crinoid concentrations made up of 1-7 mm size crinoids, iron-poor calcite	
469						shale seams whispy lamina- tions				tight	dark grey-black mudstone with whispy laminations and shale seams, interrupted by crinoid concentrations made up of 1-7 mm size crinoids, iron-poor calcite	
471						darkened grains mostly crinoids, not graded, sharp base	○ ○ ○			tight	dark grey-black mudstone with whispy laminations and shale seams, interrupted by crinoid concentrations made up of 1-7 mm size crinoids, iron-poor calcite	
473						shale seams whispy lamina- tions scattered crinoids	○ ○ ○			tight	dark grey-black mudstone with whispy laminations and shale seams, interrupted by crinoid concentrations made up of 1-7 mm size crinoids, iron-poor calcite	
475						shale seams whispy lamina- tions				tight	dark grey-black mudstone with whispy laminations and shale seams, interrupted by crinoid concentrations made up of 1-7 mm size crinoids, iron-poor calcite	
477						shale seams whispy lamina- tions scattered crinoids	○ ○ ○			tight	dark grey-black mudstone with whispy laminations and shale seams, interrupted by crinoid concentrations made up of 1-7 mm size crinoids, iron-poor calcite	
479						shale seams whispy lamina- tions scattered crinoids	○ ○ ○			tight	dark grey-black mudstone with whispy laminations and shale seams, interrupted by crinoid concentrations made up of 1-7 mm size crinoids, iron-poor calcite	
481						shale seams whispy lamina- tions scattered crinoids	○ ○ ○			tight	dark grey-black mudstone with whispy laminations and shale seams, interrupted by crinoid concentrations made up of 1-7 mm size crinoids, iron-poor calcite	
483						shale seams whispy lamina- tions scattered crinoids	○ ○ ○			tight	dark grey-black mudstone with whispy laminations and shale seams, interrupted by crinoid concentrations made up of 1-7 mm size crinoids, iron-poor calcite	

Depth	Gulf Oil Corporation Pittsburg-Midway PM-17 Cherokee, Co., KS T32S-R21E-Sec.36 Depth:483-501	Texture				Sedimentary Structures	Fossils	Abrasion			Visual Porosity	Comments (color, grains, etc.)
		M	W	P	G			N	M	A		
483						shale seams whispy laminations scattered crinoids	○ ○ ○				tight	dark grey-black mudstone with whispy laminations and shale seams, interrupted by crinoid concentrations made up of 1-7 mm size crinoids, iron-poor calcite
485						shale seams whispy laminations scattered crinoids	○ ○ ○				tight	dark grey-black mudstone with whispy laminations and shale seams, interrupted by crinoid concentrations made up of 1-7 mm size crinoids, iron-poor calcite
487						shale seams whispy laminations scattered crinoids	○ ○ ○				tight	dark grey-black mudstone with whispy laminations and shale seams, interrupted by crinoid concentrations made up of 1-7 mm size crinoids, iron-poor calcite
489						shale seams whispy laminations scattered crinoids	○ ○ ○				tight	dark grey-black mudstone with whispy laminations and shale seams, interrupted by crinoid concentrations made up of 1-7 mm size crinoids, iron-poor calcite
491						shale seams whispy laminations scattered crinoids	○ ○ ○				tight	dark grey-black mudstone with whispy laminations and shale seams, interrupted by crinoid concentrations made up of 1-7 mm size crinoids, iron-poor calcite
493						shale seams whispy laminations scattered crinoids	○ ○ ○				tight	dark grey-black mudstone with whispy laminations and shale seams, interrupted by crinoid concentrations made up of 1-7 mm size crinoids, iron-poor calcite
495						shale seams whispy laminations scattered crinoids	○ ○ ○				tight	dark grey-black mudstone with whispy laminations and shale seams, interrupted by crinoid concentrations made up of 1-7 mm size crinoids, iron-poor calcite
497						shale seams whispy laminations scattered crinoids	○ ○ ○				tight	dark grey-black mudstone with whispy laminations and shale seams, interrupted by crinoid concentrations made up of 1-7 mm size crinoids, iron-poor calcite
499						shale seams 50 mm crinoid bed whispy laminations	○ ○ ○ ○ ○ ○				tight	dark grey-black mudstone with whispy laminations and shale seams, interrupted by crinoid concentrations made up of 1-7 mm size crinoids, iron-poor calcite
501						whispy laminations						

Depth	Gulf Oil Corporation Pittsburg-Midway PM-17 Cherokee, Co., KS T32S-R21E-Sec.36 Depth: 537-555	Texture				Sedimentary Structures	Fossils	Abrasion			Visual Porosity	Comments (color, grains, etc.)	
		M	W	P	G			N	M	A			
537						massive white chert with grey mottles					3-5 mm open vugs	massive white-grey mottled chert with 3-5 mm open vugs, also contain elongate porous areas possibly sponges?	
539						massive white chert with grey mottles					3-5 mm open vugs	massive white-grey mottled chert with 3-5 mm open vugs, also contain elongate porous areas possibly sponges?	
541						missing 2 feet						missing core	
543						white chert rubble forams						very porous	white porous chalky brecciated chert, held together in areas, others are just rubble, ferroan dolomite-ankerite
545						brecciated bivalves and bryozoans shaly seams						very porous	chalky white tripolitic chert slightly to highly brecciated with dark grey circular to elongate replacement spots, ferroan dolomite-ankerite
547						brecciated						very porous	chalky white tripolitic chert slightly to highly brecciated with dark grey circular to elongate replacement spots, ferroan dolomite-ankerite
549						white chert rubble						fracture, porous	white porous chalky brecciated chert, held together in areas, others are just rubble, ferroan dolomite-ankerite
551						styolites whispy shale seams						tight	autoclastically brecciated chert interbedded with dark grey wackestone-packstone, whispy shale seams, styolites, vertical fractures, iron-poor calcite
553						brecciated						very porous	chalky white tripolitic chert slightly to highly brecciated with dark grey circular to elongate replacement spots, ferroan dolomite-ankerite
555													

Depth	Gulf Oil Corporation Pittsburg-Midway PM-17 Cherokee, Co., KS T32S-R21E-Sec.36 Depth:555-573	Texture				Sedimentary Structures	Fossils	Abrasion			Visual Porosity	Comments (color, grains,etc.)
		M	W	P	G			N	M	A		
555						stylolites whispy shale seams				tight	autoclastically brecciated chert interbedded with dark grey wackestone-packstone, whispy shale seams, stylolites, vertical fractures, iron-poor calcite	
557						autoclastically brecciated chert				fracture	autoclastically brecciated white/grey chert 4-20 mm angular clasts with dark grey infill, larger openings contain mm size chert clasts.infill is iron-poor calcite	
559						autoclastically brecciated chert				fracture	autoclastically brecciated white/grey chert 4-20 mm angular clasts with dark grey infill, larger openings contain mm size chert clasts.infill is iron-poor calcite	
561						mottled blue- white chert, autoclastic brecciation to crackle brecciated				fracture	mottled blue-white chert, autoclastically brecciated to massive, fractures sometimes filled with chalcedony	
563						mottled blue- white chert, autoclastic brecciation to crackle brecciated				fracture	mottled blue-white chert, autoclastically brecciated to massive, fractures sometimes filled with chalcedony	
565						mottled blue- white chert, autoclastic brecciation to crackle brecciated				fracture	mottled blue-white chert, autoclastically brecciated to massive, fractures sometimes filled with chalcedony	
567						stylolites whispy shale seams				tight	autoclastically brecciated chert interbedded with dark grey wackestone-packstone, whispy shale seams, stylolites, vertical fractures, iron-poor calcite	
569						autoclastically brecciated chert				fracture	autoclastically brecciated white/grey chert 4-20 mm angular clasts with dark grey infill, larger openings contain mm size chert clasts.infill is iron-poor calcite	
571						autoclastically brecciated chert				fracture	autoclastically brecciated white/grey chert 4-20 mm angular clasts with dark grey infill, larger openings contain mm size chert clasts.infill is iron-poor calcite	
573												

Depth	Gulf Oil Corporation Pittsburg-Midway PM-17 Cherokee, Co., KS T32S-R21E-Sec.36 Depth: 573-591	Texture				Sedimentary Structures	Fossils	Abrasion			Visual Porosity	Comments (color, grains, etc.)
		M	W	P	G			N	M	A		
573						autoclastically brecciated chert					fracture	autoclastically brecciated white/grey chert 4-20 mm angular clasts with dark grey infill, larger openings contain mm size chert clasts. infill is iron-poor calcite
575						autoclastically brecciated chert					fracture	autoclastically brecciated white/grey chert 4-20 mm angular clasts with dark grey infill, larger openings contain mm size chert clasts. infill is iron-poor calcite
577						stylolites whispy shale seams					tight	dark grey wackestone- packstone, whispy shale seams, stylolites, vertical fractures, iron-poor calcite
579						chert bed full of 1-2 mm silicified crinoids					tight	mottled massive blue-white chert (bed of silicified crinoids) interbedded with dark grey wackestone- packstone
						interbedded chert and wacke- packstone					tight	mottled massive blue-white chert interbedded with dark grey wackestone-packstone
583						mottled blue- white chert, autoclastic brecciation					fracture	mottled blue-white chert, autoclastically brecciated to massive, fractures often filled with chalcedony
585						stylolites whispy shale seams					tight	dark grey wackestone- packstone, whispy shale seams, stylolites, vertical fractures, iron-poor calcite
587						stylolites whispy shale seams abundant 2-10 mm crinoids					tight	dark grey crinoidal packstone- wackestone, stylolites, whispy shale seams, abundant crinoids partial to complete silicification, iron-poor calcite
589						stylolites whispy shale seams abundant 2-10 mm crinoids					tight	dark grey crinoidal packstone- wackestone, stylolites, whispy shale seams, abundant crinoids partial to complete silicification, iron-poor calcite
591						stylolites whispy shale seams abundant 2-10 mm crinoids					tight	dark grey crinoidal packstone- wackestone, stylolites, whispy shale seams, abundant crinoids partial to complete silicification, iron-poor calcite

Depth	Gulf Oil Corporation Pittsburg-Midway PM-17 Cherokee, Co., KS T32S-R21E-Sec.36 Depth: 591-609	Texture				Sedimentary Structures	Fossils	Abrasion			Visual Porosity	Comments (color, grains, etc.)
		M	W	P	G			N	M	A		
591						whispy shale laminations				tight	dark grey wackestone- mudstone with whispy shale seams/laminations	
593						crackle brecciated white chert				fracture	crackle brecciated white chert, some fractures filled with chalcedoney	
595						abundant 2-10 mm crinoids autoclastically brecciated chert				tight fracture	dark grey crinoidal packstone with areas of complete silicification, stylolites, few whispy shale seams, autoclas- tically brecciated chert, iron-poor calcite	
597						abundant 2-10 mm crinoids stylolites few shale seams				tight	dark grey crinoidal packstone with areas of complete silicification, stylolites, few whispy shale seams, iron-poor calcite	
599						abundant 2-10 mm crinoids stylolites few shale seams				tight	dark grey crinoidal packstone with areas of complete silicification, stylolites, few whispy shale seams, iron-poor calcite	
601						abundant 2-10 mm crinoids stylolites few shale seams				tight	dark grey crinoidal packstone with areas of complete silicification, stylolites, few whispy shale seams, iron-poor calcite	
603						abundant 2-10 mm crinoids stylolites few shale seams				tight	dark grey crinoidal packstone with areas of complete silicification, stylolites, few whispy shale seams, iron-poor calcite	
605						abundant 2-10 mm crinoids stylolites few shale seams				tight	dark grey crinoidal packstone with areas of complete silicification, stylolites, few whispy shale seams, iron-poor calcite	
607						abundant 2-10 mm crinoids stylolites few shale seams				tight	dark grey crinoidal packstone with areas of complete silicification, stylolites, few whispy shale seams, iron-poor calcite	
609						abundant 2-10 mm crinoids stylolites few shale seams				tight	dark grey crinoidal packstone with areas of complete silicification, stylolites, few whispy shale seams, iron-poor calcite	

Depth	Gulf Oil Corporation Pittsburg-Midway PM-17 Cherokee, Co., KS T32S-R21E-Sec.36 Depth: 609-627	Texture				Sedimentary Structures	Fossils	Abrasion			Visual Porosity	Comments (color, grains, etc.)
		M	W	P	G			N	M	A		
609						abundant 2-10 mm crinoids styolites few shale seams					tight	dark grey crinoidal packstone with areas of complete silicification, styolites, few wispy shale seams, iron-poor calcite
611						abundant 2-10 mm crinoids styolites					tight	dark grey crinoidal packstone with areas of complete silicification, styolites, few wispy shale seams, iron-poor calcite
613						crinoidal chert					tight	dark grey crinoidal packstone with areas of complete silicification, styolites, few wispy shale seams, iron-poor calcite
615						crinoidal chert crackle brecciated white chert					tight	crinoidal chert with 2-10 mm crinoids crackle brecciated white chert, some fractures filled with chalcedony
617						styolites whispy shale seams abundant 2-10 mm crinoids					fracture	dark grey crinoidal packstone-wackestone, styolites, wispy shale seams, abundant crinoids partical to complete silicification, iron-poor calcite
619						styolites whispy shale seams abundant 2-10 mm crinoids					tight	dark grey crinoidal packstone-wackestone, styolites, wispy shale seams, abundant crinoids partical to complete silicification, iron-poor calcite
621						70 mm silty bed with sharp base and wispy shale seams (burrows?)					tight	dark grey crinoidal packstone-wackestone, styolites, wispy shale seams, abundant crinoids partical to complete silicification, iron-poor calcite
623						styolites whispy shale seams abundant 2-10 mm crinoids					tight	dark grey crinoidal packstone-wackestone, styolites, wispy shale seams, abundant crinoids partical to complete silicification, iron-poor calcite
625						styolites whispy shale seams abundant 2-10 mm crinoids					tight	dark grey crinoidal packstone-wackestone, styolites, wispy shale seams, abundant crinoids partical to complete silicification, iron-poor calcite
627												

Depth	Gulf Oil Corporation Pittsburg-Midway PM-17 Cherokee, Co., KS T32S-R21E-Sec.36 Depth: 627-645	Texture				Sedimentary Structures	Fossils	Abrasion			Visual Porosity	Comments (color, grains, etc.)
		M	W	P	G			N	M	A		
627						stylonites whispy shale seams abundant 2-10 mm crinoids					tight	dark grey crinoidal packstone- wackestone, stylonites, whispy shale seams, abundant crinoids partial to complete silicification, iron-poor calcite
629						stylonites whispy shale seams abundant 2-10 mm crinoids					tight	dark grey crinoidal packstone- wackestone, stylonites, whispy shale seams, abundant crinoids partial to complete silicification, iron-poor calcite
631						stylonites whispy shale seams abundant 2-10 mm crinoids					tight	dark grey crinoidal wacke- stone, stylonites, whispy shale seams, abundant crinoids partial to complete silicifica- tion, iron-poor calcite
633						stylonites whispy shale seams abundant 2-10 mm crinoids					tight	dark grey crinoidal wacke- stone, stylonites, whispy shale seams, abundant crinoids partial to complete silicifica- tion, iron-poor calcite
635						whispy shale seams					tight	dark grey mudstone with whispy shale seams/laminations, 7 mm pyrite nodules, forams
637						stylonites whispy shale seams abundant 2-10 mm crinoids					tight	dark grey crinoidal wacke- stone, stylonites, whispy shale seams, abundant crinoids partial to complete silicifica- tion, iron-poor calcite
639						whispy shale seams					tight	dark grey mudstone with whispy shale seams/laminations, 7 mm pyrite nodules, forams
641						whispy shale seams					tight	dark grey mudstone with whispy shale seams/laminations, 7 mm pyrite nodules, forams
643						whispy shale seams 3 mm forams 7 mm pyrite					tight	dark grey mudstone with whispy shale seams/laminations, 7 mm pyrite nodules, forams
645						whispy shale seams 3 mm forams 7 mm pyrite					tight	dark grey mudstone with whispy shale seams/laminations, 7 mm pyrite nodules, forams

Depth	Gulf Oil Corporation Pittsburg-Midway PM-17 Cherokee, Co., KS T32S-R21E-Sec.36 Depth: 645-663	Texture				Sedimentary Structures	Fossils	Abrasion			Visual Porosity	Comments (color, grains, etc.)	
		M	W	P	G			N	M	A			
645						whispy shale seams					tight	dark grey mudstone with whispy shale seams/laminations, 5 mm pyrite nodules	
647						strolites whispy shale seams start to loose abundant crinoids					tight	dark grey crinoidal wackestone, strolites, whispy shale seams, abundant crinoids partial to complete silicification, iron-poor calcite	
649						strolites whispy shale seams abundant 2-10 mm crinoids					tight	dark grey crinoidal wackestone, strolites, whispy shale seams, abundant crinoids partial to complete silicification, iron-poor calcite	
651						strolites whispy shale seams abundant 2-10 mm crinoids					tight	dark grey crinoidal wackestone, strolites, whispy shale seams, abundant crinoids partial to complete silicification, iron-poor calcite	
653						strolites whispy shale seams abundant 2-10 mm crinoids					tight	dark grey crinoidal wackestone, strolites, whispy shale seams, abundant crinoids partial to complete silicification, iron-poor calcite	
655						strolites whispy shale seams abundant 2-10 mm crinoids					tight	dark grey crinoidal wackestone, strolites, whispy shale seams, abundant crinoids partial to complete silicification, iron-poor calcite	
657						irregular surface with whispy shale seams below, 2-7 mm white intraclasts above					tight	dark grey crinoidal wackestone, strolites, whispy shale seams, abundant crinoids partial to complete silicification, iron-poor calcite	
659						strolites whispy shale seams abundant 2-10 mm crinoids					tight	dark grey crinoidal wackestone-packstone, strolites, abundant crinoids partial to complete silicification, iron-poor calcite	
661						strolites abundant 2-10 mm crinoids					tight	dark grey crinoidal wackestone-packstone, strolites, abundant crinoids partial to complete silicification, iron-poor calcite	
663													

Depth	Gulf Oil Corporation Pittsburg-Midway PM-17 Cherokee, Co., KS T32S-R21E-Sec.36 Depth: 663-681	Texture				Sedimentary Structures	Fossils	Abrasion			Visual Porosity	Comments (color, grains, etc.)
		M	W	P	G			N	M	A		
663						stylolites, abundant 2-10 mm crinoids					tight	dark grey lime packstone, stylolites, abundant crinoids partial to complete silicifica- tion, iron-poor calcite
665						stylolites, abundant 2-10 mm crinoids					tight	dark grey lime packstone, stylolites, abundant crinoids partial to complete silicifica- tion, iron-poor calcite
667						stylolites, abundant 2-10 mm crinoids					tight	dark grey lime packstone, stylolites, abundant crinoids partial to complete silicifica- tion, iron-poor calcite
669						stylolites, abundant 2-10 mm crinoids					tight	dark grey lime packstone, stylolites, abundant crinoids partial to complete silicifica- tion, iron-poor calcite
671						50 mm grey shale bed 2-70 mm glauco- nite seams, stylolites, abundant 2-10 mm crinoids					tight	dark grey lime packstone, 50 mm shale bed, stylolites, abundant crinoids partial to complete silicification, iron-poor calcite
673						2-70 mm glauco- nite seams, stylolites, abundant 2-10 mm crinoids					tight	dark grey lime packstone, shale seams, glauconite seams, stylolites, abundant crinoids partial to complete silicification, iron-poor calcite
675						2-70 mm glauco- nite seams, stylolites, abundant 2-10 mm crinoids					tight	dark grey lime packstone, shale seams, glauconite seams, stylolites, abundant crinoids partial to complete silicification, iron-poor calcite
677						2-70 mm glauco- nite seams, stylolites, abundant 2-10 mm crinoids					tight	dark grey lime packstone, shale seams, glauconite seams, stylolites, abundant crinoids partial to complete silicification, iron-poor calcite
679						2-70 mm glauco- nite seams, stylolites, abundant 2-10 mm crinoids					tight	dark grey lime packstone, shale seams, glauconite seams, stylolites, abundant crinoids partial to complete silicification, iron-poor calcite
681												

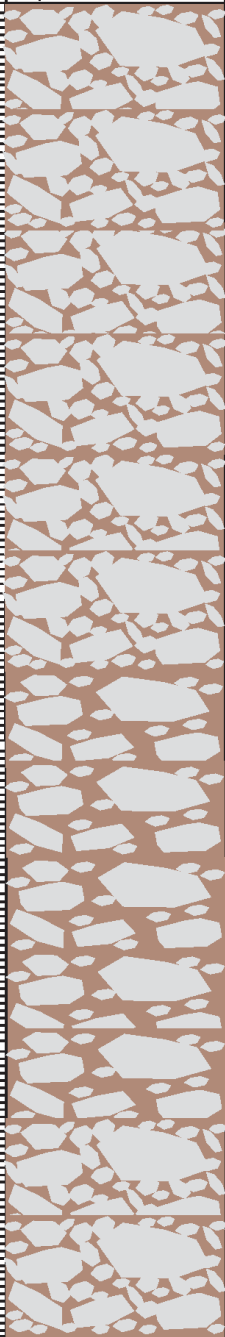
Depth	Gulf Oil Corporation Pittsburg-Midway PM-17 Cherokee, Co., KS T32S-R21E-Sec.36 Depth: 681-699	Texture				Sedimentary Structures	Fossils	Abrasion			Visual Porosity	Comments (color, grains, etc.)
		M	W	P	G			N	M	A		
681						2-5 mm glauconite seams, stylolites, abundant 2-10 mm crinoids					tight	dark grey lime packstone, shale seams, glauconite seams, stylolites, abundant crinoids partial to complete silicification, iron-poor calcite
683						2-5 mm glauconite seams, stylolites, abundant 2-10 mm crinoids					tight	dark grey lime packstone, shale seams, glauconite seams, stylolites, abundant crinoids partial to complete silicification, iron-poor calcite
685						2-5 mm shale seams, stylolites, abundant 2-10 mm crinoids					tight	dark grey lime packstone, shale seams, stylolites, abun- dant crinoids partial to complete silicification, iron-poor calcite
687						2-5 mm shale seams, stylolites, abundant 2-10 mm crinoids					tight	dark grey lime packstone, shale seams, stylolites, abun- dant crinoids partial to complete silicification, iron-poor calcite
689						2-5 mm shale seams, stylolites, abundant 2-10 mm crinoids					tight	dark grey lime packstone, shale seams, stylolites, abun- dant crinoids partial to complete silicification, iron-poor calcite
691						2-5 mm shale seams, stylolites, abundant 2-10 mm crinoids					tight	dark grey lime packstone, shale seams, stylolites, abun- dant crinoids partial to complete silicification, iron-poor calcite
693						2-5 mm shale seams, stylolites, abundant 2-10 mm crinoids					tight	dark grey lime packstone, shale seams, stylolites, abun- dant crinoids partial to complete silicification, iron-poor calcite
695						2-5 mm shale seams, stylolites, abundant 2-10 mm crinoids					tight	dark grey lime packstone, shale seams, stylolites, abun- dant crinoids partial to complete silicification, iron-poor calcite
697						2-5 mm shale seams, stylolites, abundant 2-10 mm crinoids					tight	dark grey lime packstone, shale seams, stylolites, abun- dant crinoids partial to complete silicification, iron-poor calcite
699												






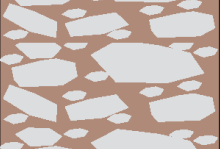
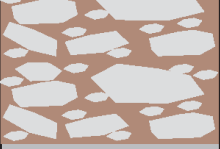
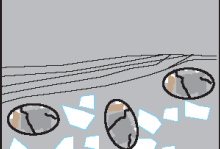
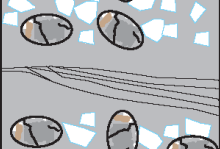

Depth	Gulf Oil Corporation Pittsburg-Midway PM-17 Cherokee, Co., KS T32S-R21E-Sec.36 Depth: 699-717	Texture				Sedimentary Structures	Fossils	Abrasion			Visual Porosity	Comments (color, grains, etc.)
		M	W	P	G			N	M	A		
699						2-5 mm shale seams, stylolites, abundant 2-10 mm crinoids					tight	dark grey lime packstone, shale seams, stylolites, abundant crinoids partial to complete silicification, iron-poor calcite
701						2-5 mm shale seams, stylolites, abundant 2-10 mm crinoids					tight	dark grey lime packstone, shale seams, stylolites, abundant crinoids partial to complete silicification, iron-poor calcite
703						2-5 mm shale seams, stylolites, abundant 2-10 mm crinoids					tight	dark grey lime packstone, shale seams, stylolites, abundant crinoids partial to complete silicification, iron-poor calcite
705						2-5 mm shale seams, stylolites, scattered 1-2 mm crinoids					tight	dark grey lime wackestone, shale seams, stylolites, scattered crinoids, iron-poor calcite
707						2-5 mm shale seams, stylolites, scattered 1-2 mm crinoids					tight	dark grey lime wackestone, shale seams, stylolites, scattered crinoids, iron-poor calcite
709						2-5 mm shale seams, stylolites, abundant 3 mm pyrite nodules					tight	dark grey lime wackestone, pyrite nodules, shale seams, coarse mineralization, iron-poor calcite
711						2-5 mm shale seams, stylolites, abundant 3 mm pyrite nodules					tight	light grey lime mud-wackestone, pyrite nodules, shale seams, coarse mineralization, iron-poor calcite
713						2-5 mm shale seams, stylolites, 10 mm coarse calcite mineralization, abundant 3 mm pyrite nodules					tight	light grey lime mud-wackestone, pyrite nodules, shale seams, coarse mineralization, iron-poor calcite
715						2-5 mm shale seams, stylolites, abundant 3 mm pyrite nodules					tight	light grey lime mud-wackestone, pyrite nodules, shale seams, iron-poor calcite
717						2-5 mm shale seams, stylolites, abundant 3 mm pyrite nodules					tight	light grey lime mud-wackestone, pyrite nodules, shale seams, iron-poor calcite

Depth	Gulf Oil Corporation Pittsburg-Midway PM-17 Cherokee, Co., KS T32S-R21E-Sec.36 Depth: 717-735	Texture				Sedimentary Structures	Fossils	Abrasion			Visual Porosity	Comments (color, grains, etc.)
		M	W	P	G			N	M	A		
717						2-5 mm shale seams, stylolites					tight	light grey lime mud-wackestone, pyrite nodules, shale seams, iron-poor calcite
719						2-5 mm shale seams, stylolites					tight	light grey lime mud-wackestone, pyrite nodules, shale seams, iron-poor calcite
721						stylolites, 1-2 mm scattered crinoids	○				tight	light grey scattered crinoidal lime mud-wackestone, pyrite nodules, shale seams, iron-poor calcite
723						2 mm pyrite nodule, stylolites, 1-2 mm scattered crinoids	○				tight	light grey scattered crinoidal lime mud-wackestone, pyrite nodules, shale seams, iron-poor calcite
725						2 mm glauconite beds vertical fracture filled with pyrite	○				tight	light grey scattered crinoidal lime mud-wackestone, small glauconite beds, pyrite nodules, shale seams, iron-poor calcite
727						2-3 mm burrows					tight	grey-green silty lime mud, no stain
729						Burrowed to slightly bioturbated, mottled texture, mostly sub-horizontal					tight	grey-green silty lime mud, no stain
731						2-3 mm burrows					tight	grey-green silty lime mud, no stain
733						2-3 mm burrows 4 mm pyrite nodule					tight	grey-green silty lime mud, no stain
735												

Gulf Oil Corporation
Pittsburg Midway
PM-12
Cherokee Co., KS
T32S-R22E-Sec. 19

Depth	Gulf Oil Corporation Pittsburg Midway PM-12 Cherokee Co., KS T32S-R22E-Sec. 19 Depth: 427-438	Texture				Sedimentary Structures	Fossils	Abrasion			Visual Porosity	Comments (color, grains, etc.)
		M	W	P	G			N	M	A		
420	TOP OF CORE											
422												
424												
426												
428												
430												
432												
434						sharp based black shale						black shale
436												
438						highly brecciated chert clasts, tight fit, nearly no matrix in areas						highly brecciated chert with fine brown silty sand infill, subangular, unsorted, 2-60mm, almost no matrix

Depth	Gulf Oil Corporation Pittsburg Midway PM-12 Cherokee Co., KS T32S-R22E-Sec. 19 Depth: 438-456	Texture				Sedimentary Structures	Fossils	Abrasion			Visual Porosity	Comments (color, grains, etc.)
		M	W	P	G			N	M	A		
438						highly brecciated chert clasts, tight fit, nearly no matrix in areas					fracture	highly brecciated chert with fine brown silty sand infill, subangular, unsorted, 2-60mm, almost no matrix in some areas
440						highly brecciated chert clasts, tight fit, nearly no matrix in areas					fracture	highly brecciated chert with fine brown silty sand infill, subangular, unsorted, 2-60mm, almost no matrix in some areas
442						highly brecciated chert clasts, tight fit, nearly no matrix in areas					fracture	highly brecciated chert with fine brown silty sand infill, subangular, unsorted, 2-60mm, almost no matrix in some areas
444						highly brecciated chert clasts, tight fit, nearly no matrix in areas					fracture	highly brecciated chert with fine brown silty sand infill, subangular, unsorted, 2-60mm, almost no matrix in some areas
446						highly brecciated chert clasts, matrix supported					fracture	highly brecciated chert with fine brown silty sand infill up to 50%, subangular, unsorted, 2-60mm
448						highly brecciated chert clasts, matrix supported					fracture	highly brecciated chert with fine brown silty sand infill up to 50%, subangular, unsorted, 2-60mm
450						highly brecciated chert clasts, matrix supported					fracture	highly brecciated chert with fine brown silty sand infill up to 50%, subangular, unsorted, 2-60mm
452						highly brecciated chert clasts, tight fit, nearly no matrix in areas					fracture	highly brecciated chert with fine brown silty sand infill, subangular, unsorted, 2-60mm, almost no matrix in some areas
454						highly brecciated chert clasts, tight fit, nearly no matrix in areas					fracture	highly brecciated chert with fine brown silty sand infill, subangular, unsorted, 2-60mm, almost no matrix in some areas
456												

Depth	Gulf Oil Corporation Pittsburg Midway PM-12 Cherokee Co., KS T32S-R22E-Sec. 19 Depth: 456-474	Texture				Sedimentary Structures	Fossils	Abrasion			Visual Porosity	Comments (color, grains, etc.)
		M	W	P	G			N	M	A		
456						highly brecciated chert clasts, tight fit, nearly no matrix in areas				fracture	highly brecciated chert with fine brown silty sand infill, subangular, unsorted, 2-60mm, almost no matrix in some areas	
458						highly brecciated chert clasts, tight fit, nearly no matrix in areas				fracture	highly brecciated chert with fine brown silty sand infill, subangular, unsorted, 2-60mm, almost no matrix in some areas	
460						highly brecciated chert clasts, tight fit, nearly no matrix in areas				fracture	highly brecciated chert with fine brown silty sand infill, subangular, unsorted, 2-60mm, almost no matrix in some areas	
462						silty-peloidal packstone with chert clasts				tight	silty-peloidal packstone with subangular white chert clasts ~20mm	
464						brecciated				fracture	highly brecciated chert in fine brown silty sand, up to 60% matrix in areas, clasts are subangular, unsorted, 2-60mm	
466						brecciated				fracture	highly brecciated chert in fine brown silty sand, up to 60% matrix in areas, clasts are subangular, unsorted, 2-60mm	
468											silty-peloidal wackestone	
470						horsetail shale seams brecciated to massive chert nodules in silty-peloidal fill				tight	mottled blue-white-brown nodular chert interbedded with silty-peloidal wackestone	
472						horsetail shale seams brecciated to massive chert nodules in silty-peloidal fill				tight	mottled blue-white-brown nodular chert interbedded with silty-peloidal wackestone	
474						horsetail shale seams brecciated to massive chert nodules in silty-peloidal fill						

Depth	Gulf Oil Corporation Pittsburg Midway PM-12 Cherokee Co., KS T32S-R22E-Sec. 19 Depth: 474-492	Texture				Sedimentary Structures	Fossils	Abrasion			Visual Porosity	Comments (color, grains, etc.)
		M	W	P	G			N	M	A		
474						brecciated to massive chert nodules in silty-peloidal fill					tight	mottled blue-white-brown nodular chert interbedded with silty-peloidal wackestone
476						brecciated chert nodules in silty-peloidal fill					tight	mottled blue-white-brown nodular chert interbedded with silty-peloidal wackestone
478						lenticular bioturbation, parallel laminations					tight	dark grey-black mudstone, fine skeletal debris crinoid concentrations
480						lenticular bioturbation, parallel laminations					tight	dark grey-black mudstone, fine skeletal debris crinoid concentrations
482						30 mm crinoid bed lenticular bioturbation, parallel laminations					tight	dark grey-black mudstone, fine skeletal debris crinoid concentrations
484						lenticular bioturbation, parallel laminations					tight	dark grey-black mudstone, fine skeletal debris crinoid concentrations
486						lenticular bioturbation, parallel laminations					tight	dark grey-black mudstone, fine skeletal debris crinoid concentrations
488						lenticular bioturbation, parallel laminations					tight	dark grey-black mudstone, fine skeletal debris crinoid concentrations
490						lenticular bioturbation, parallel laminations					tight	dark grey-black mudstone, fine skeletal debris crinoid concentrations
492						5-8 mm crinoids					tight	dark grey-black mudstone, fine skeletal debris crinoid concentrations

Depth	Gulf Oil Corporation Pittsburg Midway PM-12 Cherokee Co., KS T32S-R22E-Sec. 19 Depth: 492-510	Texture				Sedimentary Structures	Fossils	Abrasion			Visual Porosity	Comments (color, grains, etc.)
		M	W	P	G			N	M	A		
492						lenticular bioturbation					tight	dark grey-black mudstone, fine skeletal debris crinoid concentrations
494											tight	25 mm black shale bed
496											tight	crinoid wackestone
498						fully to partially silicified fossil fragments					tight	crinoid wackestone 60 mm black shale bed
500						highly brecciated, matrix supported					fracture	dense chert, crinoid wackestone breccia, dark brown-black shale infill, karstic features
502						highly brecciated, matrix supported					fracture	dense chert, crinoid wackestone breccia, dark brown-black infill, karstic features
504						collapse feature, slickensides, debris clasts					fracture	crinoid wackestone fill
506						massive, dense, mottled, chert					tight	dense mottled blue chert, sharp base,
508						brecciated					very porous slightly moldic	chalky white tripolitic chert breccia, rounded clasts in white matrix, stains ankerite
510												

Depth	Gulf Oil Corporation Pittsburg Midway PM-12 Cherokee Co., KS T32S-R22E-Sec. 19 Depth: 510-528	Texture				Sedimentary Structures	Fossils	Abrasion			Visual Porosity	Comments (color, grains, etc.)
		M	W	P	G			N	M	A		
510						brecciated					very porous slightly moldic	chalky white tripolitic chert breccia, rounded clasts in white matrix, stains ankerite
512						brecciated					very porous slightly moldic	chalky white tripolitic chert breccia, rounded clasts in white matrix, stains ankerite
514						brecciated					very porous slightly moldic	chalky white tripolitic chert breccia, rounded clasts in white matrix, stains ankerite
516						brecciated					very porous slightly moldic	chalky white tripolitic chert breccia, rounded clasts in white matrix, stains ankerite
518						brecciated					very porous slightly moldic	chalky white tripolitic chert breccia, rounded clasts in white matrix, stains ankerite
520						silicified burrows					very porous slightly moldic	chalky white tripolitic chert breccia, rounded clasts in grey silty infill with chards of chert
522											tight	
524						horizontal shale seams					tight	crinoidal packstone, no sorting, unabraded, tend to accumulate in beds varies with increase shale areas of wackestone
526						horizontal shale seams					tight	crinoidal packstone, no sorting, unabraded, tend to accumulate in beds varies with increase shale areas of wackestone
528						chert						

Depth	Gulf Oil Corporation Pittsburg Midway PM-12 Cherokee Co., KS T32S-R22E-Sec. 19 Depth: 528-546	Texture				Sedimentary Structures	Fossils	Abrasion			Visual Porosity	Comments (color, grains, etc.)
		M	W	P	G			N	M	A		
528						stylolites					tight	crinoidal packstone, no sorting, unbraided, tend to accumulate in beds
530						horizontal shale seams chert					tight	crinoidal packstone, no sorting, unbraided, tend to accumulate in beds varies with increase shale areas of wackestone
532											tight	crinoidal packstone, no sorting, unbraided, tend to accumulate in beds
534						horizontal shale seams					tight	sharp based, shaly crinoidal wackestone, not sorted, unbraided
536						medium-highly brecciated dense mottled chert					fracture	light grey mottled chert breccia with angular sand sized fragments in fill (chert shards?)
538						medium-highly brecciated dense mottled chert					fracture	light grey mottled chert breccia with angular sand sized fragments in fill (chert shards?)
540						medium-highly brecciated dense mottled chert					fracture	light grey mottled chert breccia with angular sand sized fragments in fill (chert shards?)
542						medium-highly brecciated dense mottled chert					fracture	mottled dense white chert
544						medium-highly brecciated dense mottled chert					fracture	mottled dense white chert
546												

Depth	Gulf Oil Corporation Pittsburg Midway PM-12 Cherokee Co., KS T32S-R22E-Sec. 19 Depth: 546-564	Texture				Sedimentary Structures	Fossils	Abrasion			Visual Porosity	Comments (color, grains, etc.)
		M	W	P	G			N	M	A		
546						highly brecciated chert clasts in brown matrix					fracture tight	 mottled dense white chert
548						slightly brecciated dense mottled chert					fracture tight	highly brecciated white 3-40 mm angular chert clasts in dark brown matrix. very ratty looking, no sorting
550						slightly brecciated dense mottled chert					tight	mottled dense white chert
552						highly brecciated chert clasts in brown matrix					tight	highly brecciated white 3-40 mm angular chert clasts in dark brown matrix. very ratty looking, no sorting
554						dense mottled					tight	mottled dense white chert
556						medium intensity fractured white marble textured chert					dense with few 10 mm spar filled vugs	medium intensity fractured white marbly chert
558						medium intensity fractured white marble textured chert					dense with few 10 mm spar filled vugs	slightly fractured white marbly chert increase brecciation up section
560						slightly fractured white marble textured chert					dense with few 10 mm spar filled vugs	slightly fractured white marbly chert
562						highly brecciated chert clasts in brown matrix					fractures	highly brecciated white 3-40 mm angular chert clasts in dark brown matrix. very ratty looking, no sorting
564												

Depth	Gulf Oil Corporation Pittsburg Midway PM-12 Cherokee Co., KS T32S-R22E-Sec. 19 Depth: 564-582	Texture				Sedimentary Structures	Fossils	Abrasion			Visual Porosity	Comments (color, grains, etc.)
		M	W	P	G			N	M	A		
564						highly brecciated chert clasts in brown matrix					fracture	highly brecciated white 3-40 mm angular chert clasts in dark brown matrix. very ratty looking, no sorting
566						highly brecciated chert clasts in brown matrix					fracture	highly brecciated white 3-40 mm angular chert clasts in dark brown matrix. very ratty looking, no sorting
568						small fractures					tight	
570											tight	slightly fractured, marbly textured chert, 15 mm bryozoans
572						highly brecciated					fracture	fossiliferous mottled dense white chert
574						mottled dense white chert					tight	
576						mottled dense white chert					tight	fossiliferous mottled dense white chert
578						highly brecciated chert clasts in brown matrix					fracture	highly brecciated white 3-40 mm angular chert clasts in dark brown matrix. very ratty looking, no sorting
580						autoclastic brecciated chert with brown infill					fracture	autoclastic brecciated white angular chert clasts with brown infill
582						mottled blue- brown chert faint low angle laminations (>mm)					tight	mottled blue-white-brown chert interbedded with burrowed peloidal wacke- stone

Depth	Gulf Oil Corporation Pittsburg Midway PM-12 Cherokee Co., KS T32S-R22E-Sec. 19 Depth: 582-600	Texture				Sedimentary Structures	Fossils	Abrasion			Visual Porosity	Comments (color, grains, etc.)
		M	W	P	G			N	M	A		
		582										
584										tight	mottled blue-white-brown chert interbedded with burrowed peloidal wackestone	
586										tight	mottled blue-white-brown chert interbedded with burrowed peloidal wackestone	
588										tight	mottled blue-white-brown chert interbedded with burrowed peloidal wackestone	
590										tight	mottled blue-white-brown chert interbedded with burrowed peloidal wackestone	
592										tight	mottled blue-white-brown chert interbedded with burrowed peloidal wackestone	
594										tight	mottled blue-white-brown chert	
596										3-7 mm vugs	grey peloidal wackestone, crinoid debris	
598										1-5 mm vugs	grey peloidal wackestone, crinoid debris	
600												

Depth	Gulf Oil Corporation Pittsburg Midway PM-12 Cherokee Co., KS T32S-R22E-Sec. 19 Depth: 600-618	Texture				Sedimentary Structures	Fossils	Abrasion			Visual Porosity	Comments (color, grains, etc.)
		M	W	P	G			N	M	A		
600						burrows 4 mm shale bed				porous	dense porcellanite chert slightly brecciated interbedded with silty burrowed packstone	
602						burrows chalcidoney in fractures				porous	dense porcellanite chert slightly brecciated interbedded with silty burrowed packstone	
604						nodular chert replacement backfilled burrows				porous	dense porcellanite chert slightly brecciated interbedded with silty burrowed packstone	
606						backfilled burrows 6-15 mm shale beds				porous	dense porcellanite chert slightly brecciated interbedded with silty burrowed packstone	
608						burrows chalcidoney in fractures				porous	dense porcellanite chert slightly brecciated interbedded with silty burrowed packstone	
610						chert slightly brecciated, no matrix burrows				porous 5 mm vugs	dense porcellanite chert slightly brecciated interbedded with silty burrowed packstone	
612						chert slightly brecciated, no matrix burrows				porous 5 mm vugs	dense porcellanite chert slightly brecciated interbedded with silty burrowed packstone	
614						chert slightly brecciated, no matrix burrows				porous 5 mm vugs	dense porcellanite chert slightly brecciated interbedded with silty burrowed packstone	
616						chert slightly brecciated, no matrix burrows				porous	dense porcellanite chert slightly brecciated interbedded with silty burrowed packstone	
618						burrows						

Depth	Gulf Oil Corporation Pittsburg Midway PM-12 Cherokee Co., KS T32S-R22E-Sec. 19 Depth: 618-636	Texture				Sedimentary Structures	Fossils	Abrasion			Visual Porosity	Comments (color, grains, etc.)
		M	W	P	G			N	M	A		
618						scattered fossils molds					porous 1-5 mm molds	light grey silty, burrowed, crinoidal packstone increase molds up section silicified crinoids
620						whispy burrows scattered fossils molds					porous 1-5 mm molds	light grey silty, burrowed, crinoidal packstone increase molds up section silicified crinoids
622						whispy burrows scattered fossils molds					porous 1-5 mm molds	light grey silty, burrowed, crinoidal packstone silicified crinoids
624						whispy burrows scattered fossils shale seams					porous 1-5 mm molds	light grey silty, burrowed, crinoidal packstone silicified crinoids
626						whispy burrows scattered fossils concentration of crinoids					porous	light grey silty, burrowed, crinoidal packstone silicified crinoids
628						whispy burrows scattered fossils					porous	light grey silty, burrowed, crinoidal packstone silicified crinoids
630						whispy burrows scattered fossils					porous	light grey silty, burrowed, crinoidal packstone silicified crinoids
632						whispy burrows concentration of crinoids					porous	light grey silty, burrowed, crinoidal wackestone- packstone silicified crinoids
634						laminated shale seams					tight	light grey wackestone 1-10 mm crinoids
636												

Depth	Gulf Oil Corporation Pittsburg Midway PM-12 Cherokee Co., KS T32S-R22E-Sec. 19 Depth: 636-654	Texture				Sedimentary Structures	Fossils	Abrasion			Visual Porosity	Comments (color, grains, etc.)
		M	W	P	G			N	M	A		
636						laminated shale seams					tight	dark grey wackestone 1-10 mm crinoids
638						laminated shale seams					tight	dark grey wackestone 1-10 mm crinoids
640						laminated shale seams					tight	dark grey wackestone 1-10 mm crinoids
642						laminated shale seams					tight	dark grey wackestone 1-10 mm crinoids
644						laminated shale seams					tight	dark grey wackestone 1-10 mm crinoids
646						laminated shale seams					tight	dark grey wackestone 1-10 mm crinoids
648						laminated shale seams					tight	dark grey wackestone 1-10 mm crinoids
650						laminated shale seams					tight	dark grey wackestone 1-10 mm crinoids
652						laminated shale seams					tight	dark grey wackestone 1-10 mm crinoids
654						laminated shale seams					tight	dark grey wackestone 1-10 mm crinoids

Depth	Gulf Oil Corporation Pittsburg Midway PM-12 Cherokee Co., KS T32S-R22E-Sec. 19 Depth: 654-672	Texture				Sedimentary Structures	Fossils	Abrasion			Visual Porosity	Comments (color, grains, etc.)
		M	W	P	G			N	M	A		
654						laminated shale seams					tight	dark grey wackestone 1-10 mm crinoids
656						laminated shale seams					tight	dark grey wackestone 1-10 mm crinoids
658						laminated shale seams					tight	dark grey wackestone 1-10 mm crinoids
660						burrowed-whispy bedding 20-30 mm chalcondny with calcite center					tight	light grey wackestone, increased silt 1-10 mm crinoids
662						burrowed-whispy bedding 20-30 mm chalcondny with calcite center					tight	light grey wackestone, increased silt 1-10 mm crinoids
664						laminated shale seams					tight	dark grey wackestone 1-10 mm crinoids
666						laminated shale seams					tight	dark grey wackestone 1-10 mm crinoids
668						laminated shale seams					tight	dark grey wackestone 1-10 mm crinoids
670						burrowed-whispy bedding 30 mm chalcondny					tight	light grey wackestone 1-10 mm crinoids
672												

Depth	Gulf Oil Corporation Pittsburg Midway PM-12 Cherokee Co., KS T32S-R22E-Sec. 19 Depth: 672-690	Texture				Sedimentary Structures	Fossils	Abrasion			Visual Porosity	Comments (color, grains, etc.)
		M	W	P	G			N	M	A		
672						burrowed-whispy bedding 40 mm chalcodny with calcite center					tight	light grey bioturbated wackestone, increased shale
674						burrowed-whispy bedding concentration of grains					tight	light grey fossiliferous wackestone packstone large 20 mm crinoids
676						sharp base, poorly sorted, normally graded					tight	light grey fossiliferous wackestone packstone large 20 mm crinoids
678						laminated shale seams					tight	light grey crinoidal wackestone large 20 mm crinoids
680						laminated shale seams					tight	grey bioturbated wackestone
682						burrowed-whispy bedding					tight	light grey wackestone, increased silt
684						burrowed-whispy bedding nodular silica replacement					tight	light grey wackestone, increased silt
686						30 mm chalcodny concentration of grains silica replacement					tight	dark grey fossiliferous wackestone packstone
688						laminated shale seams silica replacement					tight	dark grey crinoidal wackestone 1-10 mm crinoids
690												

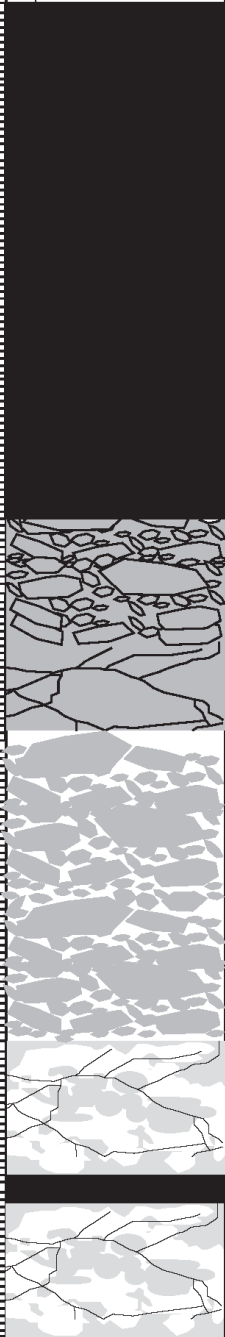
Depth	Gulf Oil Corporation Pittsburg Midway PM-12 Cherokee Co., KS T32S-R22E-Sec. 19 Depth: 690-708	Texture				Sedimentary Structures	Fossils	Abrasion			Visual Porosity	Comments (color, grains, etc.)
		M	W	P	G			N	M	A		
690						laminated shale seams silica replacement					tight	dark grey crinoidal wackestone 1-10 mm crinoids
692						laminated shale seams					tight	dark grey crinoidal wackestone 1-10 mm crinoids
694						laminated shale seams					tight	dark grey crinoidal wackestone 1-10 mm crinoids
696						laminated shale seams 50 mm chalcedony with calcite center silica replacement					tight	dark grey crinoidal wackestone coarse mineralization 1-10 mm crinoids
698						laminated shale seams					tight	dark grey crinoidal wackestone 1-10 mm crinoids
700						silica replacement					tight	dark grey crinoidal wackestone 1-10 mm crinoids
702						laminated shale seams					tight	dark grey crinoidal wackestone 1-10 mm crinoids
704						laminated shale seams					tight	dark grey crinoidal wackestone with black shale seams
706						silica replacement 25 mm chalcedony with calcite center					tight	silica replacement beds coarse mineralization
708												



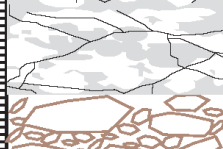
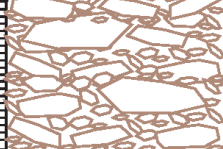
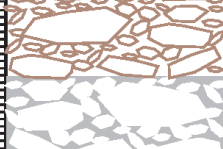

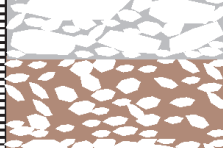
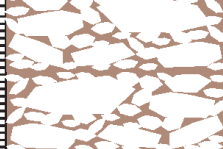


Depth	Gulf Oil Corporation Pittsburg Midway PM-12 Cherokee Co., KS T32S-R22E-Sec. 19 Depth: 708-726	Texture				Sedimentary Structures	Fossils	Abrasion			Visual Porosity	Comments (color, grains, etc.)
		M	W	P	G			N	M	A		
708						15 mm chalcidony with calcite center					tight	dark grey crinoidal wackestone
710						2 mm burrows stylolites					tight	light grey crinoidal lime wackestone
712						stylolites replacement seams following fractures					tight	light grey crinoidal lime mudstone
714						silty-shale package					tight	light grey crinoidal lime wackestone-mudstone
716						40 mm coarse white chalcidony with calcite center stylolites					tight	light grey crinoidal lime wackestone
718						10 mm coarse white chalcidony 40 mm shale seam stylolites					tight	light grey crinoidal lime wackestone
720						stylolites 2 mm shale seam					tight	light grey crinoidal lime wackestone
722						stylolites 2 mm shale seam					tight	light grey crinoidal lime wackestone
724						6 mm shale seam 5 mm shale seam stylolites 3 mm shale seam					tight	light grey fossiliferous lime wackestone
726						3 mm shale seam						

Depth	Gulf Oil Corporation Pittsburg Midway PM-12 Cherokee Co., KS T32S-R22E-Sec. 19 Depth: 726-744	Texture				Sedimentary Structures	Fossils	Abrasion			Visual Porosity	Comments (color, grains, etc.)
		M	W	P	G			N	M	A		
726						6 mm shale seam					tight	light grey fossiliferous lime wackestone
728											tight	light grey fossiliferous lime wackestone
730						shale seam					tight	light grey fossiliferous lime wackestone
732						3-5 mm shale seams bioturbated, mottled texture					tight	light grey fossiliferous lime wackestone
734						5 mm shale seams					tight	light grey crinoid (1-4 mm) rich lime wackestone
736						bioturbated, mottled texture with random 1-3 mm pyrite					tight	light grey lime wackestone, bioturbated, pyrite nodules
738						deformed and drapped beds, slickensides 4-10 mm spar					fracture	fossiliferous wackestone, angular breccia clasts 4-25 mm with dark grey shaly infill normal fault
740						bioturbated, mottled texture					tight	grey-green silty lime mud
742						bioturbated, mottled texture					tight	grey-green silty lime mud
744						4-9 mm pyrite nodules						

Depth	Gulf Oil Corporation Pittsburg Midway PM-12 Cherokee Co., KS T32S-R22E-Sec. 19 Depth: 744-760	Texture				Sedimentary Structures	Fossils	Abrasion			Visual Porosity	Comments (color, grains, etc.)
		M	W	P	G			N	M	A		
744						burrowed to bioturbated, mottled texture, mostly sub-horizontal					tight	grey-green silty lime mud
746						2-3 mm light grey filled burrows 3-4 mm black lined burrows with light grey fill					tight	grey-green silty lime mud
748						network of burrows					tight	grey-green silty lime mud
750						1 mm laminations						light grey, peloidal interbedded with thin laminations
752						small (1-4 mm) rip-up clasts					open vug (12 mm) partially spar filled	white angular rip-up clasts
754						floating brecciated clasts 7 mm pyrite bed 2-6 mm backfilled burrows					open vugs (2-8 mm) partially spar filled	light grey, peloidal packstone white brecciated subrounded interclasts (5-15 mm)
754						planar bedding					tight	light grey mud disrupted by dark grey burrow mud intraclasts subrounded 4-20 mm surrounded by quartz sand matrix
756						horizontal to vertical burrows 4 mm pyrite coarse pink dolomite					tight	medium to dark grey peloidal packstone mostly peloidal
758						autoclastic brecciation					fracture	medium to dark grey peloidal packstone mostly peloidal 1-4 mm crinoids
760	Base of Mississippian											

Gulf Oil Corporation
Pittsburg-Midway
PM-21
Cherokee Co., KS
T32S-R22E-Sec.13

Depth	Gulf Oil Corporation Pittsburg-Midway PM-21 Cherokee Co., KS T32S-R22E-Sec.13 Depth: 381-399	Texture				Sedimentary Structures	Fossils	Abrasion			Visual Porosity	Comments (color, grains, etc.)
		M	W	P	G			N	M	A		
381						black shale				tight	black shale	
383						black shale				tight	black shale	
385						black shale				tight	black shale	
387						black shale				tight	black shale	
389						ashy loose rubble				fracture	fracture	ashy rubble to whole ashy-like substance completely fractured
391						loose brecciated rubble				fracture	fracture	dirty grey loose brecciated chert rubble, 5-60 mm angular clasts, some are plate-like with slickensides
393						loose brecciated rubble				fracture	fracture	dirty grey loose brecciated chert rubble, 5-60 mm angular clasts, some are plate-like with slickensides
395						mottled white-blue chert autoclastically brecciated				fracture	fracture	mottled white-blue chert autoclastically brecciated
397					150 mm shale bed				fracture	fracture	mottled white-blue chert autoclastically brecciated	
399												

Depth	Gulf Oil Corporation Pittsburg-Midway PM-21 Cherokee Co., KS T32S-R22E-Sec.13 Depth: 399-417	Texture				Sedimentary Structures	Fossils	Abrasion			Visual Porosity	Comments (color, grains, etc.)
		M	W	P	G			N	M	A		
399						mottled white-blue chert autoclastically brecciated				fracture	mottled white-blue chert autoclastically brecciated	
401						mottled white-blue chert autoclastically brecciated				fracture	mottled white-blue chert autoclastically brecciated	
403						mottled white-blue chert autoclastically brecciated				fracture	mottled white-blue chert autoclastically brecciated	
405						loose chert rubble				fracture	white angular chert clasts 2-20 mm, loose rubble in box, clasts have brown tint to completely brown sides	
407						loose chert rubble				fracture	white angular chert clasts 2-20 mm, loose rubble in box, clasts have brown tint to completely brown sides	
409						white brecciated chert clasts				fracture	white angular chert clasts 2-20 mm in light grey matrix, clast supported	
411						white brecciated chert clasts				fracture	white angular chert clasts 2-5 mm in light brown matrix, matrix supported	
413						white brecciated chert clasts				fracture	white angular chert clasts 2-20 mm in light brown matrix, clast supported	
415						massive white chert				porous	massive white chert, porous, possibly tripolitic chert	
417												

Depth	Gulf Oil Corporation Pittsburg-Midway PM-21 Cherokee Co., KS T32S-R22E-Sec.13 Depth: 417-435	Texture				Sedimentary Structures	Fossils	Abrasion			Visual Porosity	Comments (color, grains, etc.)
		M	W	P	G			N	M	A		
417						massive white chert				porous	massive white chert, porous, possibly tripolitic chert	
419						massive white chert				porous	massive white chert, porous, possibly tripolitic chert	
421						loose chert rubble with partially whole mottled white-blue chert				fracture	white angular chert clasts 2-20 mm, loose rubble in box, loose brownish color, mostly white-grey clasts, interbedded with 20-60 mm beds of mottled white-blue chert	
423						loose chert rubble with partially whole mottled white-blue chert				fracture	white angular chert clasts 2-20 mm, loose rubble in box, loose brownish color, mostly white-grey clasts, interbedded with 20-60 mm beds of mottled white-blue chert	
425						loose chert rubble with partially whole mottled white-blue chert				fracture	white angular chert clasts 2-20 mm, loose rubble in box, loose brownish color, mostly white-grey clasts, interbedded with 20-60 mm beds of mottled white-blue chert	
427						loose chert rubble				fracture	white angular chert clasts 2-20 mm, loose rubble in box, loose brownish color, mostly white-grey clasts	
429						loose chert rubble				fracture	white angular chert clasts 2-20 mm, loose rubble in box, clasts have brown tint to completely brown sides	
431						loose chert rubble				fracture	white angular chert clasts 2-20 mm, loose rubble in box, clasts have brown tint to completely brown sides	
433						white brecciated chert clasts				fracture	white angular chert clasts 2-20 mm in light brown matrix, clast supported	
435												

Depth	Gulf Oil Corporation Pittsburg-Midway PM-21 Cherokee Co., KS T32S-R22E-Sec.13 Depth: 435-453	Texture				Sedimentary Structures	Fossils	Abrasion			Visual Porosity	Comments (color, grains, etc.)
		M	W	P	G			N	M	A		
435						white brecciated chert clasts				fracture	white angular chert clasts 2-20 mm in light brown matrix, clast supported	
437						white brecciated chert clasts				fracture	white angular chert clasts 2-20 mm in light grey matrix, clast supported	
439						fractured mottled dense white-blue chert				tight	white-blue mottled massive chert, fractures filled with chalcedony	
441						mottled dense blue-white chert 15 mm pyrite nodule				tight	blue-white mottled massive chert abundant pyrite, internal quartz silt infill	
443						fossiliferous packstone				tight	light grey crinoidal packstone, dominantly crinoids ranging from 1-3 mm, contains other fossils, autoclastically breccia- ted, abundant stylonites, iron-poor calcite	
445						fossiliferous packstone				tight	light grey crinoidal packstone, dominantly crinoids ranging from 1-3 mm, contains other fossils, abundant stylonites, iron-poor calcite	
447						mottled dense white-blue chert				tight	white-blue mottled massive chert	
449						slightly brecciated				very porous	chalky white tripolitic chert slightly to highly brecciated with dark grey circular to elongate replacement spots, iron-poor calcite	
451						slightly brecciated				very porous	chalky white tripolitic chert slightly to highly brecciated with dark grey circular to elongate replacement spots, iron-poor calcite	
453												

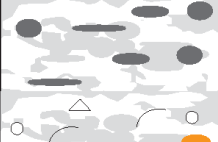

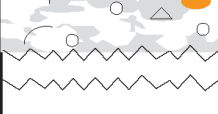
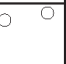

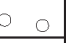
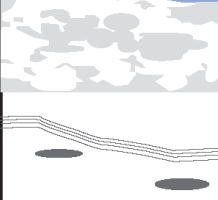
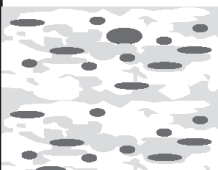
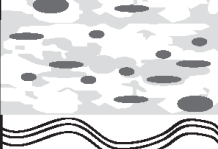

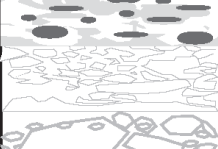

Depth	Gulf Oil Corporation Pittsburg-Midway PM-21 Cherokee Co., KS T32S-R22E-Sec.13 Depth:453-471	Texture				Sedimentary Structures	Fossils	Abrasion			Visual Porosity	Comments (color, grains, etc.)
		M	W	P	G			N	M	A		
453						slightly brecciated					very porous	chalky white tripolitic chert slightly to highly brecciated with dark grey circular to elongate replacement spots, iron-poor calcite
455						slightly brecciated					very porous	chalky white tripolitic chert slightly to highly brecciated with dark grey circular to elongate replacement spots, iron-poor calcite
457						2 mm shale bed with iron stain on both sides						
457						slightly brecciated					very porous	chalky white tripolitic chert slightly to highly brecciated with dark grey circular to elongate replacement spots, iron-poor calcite
459						slightly brecciated					very porous	chalky white tripolitic chert slightly to highly brecciated with dark grey circular to elongate replacement spots, iron-poor calcite
461						whispy laminations					very porous	chalky white tripolitic chert fairly massive with fine whispy laminations, iron-poor calcite
463						whispy laminations					very porous	chalky white tripolitic chert fairly massive with fine whispy laminations, iron-poor calcite
465						slightly brecciated					very porous	chalky white tripolitic chert slightly to highly brecciated with dark grey circular to elongate replacement spots, iron-poor calcite
467						slightly brecciated					very porous	chalky white tripolitic chert slightly to highly brecciated with dark grey circular to elongate replacement spots, iron-poor calcite
469						slightly brecciated					very porous	chalky white tripolitic chert slightly to highly brecciated with dark grey circular to elongate replacement spots, iron-poor calcite
471												

Depth	Gulf Oil Corporation Pittsburg-Midway PM-21 Cherokee Co., KS T32S-R22E-Sec.13 Depth: 471-489	Texture				Sedimentary Structures	Fossils	Abrasion			Visual Porosity	Comments (color, grains, etc.)
		M	W	P	G			N	M	A		
471						slightly brecciated					very porous	chalky white tripolitic chert slightly to highly brecciated with dark grey circular to elongate replacement spots, iron-poor calcite
473						slightly brecciated					very porous	chalky white tripolitic chert slightly to highly brecciated with dark grey circular to elongate replacement spots, iron-poor calcite
475						slightly brecciated					very porous	chalky white tripolitic chert slightly to highly brecciated with dark grey circular to elongate replacement spots, iron-poor calcite
477						slightly brecciated					very porous	chalky white tripolitic chert slightly to highly brecciated with dark grey circular to elongate replacement spots, iron-poor calcite
479						slightly brecciated					very porous	chalky white tripolitic chert slightly to highly brecciated with dark grey circular to elongate replacement spots, iron-poor calcite
481						mottled dense white-blue chert					porous	white-blue mottled massive chert, contains dark grey circular to elongate replacement spots, iron-poor calcite
483						mottled dense white-blue chert iron-stained bed					porous	white-blue mottled massive chert, contains dark grey circular to elongate replacement spots
485						mottled dense white-blue chert					porous	white-blue dense mottled chert, with iron-stained beds microkarstic surface with internal sediment infill
487						fossiliferous packstone stylolites					tight	dark grey fossiliferous packstone, dominantly crinoids with abundant bivalves/brachs ranging from 2-4 mm, stylolites, iron-poor calcite
489												

Depth	Gulf Oil Corporation Pittsburg-Midway PM-21 Cherokee Co., KS T32S-R22E-Sec.13 Depth: 489-507	Texture				Sedimentary Structures	Fossils	Abrasion			Visual Porosity	Comments (color, grains, etc.)
		M	W	P	G			N	M	A		
489						fossiliferous packstone 3 mm shale bed no visible whole fossils					tight	dark grey fossiliferous packstone, fossils 2-5 mm, stylolites, iron-poor calcite
491						mottled dense white-blue chert 3 mm shale bed with iron stain					tight	white-blue dense mottled chert 3 mm shale bed iron stained above
493						mottled dense white-blue chert					fracture	white-blue dense mottled chert autoclastically brecciated
495						highly brecciated chert					fracture	highly brecciated angular 2-15 mm white chert clasts in brown-ashy matrix
497						mottled dense white-blue chert					tight	dark grey fossiliferous packstone, fossils 2-5 mm, stylolites, iron-poor calcite, interbedded with mottled dense white-blue chert
499						fossiliferous packstone mottled dense white-blue chert					tight	dark grey fossiliferous packstone, fossils 2-5 mm, stylolites, iron-poor calcite, interbedded with mottled dense white-blue chert
501						fossiliferous packstone autoclastic brecciated					tight fracture	dark grey fossiliferous packstone, autoclastically brecciated, fossils 2-5 mm, stylolites, iron-poor calcite
503						faint horizontal laminations white chert with silicified fossil fragments					tight	dark grey fossiliferous packstone interbedded with white dense chert with silicified fossil fragments
505						fossiliferous packstone mottled dense white-blue chert					tight	dark grey fossiliferous packstone interbedded with mottled dense white-blue chert, iron-poor calcite
507						mottled dense white-blue chert						

Depth	Gulf Oil Corporation Pittsburg-Midway PM-21 Cherokee Co., KS T32S-R22E-Sec.13 Depth: 507-525	Texture				Sedimentary Structures	Fossils	Abrasion			Visual Porosity	Comments (color, grains, etc.)
		M	W	P	G			N	M	A		
507						mottled blue-white chert					tight	mottled dark grey-white chert massive
509						fossiliferous packstone					tight	dark grey fossiliferous packstone, dominately crinoids with abundant bivalves/brachs ranging from 2-10 mm, strolites, iron-poor calcite
511						autoclastic brecciation strolites					fracture	dark grey fossiliferous packstone, interrupted by 3 surfaces of mm shale beds with iron staining surrounding both sides of shale, autoclastic brecciation, strolites
513						autoclastic brecciation strolites					fracture	dark grey fossiliferous packstone, interrupted by 3 surfaces of mm shale beds with iron staining surrounding both sides of shale, autoclastic brecciation, strolites
515						fossiliferous packstone strolites					tight	dark grey fossiliferous packstone, dominately crinoids with abundant bivalves/brachs ranging from 2-10 mm, strolites, iron-poor calcite
517						fossiliferous packstone strolites					tight	dark grey fossiliferous packstone, dominately crinoids with abundant bivalves/brachs ranging from 2-4 mm, strolites, iron-poor calcite
519						fossiliferous packstone strolites					tight	dark grey fossiliferous packstone, dominately crinoids with abundant bivalves/brachs ranging from 2-10 mm, strolites, iron-poor calcite
521						fossiliferous packstone strolites					tight	dark grey fossiliferous packstone, dominately crinoids with abundant bivalves/brachs ranging from 2-10 mm, strolites, iron-poor calcite
523						fossiliferous packstone strolites					tight	dark grey fossiliferous packstone, dominately crinoids with abundant bivalves/brachs ranging from 2-10 mm, strolites, iron-poor calcite
525						fossiliferous packstone strolites					tight	dark grey fossiliferous packstone, dominately crinoids with abundant bivalves/brachs ranging from 2-10 mm, strolites, iron-poor calcite

Depth	Gulf Oil Corporation Pittsburg-Midway PM-21 Cherokee Co., KS T32S-R22E-Sec.13 Depth: 525-543	Texture				Sedimentary Structures	Fossils	Abrasion			Visual Porosity	Comments (color, grains, etc.)
		M	W	P	G			N	M	A		
525						fossiliferous packstone stylolites					tight	dark grey fossiliferous packstone, dominately crinoids ranging from 2-10 mm, stylolites, iron-poor calcite
527						fossiliferous packstone stylolites					tight	dark grey fossiliferous packstone, dominately crinoids ranging from 2-10 mm, stylolites, iron-poor calcite
529						fossiliferous packstone stylolites					tight	dark grey fossiliferous packstone, dominately crinoids ranging from 2-10 mm, stylolites, iron-poor calcite
531						fossiliferous packstone stylolites					tight	dark grey fossiliferous packstone, dominately crinoids ranging from 2-10 mm, stylolites, iron-poor calcite
533						fossiliferous packstone stylolites					tight	dark grey fossiliferous packstone, dominately crinoids ranging from 2-10 mm, stylolites, iron-poor calcite
535						fine horizontal laminations fossiliferous packstone iron-stained stylolites					tight	dark grey fossiliferous packstone, dominately crinoids ranging from 2-10 mm, stylolites, fine horizontal laminations, iron-poor calcite
537						fossiliferous packstone stylolites					tight	dark grey fossiliferous packstone, dominately crinoids ranging from 2-10 mm, stylolites, fine horizontal laminations, iron-poor calcite
539						massive white- blue chert autoclastically brecciated					fracture	dark grey fossiliferous packstone, dominately crinoids ranging from 2-10 mm, interbedded with massive white-blue chert autoclastically brecciated,
541						fine horizontal laminations fossiliferous packstone					tight	dark grey fossiliferous packstone, stylolites, loose large fossils, visible fossils 2-4 mm but packstone probably made of abraided fossil fragments
543												

Depth	Gulf Oil Corporation Pittsburg-Midway PM-21 Cherokee Co., KS T32S-R22E-Sec.13 Depth: 561-579	Texture				Sedimentary Structures	Fossils	Abrasion			Visual Porosity	Comments (color, grains, etc.)
		M	W	P	G			N	M	A		
561						massive blue-white chert 10 mm iron stained nodules					fracture	blue-white to white-blue mottled massive chert. contains dark grey circular to elongate replacement spots, silicified fossils, no stain
563						massive blue-white chert packstone					fracture	blue-white to white-blue mottled massive chert. contains dark grey circular to elongate replacement spots, silicified fossils, packstone is fine grained
565						massive blue-white chert, coarse calcite filling in fractures					fracture	blue-white to white-blue mottled massive chert. contains dark grey circular to elongate replacement spots, poss. replaced burrows? no stain
567						white chalky chert, wispy seams					fracture	white porous chalky chert, with grey wispy seams, circular to elongate replacement spots,
569						massive blue-white chert					fracture	blue-white to white-blue mottled massive chert. contains dark grey circular to elongate replacement spots, poss. replaced burrows? no stain
571						massive blue-white chert					fracture	blue-white to white-blue mottled massive chert. contains dark grey circular to elongate replacement spots, poss. replaced burrows? no stain
573						wispy shale seams fine horizontal laminations					tight	light grey burrowed packstone with fine horizontal laminations black shale bed
575						brecciated white chert					fracture, 3-5 mm vugs	white porous chalky brecciated chert
577						white chert rubble					fracture	white porous chalky chert rubble, ferroan dolomite
579												

Depth	Gulf Oil Corporation Pittsburg-Midway PM-21 Cherokee Co., KS T32S-R22E-Sec.13 Depth: 579-597	Texture				Sedimentary Structures	Fossils	Abrasion			Visual Porosity	Comments (color, grains, etc.)
		M	W	P	G			N	M	A		
579						white chert rubble 3 mm shale bed				fracture	white porous chalky chert rubble, ferroan dolomite	
581						white chert rubble				fracture	white porous chalky chert rubble, ferroan dolomite forams found in some loose nodules	
583						white chert rubble				fracture	white porous chalky chert rubble, ferroan dolomite	
585						brecciated white chert				fracture, porous	white porous chalky brecciated chert, held together in areas, others are just rubble, ferroan dolomite	
587						brecciated white chert white chert rubble				fracture, porous	white porous chalky brecciated chert, held together in areas, others are just rubble, ferroan dolomite	
589						brecciated white chert				fracture, porous	white porous chalky brecciated chert, held together in areas, others are just rubble, ferroan dolomite	
591						white chert rubble brecciated white chert				fracture porous	white porous chalky brecciated chert, held together in areas, others are just rubble, ferroan dolomite contains sparse forams and bivalves within a 50 mm bed	
593						white chert rubble				fracture	white porous chalky chert rubble 5-40 mm nodules, ferroan dolomite	
595						white chert rubble 25 mm coarse pink baroque dolomite				fracture	white porous chalky chert rubble 5-40 mm nodules, ferroan dolomite	
597												

Depth	Gulf Oil Corporation Pittsburg-Midway PM-21 Cherokee Co., KS T32S-R22E-Sec.13 Depth: 597-615	Texture				Sedimentary Structures	Fossils	Abrasion			Visual Porosity	Comments (color, grains, etc.)
		M	W	P	G			N	M	A		
597						faint horizontal laminations				tight	light grey fine-grained packstone with faint horizontal laminations	
599						massive blue-white chert				fracture	blue-white to white-blue mottled massive chert. contains dark grey 2-5 mm circular to elongate replacement spots, poss. replaced burrows? no stain	
601						massive blue-white chert				fracture	blue-white to white-blue mottled massive chert. contains dark grey 2-5 mm circular to elongate replacement spots, poss. replaced burrows? no stain	
603						white chert rubble				fracture, some vugs	loose white chert rubble in box	
605						massive blue-white chert				fracture	blue-white to white-blue mottled massive chert. contains dark grey 2-5 mm circular to elongate replacement spots, poss. replaced burrows? no stain	
607						crackle-brecciated blue-white chert interbedded with burrowed wackstone with fine horizontal laminae				fracture	crackle brecciated mottled blue-white dense chert, some fractures filled with chalcedony, interbedded with wackstone- iron-poor calcite	
609						crackle-brecciated blue-white chert interbedded with wackstone				fracture	crackle brecciated mottled blue-white dense chert, some fractures filled with chalcedony, interbedded with wackstone-iron-poor calcite	
611						missing core					missing core	
613						crackle-brecciated blue-white chert interbedded with wackstone				fracture	crackle brecciated mottled blue-white dense chert, some fractures filled with chalcedony, interbedded with wackstone iron-poor calcite	
615						crackle-brecciated blue-white chert interbedded with wackstone				fracture	crackle brecciated mottled blue-white dense chert, some fractures filled with chalcedony, interbedded with wackstone iron-poor calcite	

Depth	Gulf Oil Corporation Pittsburg-Midway PM-21 Cherokee Co., KS T32S-R22E-Sec.13 Depth: 615-633	Texture				Sedimentary Structures	Fossils	Abrasion			Visual Porosity	Comments (color, grains, etc.)
		M	W	P	G			N	M	A		
615						crackle-brecciated blue-white chert interbedded with wackstone				fracture	crackle brecciated mottled blue-white dense chert, some fractures filled with chalcedony, interbedded with wackstone-iron-poor calcite	
617						crackle-brecciated blue-white chert interbedded with wackstone				fracture	crackle brecciated mottled blue-white dense chert, some fractures filled with chalcedony, interbedded with wackstone-iron-poor calcite	
619						crackle-brecciated blue-white chert interbedded with wackstone				fracture	crackle brecciated mottled blue-white dense chert, some fractures filled with chalcedony, interbedded with wackstone-iron-poor calcite	
621						crackle-brecciated blue-white chert				fracture	variable mottled blue-white dense chert, fractured to completely crackle brecciated, some fractures filled with chalcedony	
623						crackle-brecciated blue-white chert				fracture	variable mottled blue-white dense chert, fractured to completely crackle brecciated, some fractures filled with chalcedony	
625						burrowed wackstone with fine horizontal laminations				fracture	variable mottled blue-white dense chert, fractured to completely crackle brecciated, some fractures filled with chalcedony	
627						crackle-brecciated blue-white chert				fracture	variable mottled blue-white dense chert, fractured to completely crackle brecciated, some fractures filled with chalcedony	
629						crackle-brecciated blue-white chert				fracture, 10 mm vugs	variable mottled blue-white dense chert, fractured to completely crackle brecciated, some fractures filled with chalcedony	
631						crackle-brecciated blue-white chert				fracture	variable mottled blue-white dense chert, fractured to completely crackle brecciated, some fractures filled with chalcedony, completely silicified, no fizz, no stain	
633						crackle-brecciated blue-white chert				fracture	variable mottled blue-white dense chert, fractured to completely crackle brecciated, some fractures filled with chalcedony, completely silicified, no fizz, no stain	

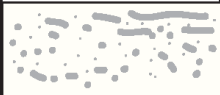
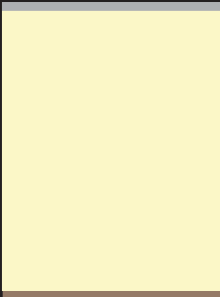



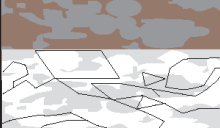
Depth	Gulf Oil Corporation Pittsburg-Midway PM-21 Cherokee Co.,KS T32S-R22E-Sec.13 Depth:633-651	Texture				Sedimentary Structures	Fossils	Abrasion			Visual Porosity	Comments (color, grains,etc.)
		M	W	P	G			N	M	A		
633						burrowed wackestone with fine horizontal laminations, can be wispy around nodular chert					fracture	mottled white-blue chert interbedded with wackestone
635						crackle-brecciated white chert					fracture	crackle brecciated white chert
637						crackle-brecciated white chert variable white-blue mottled chert					fracture	crackle brecciated white chert with mottled white-blue chert
639						missing core (box messed up)						missing core
641						variable blue-white mottled chert					fracture	variable mottled blue-white dense chert, fractured, fractures filled with chalcedony
643						burrowed wackestone with fine horizontal laminations, can be wispy around nodular chert					fracture	crackle brecciated white chert interbedded with wackestone
645						crackle-brecciated white chert variable blue-white mottled chert					fracture	crackle brecciated white chert with mottled blue-white chert
647						massive white chert white chert rubble in box					fracture	mottled white-blue dense chert, loose white chert rubble
649						variable blue-white mottled chert, highly brecciated-crackle breccia					fracture	variable mottled blue-white dense chert, often fractured to brecciated, fractures filled with chalcedony, interbedded with small beds/nodules of wackestone
651												

Depth	Gulf Oil Corporation Pittsburg-Midway PM-21 Cherokee Co., KS T32S-R22E-Sec.13 Depth: 651-669	Texture				Sedimentary Structures	Fossils	Abrasion			Visual Porosity	Comments (color, grains, etc.)
		M	W	P	G			N	M	A		
651						burrowed wackestone with fine horizontal laminations, can be wispy around nodular chert				fracture	variable mottled blue-white dense chert, often fractured to brecciated, fractures filled with chalcedony, interbedded with beds of wackestone	
653						variable blue-white mottled chert				fracture	variable mottled blue-white dense chert, often fractured to brecciated, fractures filled with chalcedony, interbedded with beds of wackestone	
655						variable blue-white mottled chert				fracture	variable mottled blue-white dense chert, often fractured to brecciated, fractures filled with chalcedony, interbedded with beds of wackestone	
657						variable blue-white mottled chert				fracture	variable mottled blue-white dense chert, often fractured to brecciated, fractures filled with chalcedony, interbedded with beds of wackestone	
659						variable blue-white mottled chert interbedded with burrowed wackestone				fracture	variable mottled blue-white dense chert, often fractured to brecciated, fractures filled with chalcedony, interbedded with beds of wackestone	
661						variable blue-white mottled chert				fracture	variable mottled blue-white dense chert, often fractured to brecciated, interbedded with beds of wackestone	
663						variable blue-white mottled chert				fracture	variable mottled blue-white dense chert, often fractured to brecciated, interbedded with beds of wackestone	
665						30 mm coarse quartz				fracture	mottled blue-white dense chert with coarse quartz mineralization, completely silicified, no fizz, no stain	
667						burrowed wackestone with fine horizontal laminations blue-white mottled chert				fracture	mottled blue-white dense chert slightly fractured overlain by dark grey burrowed wackestone	
669						blue-white mottled chert						

Depth	Gulf Oil Corporation Pittsburg-Midway PM-21 Cherokee Co., KS T32S-R22E-Sec.13 Depth: 699-687	Texture				Sedimentary Structures	Fossils	Abrasion			Visual Porosity	Comments (color, grains, etc.)
		M	W	P	G			N	M	A		
669						50 mm coarse chalcidony/quartz				tight	large 50 mm coarse chalcidony with quartz center mineralization	
671						dense mottled chert					mottled blue-white dense chert	
673						burrowed wacke- stone autoclastically brecciated white chert				fracture	autoclastically brecciated white chert overlain by dark grey burrowed packstone	
675						dense mottled chert, fractured				fracture	mottled blue-white dense chert slightly fractured overlain by dark grey burrowed packstone	
677						burrowed wacke- stone with 10-40 mm chert nodules				tight	dark grey burrowed wacke- stone interbedded with 10-40 mm chert nodules	
679						missing core					missing core	
682						1-4 mm planar beds and short 2-5 mm dark horizon- tal lines, possibly burrows or organic matter				tight	dark grey silty wackestone with horizontal planar lamina- tions and horizontal wispy lamination possibly from burrows, increase in silt upsection, iron-poor calcite	
683						1-4 mm planar beds and short 2-5 mm dark horizon- tal lines, possibly burrows or organic matter				tight	dark grey to black mudstone with horizontal planar lamina- tions and horizontal wispy lamination possibly from burrows, iron-poor calcite	
685						1-2 mm planar beds and short 2-5 mm dark horizon- tal laminations, possibly burrows				tight	dark grey to black mudstone with horizontal planar lamina- tions and horizontal wispy lamination possibly from burrows, iron-poor calcite	
687						1-2 mm planar beds and short 2-5 mm dark horizon- tal laminations, possibly burrows				tight	dark grey to black mudstone with horizontal planar lamina- tions and horizontal wispy lamination possibly from burrows, iron-poor calcite	

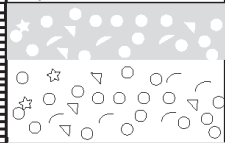

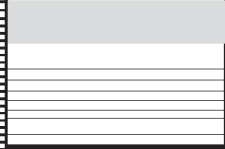
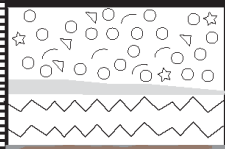



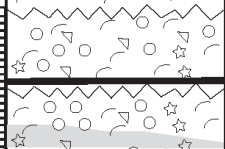



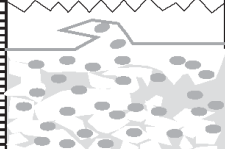


Depth	Gulf Oil Corporation Pittsburg-Midway PM-21 Cherokee Co., KS T32S-R22E-Sec.13 Depth: 687-705	Texture				Sedimentary Structures	Fossils	Abrasion			Visual Porosity	Comments (color, grains, etc.)
		M	W	P	G			N	M	A		
687						1-2 mm planar beds and short 2-5 mm dark horizontal laminations, possibly burrows				tight	dark grey to black mudstone with horizontal planar laminations and horizontal whispy laminations possibly from burrows, iron-poor calcite	
689						thick 4 mm planar beds and short 2-5 mm dark horizontal laminations, possibly burrows				tight	dark grey to black mudstone with horizontal planar laminations and horizontal whispy laminations possibly from burrows, iron-poor calcite	
691						30 mm chalcidony planar beds and short 2-5 mm dark horizontal laminations, possibly burrows				tight	dark grey to black mudstone with horizontal planar laminations and horizontal whispy laminations possibly from burrows, iron-poor calcite	
693						planar beds and short 2-5 mm dark horizontal laminations, possibly burrows				tight	dark grey to black mudstone with horizontal planar laminations and horizontal whispy laminations possibly from burrows, iron-poor calcite	
695						20-35 mm coarse chalcidony almost breccia texture ??				porous	silty grainy packstone with horizontal and vertical burrows, coarse mineralization, darkend grains, porous, iron-poor calcite	
697						burrows 15 mm coarse chalcidony mottled texture with dark grains				porous	silty grainy packstone with horizontal and vertical burrows, coarse mineralization, darkend grains, porous, iron-poor calcite	
699						5-10 mm coarse quartz surrounded by pyrite planar beds mottled texture				tight porous	silty grainy mottled packstone increased mud with planar beds cause loss of porosity, coarse mineralization with draped beds	
701						stylonites mottled texture				porous	silty grainy packstone with horizontal and vertical burrows, pyrite nodules, darkend grains, porous, iron-poor calcite	
703						1-3 mm dark grains 1-4 mm pyrite nodules horizontal and vertical burrows				porous	silty grainy packstone with horizontal and vertical burrows, pyrite nodules, darkend grains, porous, iron-poor calcite	
705						horizontal and vertical burrows						










Gulf Oil Corporation
Pittsburg Midway
PM-8
Cherokee Co., KS
T32S-R23E-Sec. 5

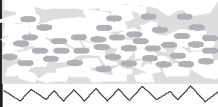



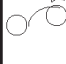
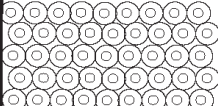






Depth	Gulf Oil Corporation Pittsburg Midway PM-8 Cherokee Co., KS T32S-R23E-Sec. 5 Depth: 384-398	Texture				Sedimentary Structures	Fossils	Abrasion			Visual Porosity	Comments (color, grains, etc.)
		M	W	P	G			N	M	A		
380												
382												
384	TOP OF CORE											
384						white tripolitic chert, mottled to furry-like				very porous	porous white tripolitic chert slightly mottled, almost looks fur tree like in areas of high concentration, others are just spots or blotchy	
386						10 mm black shale 50 mm ashy-like rubble				surface very porous	porous white tripolitic chert slightly mottled ashy-like rubble topped with black shale very porous tan tripolitic chert massive, stain ankerite	
388						tan tripolitic chert				very porous	very porous tan tripolitic chert massive, stain ankerite	
390						tan tripolitic chert				porous breccia	porous tan-white tripolitic chert autoclastically breccia- ated, angular 2-25 mm clasts, infill is brown silty quartz, infill increases up section, partially stained ankerite	
392						tan-grey dirty rubble brown infill between clasts				porous breccia	porous tan-white tripolitic chert autoclastically breccia- ated, angular 2-25 mm clasts, infill is brown silty quartz, partially stained ankerite	
394						black shale ~1 ft				tight	black shale with pyrite nodules	
396						mottled chert brecciated				breccia	white-grey mottled chert autoclastically brecciated	
398						brown-grey blotchy chert mottled chert brecciated				breccia	white-grey mottled chert autoclastically brecciated interbedded with brown-grey blotchy cherty-ls	

Depth	Gulf Oil Corporation Pittsburg Midway PM-8 Cherokee Co., KS T32S-R23E-Sec. 5 Depth: 398-416	Texture				Sedimentary Structures	Fossils	Abrasion			Visual Porosity	Comments (color, grains, etc.)
		M	W	P	G			N	M	A		
398						mottled chert brecciated brown-grey blotchy chert					breccia	white-grey mottled chert autoclastically brecciated interbedded with brown-grey blotchy cherty-ls, sharp contacts
400						mottled chert brecciated white chert clasts in brown matrix					breccia	white-grey mottled chert autoclastically brecciated white angular 2-15 mm chert clasts in brown matrix
402						chert breccia brown-grey blotchy chert-ls					breccia	white and grey angular chert clasts 5-40 mm, clast supported, discoloration toward top, sharp contact below with brown-grey cherty-ls
404						brown-grey blotchy chert-ls mottled chert					tight	white-grey mottled massive chert, sharp contacts brown-grey blotchy cherty limestone, iron-poor calcite (hard to describe texture) possibly contains clasts
406						white chert clasts in cherty matrix which grades into brown brown-grey blotchy chert-ls					breccia	white angular 2-15 mm chert clasts in cherty matrix. matrix grades into brown. also grades from clast supported to matrix supported, sharp contact below, gradational above
408						7 mm shale bed mottled chert brown-grey blotchy chert-ls					tight	white-grey mottled massive chert, sharp contacts brown-grey blotchy cherty limestone, iron-poor calcite (hard to describe texture) possibly contains clasts
410						white chert clasts in brown matrix slight fractures white-grey mottled chert					breccia fracture	angular 2-25mm chert clasts in brown matrix, clast supported white-grey chert massive to slightly fractured, stylites,
412						blue-white mottled chert moderate to highly brecciated					breccia fracture	blue-white mottled chert, slightly brecciated to massive
414						blue-white mottled chert moderate to highly brecciated					breccia fracture	blue-white mottled chert, slightly brecciated to massive
416						blue-white mottled chert moderate to highly brecciated						

Depth	Gulf Oil Corporation Pittsburg Midway PM-8 Cherokee Co., KS T32S-R23E-Sec. 5 Depth: 416-434	Texture				Sedimentary Structures	Fossils	Abrasion			Visual Porosity	Comments (color, grains, etc.)
		M	W	P	G			N	M	A		
416						collapse breccia				breccia fracture	chert breccia with mm size angular chert clasts, matrix is dark grey-black limey clay-silt, also fills in fractures for ~0.5 feet	
418						blue-white mottled chert slightly brecciated				tight fracture	blue-white mottled chert, slightly brecciated to massive	
420						blue-white nodular chert stylonites fine horizontal laminations				tight fracture	brown silty lime mudstone with fine horizontal laminations, stylonites, and interbedded with blue-white nodular chert. fracture cuts both chert and mudstone, filled with chal	
422						blue-white nodular chert stylonites fine horizontal laminations				tight	brown silty lime mudstone with fine horizontal laminations, stylonites, and interbedded with blue-white nodular chert.	
424						blue-white nodular chert stylonites fine horizontal laminations				tight	brown silty lime mudstone with fine horizontal laminations, stylonites, and interbedded with blue-white nodular chert.	
426						blue-white nodular chert stylonites fine horizontal laminations				tight	brown silty lime mudstone with fine horizontal laminations, stylonites, and interbedded with blue-white nodular chert.	
428						12 mm shale bed white cherty lenses with wispy laminations				tight	brown silty dolomitic wackestone with white cherty lenses with wispy laminations, some have silicified fossil fragments	
430						white cherty lenses with wispy laminations				tight	brown silty dolomitic wackestone with white cherty lenses with wispy laminations, some have silicified fossil fragments	
432						white cherty lenses with wispy laminations				tight	brown silty dolomitic fossiliferous-crinoidal packstone, interbedded with	
434						porcellanite chert with silicified fossils						

Depth	Gulf Oil Corporation Pittsburg Midway PM-8 Cherokee Co., KS T32S-R23E-Sec. 5 Depth: 434-452	Texture				Sedimentary Structures	Fossils	Abrasion			Visual Porosity	Comments (color, grains, etc.)
		M	W	P	G			N	M	A		
434						porcellanite chert with silicified fossils crinoidal packstone					tight	brown silty dolomitic fossiliferous-crinoidal packstone, interbedded with
436						porcellanite chert fine horizontal laminations					tight	brown silty dolomitic wacke- stone with fine horizontal laminations, interbedded with nodules/lenses of blue-white porcellanite chert
438						20 mm shale bed crinoid packstone blotchy chert replacement					tight	dark grey crinoid packstone, normally graded, topped with grey shale bed
440						fossiliferous packstone stylolites partially silicified fossils					tight	fossiliferous packstone, crinoids dominate, lime mud matrix, normally graded in between stylolites
442						fossiliferous packstone 10 mm shale bed stylolites partially silicified fossils					tight	fossiliferous packstone, crinoids dominate, lime mud matrix, normally graded in between stylolites
444						fossiliferous packstone 30 mm shale bed partially silicified fossils fairly muddy					tight	fossiliferous packstone dark grey shale
446						sharp contact on chert, hard ground, corroded surface					tight	chalky white tripolitic chert slightly brecciated with dark grey circular to elongate replacement spots that increase up section, iron-poor calcite
448						slightly brecciated					very porous	chalky white tripolitic chert slightly brecciated with dark grey circular to elongate replacement spots that increase up section, iron-poor calcite
450						slightly brecciated					very porous	chalky white tripolitic chert slightly brecciated with dark grey circular to elongate replacement spots, iron-poor calcite (poss. replaced burrows?)
452												

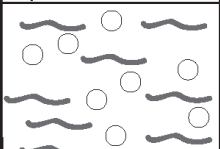





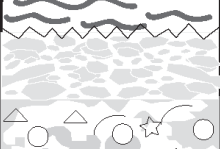




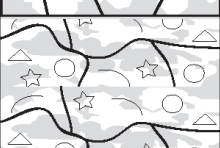

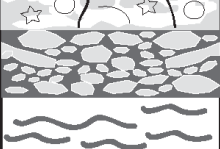

Depth	Gulf Oil Corporation Pittsburg Midway PM-8 Cherokee Co., KS T32S-R23E-Sec. 5 Depth: 452-470	Texture				Sedimentary Structures	Fossils	Abrasion			Visual Porosity	Comments (color, grains, etc.)
		M	W	P	G			N	M	A		
452						slightly brecciated				very porous	chalky white tripolitic chert slightly brecciated with dark grey circular to elongate replacement spots, iron-poor calcite (poss. replaced burrows?)	
454						slightly brecciated				very porous	chalky white tripolitic chert slightly brecciated with dark grey circular to elongate replacement spots, iron-poor calcite (poss. replaced burrows?)	
456						slightly brecciated				very porous	chalky white tripolitic chert slightly brecciated with dark grey circular to elongate replacement spots, iron-poor calcite (poss. replaced burrows?)	
458						slightly brecciated				very porous	chalky white tripolitic chert slightly brecciated with dark grey circular to elongate replacement spots, iron-poor calcite (poss. replaced burrows?)	
460						slightly brecciated				very porous	chalky white tripolitic chert slightly brecciated with dark grey circular to elongate replacement spots, iron-poor calcite (poss. replaced burrows?)	
462						slightly brecciated				very porous	chalky white tripolitic chert slightly brecciated with dark grey circular to elongate replacement spots, iron-poor calcite (poss. replaced burrows?)	
464						slightly brecciated				very porous	chalky white tripolitic chert slightly brecciated with dark grey circular to elongate replacement spots, iron-poor calcite (poss. replaced burrows?)	
466						slightly brecciated				very porous	chalky white tripolitic chert slightly brecciated with dark grey circular to elongate replacement spots, iron-poor calcite (poss. replaced burrows?)	
468						slightly brecciated				very porous	chalky white tripolitic chert slightly brecciated with dark grey circular to elongate replacement spots, iron-poor calcite (poss. replaced burrows?)	
470												




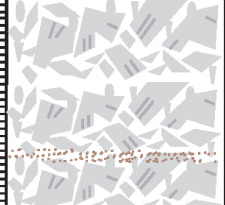
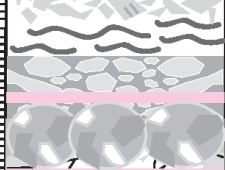

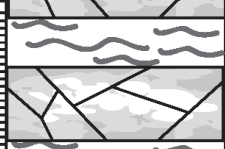
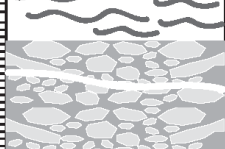
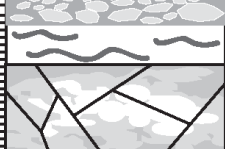

Depth	Gulf Oil Corporation Pittsburg Midway PM-8 Cherokee Co., KS T32S-R23E-Sec. 5 Depth: 470-488	Texture				Sedimentary Structures	Fossils	Abrasion			Visual Porosity	Comments (color, grains, etc.)
		M	W	P	G			N	M	A		
470										porous	chalky white tripolitic chert slightly brecciated with dark grey circular to elongate replacement spots, iron-poor calcite (poss. replaced burrows?)	
472					fossiliferous packstone ?? wackestone					tight	light grey fossiliferous packstone alternating with wackestone, diverse fauna, unsorted, stylolites, iron-rich calcite	
474					fossiliferous packstone ?? wackestone					tight	light grey fossiliferous packstone alternating with wackestone, diverse fauna, unsorted, stylolites, iron-rich calcite	
476					ooid grainstone					tight	medium-dark grey ooid grainstone, overly packed, traces of glauconite, iron-rich calcite	
478					8 mm black shale							
480					slightly brecciated					very porous slightly moldic fracture	chalky white tripolitic chert, massive to slightly autoclastic brecciated, moldic-vuggy, fizzes, mottled dark grey spots	
482					slightly brecciated					very porous slightly moldic fracture	chalky white tripolitic chert, massive to slightly autoclastic brecciated, moldic-vuggy, fizzes, mottled dark grey spots	
484					slightly brecciated mottled					very porous slightly moldic fracture	chalky white tripolitic chert, massive to slightly autoclastic brecciated, moldic-vuggy, fizzes, mottled dark grey spots	
486					slightly brecciated					very porous slightly moldic fracture	chalky white tripolitic chert, massive to slightly autoclastic brecciated, moldic-vuggy, fizzes	
488					grey-white mottled chert interbedded with wackestone					tight	white mottled grey massive chert with stylolites, fizzes, still has carbonate components	

Depth	Gulf Oil Corporation Pittsburg Midway PM-8 Cherokee Co., KS T32S-R23E-Sec. 5 Depth: 488-506	Texture				Sedimentary Structures	Fossils	Abrasion			Visual Porosity	Comments (color, grains, etc.)
		M	W	P	G			N	M	A		
488						grey- white mottled chert interbedded with wackestone					tight	white mottled grey massive chert with stylolites, fizzes, still has carbonate components
490						grey- white mottled chert interbedded with wackestone					tight	white mottled grey massive chert with stylolites, fizzes, still has carbonate components, interbedded with grey wackestone, small fossils
492						grey- white mottled chert					tight	white mottled grey massive chert with stylolites, fizzes, still has carbonate components, interbedded with grey wackestone, small fossils
494						increase in mud, fossils decrease in size, massive white- mottled chert					tight	light grey fossiliferous wacke- stone, increase mud, diverse fauna, unsorted, contacts are stylolites, sharp, iron-rich calcite, less and smaller whole fossils than down section
496						increase in mud, fossils decrease in size, massive white- mottled chert					tight	light grey fossiliferous wacke- stone, increase mud, diverse fauna, unsorted, contacts are stylolites, sharp, iron-rich calcite, less and smaller whole fossils than down section
498						increase in mud, fossiliferous wackestone disrupted by stylolites,					tight	light grey fossiliferous wacke- stone, increase mud, diverse fauna, unsorted, contacts are stylolites, sharp, iron-rich calcite, less whole fossils than down section
500						fossiliferous packstone disrupted by stylolites,					tight	light grey fossiliferous packstone, diverse fauna, unsorted, contacts are stylolites, sharp, iron-rich calcite
502						white-grey chert, silicified fossils fossiliferous packstone					tight	white chert with grey silicified fossils sharp contacts light grey fossiliferous packstone, unsorted, stylolites
504						white-grey chert, silicified fossils fossiliferous packstone					tight	white chert with grey silicified fossils sharp contacts light grey fossiliferous packstone, unsorted, stylolites
506						white-grey chert, silicified fossils fossiliferous packstone					tight	white chert with grey silicified fossils sharp contacts light grey fossiliferous packstone, unsorted, stylolites

Depth		Texture				Sedimentary Structures	Fossils	Abrasion			Visual Porosity	Comments (color, grains, etc.)
		M	W	P	G			N	M	A		
506						fossiliferous packstone disrupted by stylolites, 10-13 mm bivalves at 509'					tight	light grey fossiliferous packstone, diverse fauna, unsorted, large bivalves, contacts are stylolites, iron-poor calcite
508						fossiliferous packstone disrupted by stylolites, 10-13 mm bivalves at 509'					tight	light grey fossiliferous packstone, diverse fauna, unsorted, large bivalves, contacts are stylolites, iron-poor calcite
510						fossiliferous packstone disrupted by stylolites, coarse crystals					tight	light grey fossiliferous packstone, diverse fauna, unsorted, contacts are stylolites, iron-poor calcite
512						fossiliferous packstone disrupted by stylolites					tight	light grey fossiliferous packstone, diverse fauna, unsorted, contacts are stylolites, iron-poor calcite
514						fractured fossiliferous packstone disrupted by stylolites					fracture	light grey fossiliferous packstone, diverse fauna, unsorted, contacts are stylolites, iron-poor calcite
516						brecciated chert (fizz, not 100% silica)					fracture, breccia	white-grey mottled brecciated chert, toward top- replacement is very circular (poss. replacing burrows?), iron-poor calcite
518						fossiliferous packstone disrupted by stylolites					tight	light grey fossiliferous packstone, diverse fauna, unsorted, contacts are stylolites, iron-poor calcite
520						fossiliferous packstone disrupted by stylolites					tight	light grey fossiliferous packstone, diverse fauna, unsorted, elongate grains are imbricated, contacts are stylolites, iron-poor calcite
522						stylolites fractured laminated chert (no fizz)					tight	light grey fossiliferous packstone, unsorted, elongate grains are imbricated, contacts are stylolites.
524						fractured, laminated white chert					fracture	fractured, laminated white chert

Depth	Gulf Oil Corporation Pittsburg Midway PM-8 Cherokee Co., KS T32S-R23E-Sec. 5 Depth: 524-542	Texture				Sedimentary Structures	Fossils	Abrasion			Visual Porosity	Comments (color, grains, etc.)
		M	W	P	G			N	M	A		
524						white-grey dense mottled fossiliferous chert					tight	white-grey dense massive porcellanite chert, abundant fossils interbedded with fossiliferous packstone (iron-poor ca)
526						white-grey dense mottled fossiliferous chert					tight	white-grey dense massive porcellanite chert, abundant fossils interbedded with fossiliferous packstone (iron-poor ca)
528						fossiliferous packstone shale seam abundant fossils mostly crinoids					tight	less abundant fossils than below shale seam light grey fossiliferous packstone, stylolites
530						fossiliferous packstone					fracture	light grey fossiliferous packstone, stylolites
532						iron-stained nodule					tight	white-grey dense mottled massive porcellanite chert, fractured
534						white-grey dense mottled, fractured					fracture	light grey packstone, featureless besides iron stained
536						white-grey dense mottled fossiliferous chert					tight	white-grey dense mottled massive porcellanite chert, fractured
538						white-grey dense mottled fossiliferous chert					tight	white-grey dense massive porcellanite chert, abundant fossils interbedded with fossiliferous packstone (iron-poor ca)
540						grey fossiliferous packstone					tight	white-grey dense massive porcellanite chert, abundant fossils interbedded with fossiliferous packstone (iron-poor ca)
542						crinoid rich					tight	grey fossiliferous packstone, partially silicified

Depth	Gulf Oil Corporation Pittsburg Midway PM-8 Cherokee Co., KS T32S-R23E-Sec. 5 Depth: 542-560	Texture				Sedimentary Structures	Fossils	Abrasion			Visual Porosity	Comments (color, grains, etc.)
		M	W	P	G			N	M	A		
542						grey fossiliferous packstone crinoid rich					tight	grey fossiliferous packstone, partially silicified
544						grey fossiliferous packstone crinoid rich					tight	grey fossiliferous packstone, partially silicified
546						white-grey dense mottled fossiliferous chert					porous molds/vugs	white-grey dense porcellanite chert, fossiliferous, massive
548						wackestone white-grey chert breccia					brecciated	grey peloidal wackestone, white-grey chert angular breccia, abundant fossils
550						white-grey dense mottled chert wackestone					vuggy	white-grey dense porcellanite chert, fossiliferous, massive grey peloidal wackestone
552						white-grey dense mottled chert					fracture	white-grey mottled dense porcellanite chert, massive
554						white-grey dense mottled chert autoclastically brecciated scattered fossils					brecciated	white-grey dense porcellanite chert with scattered fossil fragments, autoclastic brecciated
556						white angular brecciated chert clasts in dark grey-black matrix wackestone					brecciated	white angular brecciated chert clasts in dark grey-black matrix grey peloidal wackestone
558						white-grey dense mottled chert					fracture	white-grey mottled dense porcellanite chert, slightly fractured
560												

Depth	Gulf Oil Corporation Pittsburg Midway PM-8 Cherokee Co., KS T32S-R23E-Sec. 5 Depth: 560-578	Texture				Sedimentary Structures	Fossils	Abrasion			Visual Porosity	Comments (color, grains, etc.)
		M	W	P	G			N	M	A		
560						white-grey dense mottled chert				fracture	white-grey mottled dense porcellanite chert, fractured	
562						white-grey dense mottled chert				fracture	white-grey mottled dense porcellanite chert, fractured, mostly silica with iron-poor calcite	
564						chert breccia				fracture-vugs	white-grey angular crackle chert breccia-highly fractured-brecciated varies with more massive to dense chert	
566						chert breccia quartz sand				fracture-vugs	white-grey angular crackle chert breccia, clast supported -highly fractured-brecciated varies with more massive to dense chert	
568						faint whispy horizontal laminae 40 mm pink baroque dolomite				fracture-vugs	blue-white mottled vuggy brecciated chert 30-60 mm grey nodular chert, baroque dolomite on both sides	
570						45 mm pink baroque dolomite slight whispy laminae mottled chert				fracture-vugs	mottled blue-white mottled vuggy chert slightly fractured alternating with brown peloidal wackestone with faint whispy horizontal laminae	
572						slight whispy laminae mottled chert				fracture-vugs	mottled blue-white mottled vuggy chert slightly fractured alternating with brown peloidal wackestone with faint whispy horizontal laminae	
574						brecciated chert clasts in light grey matrix				fracture-vugs	blue-white angular chert clasts in light grey matrix, fractures filled with white chalcedony, sharp surface above and below	
576						faint horizontal laminae-whispy mottled chert				tight fracture-vugs	brown peloidal wackestone with whispy horizontal laminae mottled blue-white chert	
578												

Depth	Gulf Oil Corporation Pittsburg Midway PM-8 Cherokee Co., KS T32S-R23E-Sec. 5 Depth: 578-596	Texture				Sedimentary Structures	Fossils	Abrasion			Visual Porosity	Comments (color, grains, etc.)
		M	W	P	G			N	M	A		
578											fractures	brown wispy wackestone interbedded with blue-white mottled massive chert slightly fractured
580											fractures	brown wispy wackestone interbedded with replace- ment chert-white-blue/grey massive to slightly brecciated chert with scattered fossil debris
582											fractures	brown wispy wackestone interbedded with replace- ment chert-white-blue/grey brecciated chert with coarse baroque dolomite (almost mottled texture)
584											fractures	brown wispy wackestone interbedded with brecciated chert white-blue/grey brecciated chert with coarse baroque dolomite (almost mottled texture)
586											fractures	brown wispy wackestone interbedded with chert breccia
588											fractures	grey-blue brecciated chert, subrounded-angular clasts, clast supported with coarse baroque dolomite
590											fracture-vugs	white-grey angular crackle chert breccia, clast supported, -highly fractured-brecciated varies with more massive to dense chert
592											fracture-vugs	white-grey angular crackle chert breccia, clast supported, -highly fractured-brecciated varies with more massive to dense chert
594											fracture-vugs	white-grey angular crackle chert breccia, clast supported, -highly fractured-brecciated varies with more massive to dense chert
596											fracture-vugs	white-grey angular crackle chert breccia, clast supported, -highly fractured-brecciated varies with more massive to dense chert

Depth	Gulf Oil Corporation Pittsburg Midway PM-8 Cherokee Co., KS T32S-R23E-Sec. 5 Depth: 596-614	Texture				Sedimentary Structures	Fossils	Abrasion			Visual Porosity	Comments (color, grains, etc.)
		M	W	P	G			N	M	A		
596						chert breccia					fracture-vugs	white-grey angular crackle chert breccia-highly fractured-brecciated varies with more massive to dense chert
598						chert breccia					fracture-vugs	white-grey angular crackle chert breccia-highly fractured-brecciated varies with more massive to dense chert
600						chert breccia					fracture-vugs	white-grey angular crackle chert breccia-highly fractured-brecciated varies with more massive to dense chert
602						chert breccia quartz sand nodular chert					fracture	white-grey crackle chert breccia mm quartz sand layer 20-45 mm white chert nodules
604						original depositional facies white-grey dense mottled chert					fracture	fractures have brown halos-filled with? highly brecciated at contact
606						white-grey dense mottled chert blue-white mottled chert					fracture	white-grey dense mottled porcellanite chert with scattered fossil fragments, segments crackle brecciated
608						original facies brecciated chert					fracture	alternating brown peloidal wackestone with chert. blue-white angular chert breccia in dark grey matrix
610						brecciated chert mottled chert					fracture, filled with chalcodny	blue-white angular chert breccia in light grey matrix blue-white mottled chert fractured with chalcodny in fractures
612						brecciated original facies mottled chert					fracture; some filled with chalcodny	brown peloidal wackestone autoclastic brecciated blue-white mottled massive chert slightly fractured
614						mottled chert						

Depth	Gulf Oil Corporation Pittsburg Midway PM-8 Cherokee Co., KS T32S-R23E-Sec. 5 Depth: 614-632	Texture				Sedimentary Structures	Fossils	Abrasion			Visual Porosity	Comments (color, grains, etc.)
		M	W	P	G			N	M	A		
614						blue-white brecciated nodules whispy-planar				fracture	blue-white brecciated vuggy chert nodules silty whispy brown peloidal wackestone, iron-poor calcite, fractured	
616						blue-white brecciated nodules dense white-grey fossiliferous chert				vuggy and fractured chert	blue-white brecciated vuggy chert nodules white-grey dense fossiliferous chert slight fractures brown unbedded wackestone	
618						no bedding scattered crinoids				chert is vuggy wackestone is tight	silty whispy brown peloidal wackestone with brecciated-dense chert nodules, iron-poor calcite	
620						highly brecciated whispy with brecciated chert nodules				fracture	silty whispy brown peloidal wackestone with brecciated chert sub-rounded to angular clasts, clast supported, iron-poor calcite	
622						whispy fractured chert				tight, vuggy	silty whispy brown peloidal wackestone, large crinoids, with dense grey-white massive fractured chert, iron-poor calcite	
624						whispy brecciated chert nodules, coarse baroque dolomite				tight, vuggy	silty whispy dark grey peloidal wackestone with brecciated dense chert nodules, iron-poor calcite, fractures filled with chalcedony	
626						whispy fractured chert, coarse baroque dolomite				tight, fractures filled with coarse mineralization	silty whispy dark grey peloidal wackestone with dense fractured mottled blue-white chert, iron-poor calcite, mineralization in fractures	
628						whispy 2 mm backfilled burrows brecciated chert nodules				fracture	silty whispy dark grey peloidal wackestone interrupted with dense brecciated chert nodules, burrowed, fractured	
630						massive chert whispy-planar				tight	silty whispy dark grey peloidal wackestone with dense mottled grey-white chert with scattered fossil debris, iron-poor calcite	
632						whispy-planar						

Depth	Gulf Oil Corporation Pittsburg Midway PM-8 Cherokee Co., KS T32S-R23E-Sec. 5 Depth: 632-650	Texture				Sedimentary Structures	Fossils	Abrasion			Visual Porosity	Comments (color, grains, etc.)
		M	W	P	G			N	M	A		
632						whispy-planar bedding, shale seams				tight	light-dark grey peloidal wackestone, dark grey horizontal whispy-planar bedding, iron-poor calcite, mottled grey-white massive chert, slightly fractured	
634						whispy-planar bedding, shale seams, scattered dense chert nodules- brecciated				tight, slight filled fractures	light-dark grey peloidal wackestone, dark grey horizontal whispy-planar bedding, iron-poor calcite, scattered dense chert nodules- replacement-	
636						whispy-planar bedding, burrows, shale seams, scattered dense chert nodules, stylolite				tight, slight filled fractures	light-dark grey peloidal wackestone, dark grey horizontal whispy-planar bedding, iron-poor calcite, scattered dense chert nodules- replacement	
638*						whispy-planar bedding, burrows, shale seams, scattered dense chert nodules				tight	light-dark grey peloidal wackestone, dark grey horizontal whispy-planar bedding, iron-poor calcite, scattered dense chert nodules- replacement	
640						whispy-planar bedding, burrows, dense shale seams, scattered dense chert nodules				tight	light-dark grey peloidal wackestone, dark grey horizontal whispy-planar bedding, iron-poor calcite, scattered dense chert	
642						whispy-planar bedding, burrows, shale seams, scattered dense chert nodules				tight	light-dark grey peloidal wackestone, dark grey horizontal whispy-planar bedding, iron-poor calcite, scattered dense chert	
644						whispy-planar bedding, burrows, shale seams, scattered dense chert nodules				tight	light-dark grey peloidal wackestone, dark grey horizontal whispy-planar bedding, iron-poor calcite, scattered dense chert	
646						whispy-planar bedding, burrows, shale seams, scattered dense chert nodules				tight	light-dark grey peloidal wackestone, dark grey horizontal whispy-planar bedding, iron-poor calcite, scattered dense chert	
648						whispy bedding, burrows, shale seams, scattered dense chert nodules				tight	light-dark grey peloidal wackestone, dark grey horizontal whispy bedding, iron-poor calcite, scattered dense chert nodules	
650												

Appendix 2
Thin Section Descriptions

Core: Depth	Grains	Abundance	Size	Grain Contacts	Mineralogy
PM-12: 437	bottom is moldic spiculite with crinoid and byozoan molds; top is clasts of the same brecciated with internal sediment	mostly spicule molds, then crinoids, then bryozoans	spicule molds ~45-60 um; crinoid molds ~50-150 um	mostly molds	all silica
PM-12: 459.5	bottom is microporous ratty looking chert clasts in dark brown clay matrix; top is crystalline dolomitic matrix with a few of the same chert clasts	bottom is angular to subround in clast support with clay matrix; top is subround in dolomitic matrix support	bottom is 0.5-2 mm; top is 2-5 mm	bottom is clast support; top is matrix support	all clasts are microporous ratty looking silica blue to light tan (not sure if grains or what?)
PM-12: 469	2 types of microporous silica; one lighter with grundgy look and random dolo rhombs; the other is very dense with spicules and random dolo rhombs	two types of silica with little dolomite matrix (possibly breccia)	if they are clasts they are large	n/a	mostly all silica with few dolomite rhombs and few calcite cements
PM-12: 478.3	brecciated chert clasts of various degree and lithology	clasts are angular to subrounded in clast support	range from 30 um to 5 mm	in clast support	mostly silica clasts: tan-light brown with rind around the clasts
PM-12: 500.6	crinoids, gastropods, bryozoans, spicules	top half is graded beds of grainstone; bottom is clay rich packstone		overly close packing, fractures, brecciated clasts, pressure solution	calcite bioclasts, silica spicules, clay matrix
PM-12: 505.2	crinoids bryozoans gastropods spicules	many of everything	40um-1 mm	packstone-grainstone; no pressure solution or grading	most replaced by silica; many are still calcite

Core: Depth	Matrix	Cements	Internal Sediment	% Porosity/Type	Compaction
PM-12: 437	moldic silica matrix; light tan in color to dark brown where denser	some moldic fossil fragments possibly had dogtooth calcite before dissolution	top is brecciated with internal sediment inbetween clasts	moldic porosity ~80%, fracture porosity ~10%	autoclastic brecciation
PM-12: 459.5	bottom matrix is dark brown clay-rich; top is crystalline dolomite that gets squished by chert clasts	some calcite cement and baroque dolomite filling in fractures	crystalline dolomite is acting like infill	all clasts are microporous; some fracture porosity	autoclastic brecciation, broken grains, pressure solution
PM-12: 469	is a section of crystalline dolomite	chalcedony filling fractures then also dolomite in those same fractures; also see calcite cements	none	microporous	fractures
PM-12: 478.3	clay rich matrix is present but mostly clasts	some fractured clasts have calcite cement	matrix is clay	some silica clasts are microporous	clasts are fractured, some pressured solution together,
PM-12: 500.6		calcite overgrowths on crinoid fragments	clay-argill. Plug below the armored surface	some interparticle porosity in top half	brecciated grains, pressure solution, overly close packing
PM-12: 505.2	matrix is silica(quartz and chalcedony) with some clays	quartz overgrowths	some clay	in upper portion highly developed inter and intra particle porosity	no features of compaction

Core: Depth	Paragenesis
PM-12: 437	deposition of normal marine material with crinoids, spicules, bryozoans; cemented with calcite overgrowths on fossils; dissolution of fossils and overgrowths; somewhere in there the matrix was all silicified; then brecciated; exposed to get internal sediment; then flooded over the top
PM-12: 459.5	silicified clasts are brecciated with dolomite matrix filling in; later calcite cement and baroque dolomite fill in some fractures
PM-12: 469	probably breccia clasts of different silica then fractures filled with chalcedony and dolomite; dolomite gets randomly distributed around silica areas
PM-12: 478.3	silicified clasts came together and fractured even more with a later calcite cement filling in those fractured clasts
PM-12: 500.6	top half is prob. High energy deposits normally graded above armored surface. Below not graded with clay rich
PM-12: 505.2	after deposition silicification of some fossils and much of the lower matrix; later dissolution of upper matrix and some intraparticle porosity development as well

Core: Depth	Grains	Abundance	Size	Grain Contacts	Mineralogy
PM-12: 509.5	clasts of microporous chert composed of spicules and fragments of crinoids and bryozoans; matrix is made of same material but less spicules	top is in clast support, bottom is in matrix support	clasts range from ~0.5-3 mm	clasts and matrix are pk-grainstones that are microporous	silica with calcitic crinoids and bryozoans
PM-12: 512.6	clasts of microporous chert composed of spicules and fragments of crinoids and bryozoans; matrix is made of same material but less spicules	clasts are microporous spiculitic crinoidal grainstones; hard in spots to decipher between clasts and matrix	clasts mostly larger 0.5-3 mm	in clast support	silica with calcitic crinoids and bryozoans
PM-12: 517	microporous silica, elongate aligned dark areas, some open cavities, baroque dolomite; breccia below	all microporous silica, many elongate spots in upper portion	elongate aligned dark areas ~300-400 um; cavity ~2mm	none	silica
PM-12: 521.6	spiculitic clasts have been dissolved out leaving matrix of calcite	in clast support	n/a	n/a	clasts are microporous spiculite that has been completely dissolved out
PM-12: 522.8	angular microporous chert clasts, angular fossiliferous chert clasts, not a lot of matrix, some calcite cement	angular microporous chert clasts and fossiliferous chert	in clast support not much matrix	grains are highly stylitized together, overly close packing	all silica grains

Core: Depth	Matrix	Cements	Internal Sediment	% Porosity/Type	Compaction
PM-12: 509.5	matrix is densely grainstone of calcitic crinoids and bryozoans highly abraided and disarticulated with some clays; unsure what is making the microporosity (whatever it was--it was holding the clasts together before dissolution)	some calcite cements	matrix is internal sediment infill	clasts are highly microporous; matrix has little microporosity	collapse breccia
PM-12: 512.6	matrix is densely grainstone of calcitic crinoids and bryozoans highly abraided and disarticulated with some clays; unsure what is making the microporosity (whatever it was--it was holding the clasts together before dissolution)	some calcite cements	internal sediment is the matrix coming in filling inbetween the clasts; clasts are made of same material but less grainy and more microporous	clasts are highly microporous; matrix has little microporosity; large fracture across slide has nice porosity	collapse breccia
PM-12: 517	elongate aligned dark areas are mostly silica; cavity has lots of carbonate w/ silt and spar on top (geopetal)	spar, baroque dolomite	internal sediment in cavities is lots of carbonate with silt	completely microporous, little fracture	stylolitization
PM-12: 521.6	matrix is calcite	none	none	highly microporous	brecciated clasts
PM-12: 522.8	not much clay matrix, some calcite cement	calcite cement	little clay matrix	all clasts are microporous	highly stylitized, overly close packed grains, in grain support

Core: Depth	Paragenesis
PM-12: 509.5	generally: subaerial exposure, solution collapse breccia, filled with marine sediment, dissolution of ?? To make microporosity
PM-12: 512.6	generally: subaerial exposure, solution collapse breccia, filled with marine sediment, dissolution of ?? To make microporosity (very much like PM12: 509.5)
PM-12: 517	original carbonate matrix (of partially spiculite) is weathered out then later cemented by quartz and followed by calcite; dark areas are possibly rhizoliths partially silica some with internal sediment and spar
PM-12: 521.6	microporous spiculite was brecciated and infilled with another porous matrix, then calcite matrix came in; later dissolution left clasts even more porous (looks like 2 matrixes?)
PM-12: 522.8	grains got crushed together; later calcite cement

Core: Depth	Grains	Abundance	Size	Grain Contacts	Mineralogy
PM-12: 528.5	Fracture: coarse crinoid debris and fine crinoid debris separated by a stylolite Matrix1: microporous chert with crinoid debris, spicules? Matrix2: increased microporosity from #1, same grains, proximal to open fractures	Fracture: abundant grains Matrix1: abundant grains Matrix2: abundant grains	Fracture: Coarse section ~150-350 um, Fine ~200 um M1: 50-200um M2: 50-200um	Fracture: stylolite cuts grains, grainstone but not overly packed M1: grainstone but not overly packed M2: grainstone but not overly packed	Fracture: calcite stain mavue M1&M2: some grains stain calcite, but not entirely
PM-12: 530	Fracture: crinoid debris Matrix: microporous chert	Fracture: crinoid debris with some calcite cements: grainstone Matrix: weird microporous chert with irregular spheres, with fenestrae bryozoans	Fracture: crinoids ~0.5-1 mm Matrix: Fenestrae bryozoans ~350 um		Fracture: Calcite Matrix: Silica
PM-12: 538	bottom is autoclastically brecciated grainstone chert; top is same grainstone chert but microporous, highly brecciated with calcitic crinoid grainstone inbetween clasts	bottom is blocky autoclastic grain rich chert; top is angular to subrounded, some is grain support some in matrix support	bottom is basically massive with open fractures; top is 0.5-5 mm clasts	variable but mostly in clast support	bottom is very grainy chert; top is same but more microporous
PM-12: 543.5	bryozoans, top of slide has fossiliferous-spiculitic Chert clast	packstone, sections of larger grains and smaller grains	40-100um for fine areas; 80-500 um for coarse areas	pressure solutions, overly close packing	completely calcite except for chert clast
PM-12: 548.5	blotchy dark tan to brown chert autoclastically brecciated; one side completely baroque dolomite	chert is fairly dense with microporous areas near fractures contains irregular vugs	almost entire slide- basically massive with few fractures	in clast support	blotchy chert clasts, various colors, unsure of fabric?,

Core: Depth	Matrix	Cements	Internal Sediment	% Porosity/Type	Compaction
PM-12: 528.5				Fracture: open fracture porosity M1&M2: microporous	stylolites
PM-12: 530				Fracture: none Matrix: microporous chert	
PM-12: 538	bottom has no matix top has calcite crinoid grainstone filling inbetween clasts	chalcedony acts as cement	suppose crinoid grainstone is internal sediment infill for the top breccia zone	bottom has open fracture porosity; top is microporous and fracture porosity	fractures, stylolitization, broken clasts
PM-12: 543.5	bioclastic matrix of varying degres of coarse-fine, layering up slide	none	none	tight excpt for chert clast which has high interparticle porosity	pressure solution, overly close packing
PM-12: 548.5	no real matrix	baroque dolomite	none	microporous areas are proximal to fracture openings, vugs?	internal fractures are faint but open/larger fractures are more visible

Core: Depth	Paragenesis
PM-12: 528.5	<p>microporous grainstone was deposited uniformly then later fractures influenced the porosity to allow a zone of more microporosity and less, with this fracture event allowed deposition of the crinoid grainstone along side this microporous chert. Grainstone was compacted and stylolites</p>
PM-12: 530	<p>microporous chert had to be in tact before fracture formed and filled with crinoid grainstone</p>
PM-12: 538	<p>top is different from the bottom; seems to be some kind of surface here; not sure??</p>
PM-12: 543.5	<p>fine-coarse bedding helps depo env. Clast of chert maybe from reworking.; chert clast has silicified fossils as well as many spicules with high degree of interparticle porosity</p>
PM-12: 548.5	<p>original fabric?? Silicification of whatever, then brecciated, vugs created, baroque dolomite in place</p>

Core: Depth	Grains	Abundance	Size	Grain Contacts	Mineralogy
PM-12: 571.8	awkward, crazy looking silica with portions dissolved out, and some chalcedony	entire slide is silica with portions dissolved out		not really any grains?	all silica
PM-12: 581.8	bottom half is crystalline dolomite with chalcedony; top half is weird microporous silica spheres with siliceous crinoids and bryozoans and fracture filled with baroque dolomite	bottom is dolomite; top has crinoids, bryozoans and strange dissolution to create siliceous spheres remaining	larger bioclasts 0.5-3 mm	no bioclastic grain boundaries	top is all silica; bottom is dolomite and chalcedony
PM-12: 582.2	none	n/a	n/a	n/a	n/a
PM-12: 600.8	burrow= dark spots in matrix; no bioclasts, large styocumulate	n/a	n/a	n/a	n/a
PM-12: 605	bottom is crystalline dolomite; top is silicified clasts with chalcedony filled inbetween	brecciated part in clast support		none	clasts are light brown dense silica with chalcedony inbetween
PM-12: 605.8	burrow= dark spots in matrix; no bioclasts	n/a	n/a	n/a	n/a
PM-12: 616	bottom; angular brecciated light to dark tan microporous chert clasts, chalcedony in fractures; top is more of same clasts in crystalline dolomite matrix	bottom is clast supported; top is matrix support	bottom clasts are 100 um-1.5 mm; top is .5-3 mm	brecciated grains are bounded by fractures that are either open or filled with chalcedony	all silica clasts with varying degrees of microporosity; some baroque dolomite

Core: Depth	Matrix	Cements	Internal Sediment	% Porosity/Type	Compaction
PM-12: 571.8	silica fabric is hard to describe; blotchy-awkwardly veiny-with blobs dissolved out	chalcedony	none	microporous blotches	none
PM-12: 581.8	top matrix is siliceous spheres with siliceous bioclasts, fracture filled with baroque dolomite, and dark brown silica areas; bottom is mostly crystalline dolomite with some chacedony replacement	chalcedony overgrowths, baroque dolomite fills fracture	none	very microporous on top; fractrues have some porosity along margins, and large open pore space between top and bottom	fracturing
PM-12: 582.2	subhedral dolomite 20-60um, many xl junctions, low intercrystalline matrix	calcite cement fills intercrystalline porosity	none	~5% intercrystalline	stylolitization
PM-12: 600.8	subhedral crystalline dolomite 20-60um, many xl junctions, low intercrystalline porosity	none	none	fracture through styocumulate; no intercrystalline porosity	open fracture in 2.5 mm styocumulate
PM-12: 605	bottom half is crystalline dolomite matrix; toward silica clasts it appears that dolomite is attacking the silica (possibly?)	chalcedony acting as cement binding the brecciated clasts together		some microporosity developed	brecciated clasts
PM-12: 605.8	subhedral crystalline dolomite 20-60um, many xl junctions	none	none	~5-10% intercrystalline porosity	none
PM-12: 616	matrix on top is crystalline dolomite with some intercrystalline porosity; chalcedony filling fractures is also porous	baroque dolomite and chalcedony acting as cement	none	chalcedony is microporous; some open fracture porosity; clasts are microporous silica; crystalline dolomite has intercrystalline porosity; breccia porosity	fractures; broken grains

Core: Depth	Paragenesis
PM-12: 571.8	possibly that porous areas were dolomitized early on and non-porous areas were not, then later the dolomite was dissolved out
PM-12: 581.8	top original fabric has been dissolved away leaving silica sphere and siliceous bioclasts--so stage of silicification then dissolution
PM-12: 582.2	burrows are present (subround dark spots) and pyrite, and stylolites
PM-12: 600.8	some burrows are present; major feature here is the styocumulate
PM-12: 605	silica clasts brecciated then later filled fractures with chalcedony; dolomitization of lower silica clasts appears to be later as dolomite is replacing the silica?
PM-12: 605.8	burrows are present as subround dark spots
PM-12: 616	brecciated silica into clasts; some fractures get filled with chalcedony; later baroque dolomite fills in

Core: Depth	Grains	Abundance	Size	Grain Contacts	Mineralogy
PM-12: 623.3	crinoids spicules forams gastropods bryozoans	few most few few few	~600-800 um ~25-70 um ~300 um ~300 um ~500um	no compactional features	mostly to all silicified
PM-12: 672	few calcitic bioclasts	few	none	none	dolomite matrix, calcite fossils, chalcedony with calcite mineralization
PM-12: 675	bottom 3/4 is baroque dolomite; top 1/4 is crystalline dolomite with few calcitic bioclasts	few	200-700 um	none	bioclasts are calcite
PM-12: 705	crinoids, gastropods, bryozoans, spicules	few, many, few	0.5-2.5 mm, ~500 um, 1-2.5 um	none	upper 1/4 of sample has more silica, lower 3/4 more calcite
PM-12: 707.5	few calcitic bioclasts	few	none	none	dolomite matrix, calcite fossils, chalcedony with calcite mineralization
PM-12: 716.3	disarticulated bryozoans, gastropods, crinoids, spicules	wackestone- packstone	150-800 um	none really	calcitic fossil fragments with dolomite matrix and large chalcedony and calcite mineralization
PM-12: 752.7	muddy intraclasts, burrows, no bioclasts, pyrite	few	up to the length of slide, to smaller	none	intraclasts look muddy
PM-12: 571.5	none	n/a	n/a	n/a	n/a
PM-17: 404	spicules crinoids bryozoans gastropods	many of all	50-300 um	pkstone-grainstone	mostly all calcite
PM-17: 407.5	spicules fragments of everything else	mostly spicules	15-30 um	pkstone-grainstone	calcitic fossil fragments and spicule molds

Core: Depth	Matrix	Cements	Internal Sediment	% Porosity/Type	Compaction
PM-12: 623.3	highly porous silica with some micrite	chalcedony replacement	none	modalic-intraparticle ~40%, interparticle ~60%, entire porosity ~80%	open fracture cuts grains, mechanical fracturing of grains
PM-12: 672	matrix is 15-50 um dolomite rhombs with 3/4 of the slide being coarse chalcedony xls	chalcedony replacement	none	none	none
PM-12: 675	matrix is crystalline dolomite on top; baroque dolomite with chalcedony on bottom	none	none	none	none
PM-12: 705	lower 3/4 has dolomite rhombs with micrite, upper 1/4 is mostly micrite	megaquartz in some modalic insides of gastropods	none	none	is boundary a stylolite or something else?
PM-12: 707.5	matrix is 15-50 um dolomite rhombs with 3/4 of the slide being coarse chalcedony xls	chalcedony replacement	none	none	none
PM-12: 716.3	matrix is 15-50 um dolomite rhombs with 3/4 of the slide being coarse chalcedony xls	chalcedony replacement with calcite	none	none	none
PM-12: 752.7	matrix is mostly 50-125 um dolomite rhoms with some intercrystalline calcite and open porosity	intercrystalline calcite could be cement		matrix has intercrystalline porosity, also fracture porosity	open fractures, cross-cut matrix and intraclasts
PM-12: 571.5	all baroque dolomite with corner of silica (?)	none	none	some fracture porosity ~3-5%	fractures
PM-17: 404	fine calcite matrix with coarse calcite fracture fill and lots of pyrite	calcite cements	none	few modalic pores	large fracture filled with coarse calcite and pyrite
PM-17: 407.5	matrix is silica	chalcedony cements	none	spicules are molds; good modalic porosity developed	none

Core: Depth	Paragenesis
PM-12: 623.3	stage of silicification, stage of dissolution to create moldic porosity, in what order? Prob molds first. Last is fracturing- cuts silicified moldic grains
PM-12: 672	dolomite rhombs cut chalcedony boundaries, chalc is almost clast-like with calcite inbetween, some chalcedony looks brecciated then later calcite cement fills in breccia openings
PM-12: 675	matrix replaced by crystalline dolomite; fossils were left calcite; mineralization is baroque dolomite with radiating chalcedony spheres; both of those were later
PM-12: 705	
PM-12: 707.5	dolomite rhombs cut chalcedony boundaries, chalc is almost clast-like with calcite inbetween, some chalcedony looks brecciated then later calcite cement fills in breccia openings
PM-12: 716.3	fossils are still calcite with a dolomite matrix
PM-12: 752.7	fractures had to come after deposition of intraclasts and after dolomitization, calcite could be remnant of original fabric
PM-12: 571.5	very coarse dolomite along with silica phase both cut by fractures
PM-17: 404	high energy disarticulated abraided fossils deposited; some moldic porosity development; fractured; later fracture filled with coarse calcite phase
PM-17: 407.5	high energy deposits, stage of silicification, stage of dissolution, clasts of moldic porosity and clasts of non

Core: Depth	Grains	Abundance	Size	Grain Contacts	Mineralogy
PM-17: 423.5	spicules crinoids bryozoans gastropods	many of all	50-300 um	pkstone-grainstone	mostly all calcite
PM-17: 428.2	clasts of spiculitic silica and matrix of dolomite	in matrix support	n/a	n/a	clasts are dark brown spiculitic silica
PM-17: 456.5	none; some spicules in concentrated areas	n/a	n/a	n/a	n/a
PM-17: 506.5	crinoids bryozoans gastropods	mostly few few	.05-3 mm	pkstone-grainstone	all calcite
PM-17: 514.2	crinoids bryozoans gastropods spicules	lots of everything	50-1000 um	packstone	mostly silica with calcitic fossils
PM-17: 516.1	highly abraded and disarticulated crinoids, gastropods, bryozoans, spicules	many of all; can't decipher all of them since they are so small	50-200 um	pkstone-grainstone, but no compactional features	mostly calcitic fossil fragments
PM-17: 540.2	completely silica; hard to tell if clasts or not; some possible clasts are separated by white wispy silica that is slightly less porous	all silica	n/a	pretty much all the same matrix with possible clasts	microporous silica
PM-17: 606.6	crinoids, bryozoans, gastropods, spicules	packstone	0.5-2 mm	not overly close but pkstone	completely silicified and highly dissolved
PM-17: 641.7	n/a	mostly spicules with whole bryozoans and fragments of crinoids	30-3000 um	wack-packstone	almost all silica

Core: Depth	Matrix	Cements	Internal Sediment	% Porosity/Type	Compaction
PM-17: 423.5	fine calcite matrix with coarse calcite fracture fill and lots of pyrite	calcite cements	none	few moldic pores	large fracture filled with coarse calcite and pyrite
PM-17: 428.2	matrix is dolomite rhombs with other bioclasts and calcitic fragments; stain calcite	chalcedony filling in fractures along silica clasts	none	none; silica clast is tight	brecciated clasts
PM-17: 456.5	matrix is calcite with few dolo-rhombs, and siliceous areas with spicules	none	none	none-tight	stylolitization
PM-17: 506.5	some micritic matrix	calcite cements all over the place	none	none	overly close packing, pressure solution seams, broken grains, large stylolites cut into grains
PM-17: 514.2	silica	calcite and chalcedony	none	small area of microporous interparticle chalcedony	fractured; filled with calcite
PM-17: 516.1	matrix is silica; chalcedony	chalcedony	none	one layer of microporous interparticle chalcedony	small fracture that cuts grains and later filled with chalcedony
PM-17: 540.2	all is microporous silica with black colored looking "grains" not sure what they are. Possibly clasts are made of this with matrix being white wispy-looking separations	none	none	all highly microporous	none
PM-17: 606.6	matrix is silica	none	none	inter and intra particle porosity developed; highly porous	none
PM-17: 641.7	matrix is dense silica; bottom has some dolo-rhombs	chalcedony overgrowths	none	none	tight spiculite

Core: Depth	Paragenesis
PM-17: 423.5	high energy disarticulated abraded fossils deposited; some modic porosity development; fractured; later fracture filled with coarse calcite phase
PM-17: 428.2	microporous spiculite was brecciated and infilled with bioclastic-dolomitic calcitic fossil fragments; fractures in clasts were later filled in with chalcedony
PM-17: 456.5	lime mudstone of calcite and concentrated areas of siliceous rich spicules; later some dolomite rhombs come in; later stylolites
PM-17: 506.5	calcite overgrowths came after compaction
PM-17: 514.2	highly abraded disarticulated high energy deposit; silica replacement of some fossils; fracturing; calcite overgrowths; coarse chalcedony fills vugs
PM-17: 516.1	high energy highly abraded disarticulated calcite grains; fractured; matrix later gets replaced by chalcedony and fills fractures: slide is laminated/layers of non porous chal matrix to porous chal matrix to dark silica matrix
PM-17: 540.2	all silica replaced some original fabric and then was separated by this matrix like geometry... possibly could be stylolites of white stuff ??
PM-17: 606.6	early silicification of fossils; later dissolution to create porosity
PM-17: 641.7	(top is spiculite; bottom is more Crimson) spiculite deposited with other fossil fragments later silicified; bottom has some dolo-rhombs that prob came later

Core: Depth	Grains	Abundance	Size	Grain Contacts	Mineralogy
PM-17: 701.5	crinoids, gastropods, bryozoans, spicules	top half is micritic packstone and bottom matrix has been silicified with calcite fossil fragments	100-2000 um	top is variable but not overly close packing; bottom has some pressure seams along grain boundaries	bottom is silica matrix with calcitic fossil fragments; top is all calcite
PM-21: 470.8	clasts of microporous chert composed of spicules and fragments of crinoids and bryozoans; matrix is made of same material but less spicules	clasts are microporous spiculitic crinoidal grainstones; hard in spots to decipher between clasts and matrix	clasts mostly larger 0.5-3 mm	in clast support	silica with calcitic crinoids and bryozoans
PM-21: 481	microporous silica and calcite filled burrows; some sulfides, spicules, other grains are not identifiable	appears very grainy but unsure how many are grains and how many are pits	30-90 um	packstone	mostly silica with calcite rich areas and calcite filled burrows
PM-21: 498.2	crinoids gastropods forams peloids bryozoans	many few few matrix fewer	~0.5-1 mm 1-2mm ~400um	in grain support	calcite
PM-21: 499.6	crinoids gastropods bryozoans	most few fewer	0.5-1.5 mm 0.5-1mm 1-1.5 mm	solution seams, overly close packing	calcite
PM-21: 571.8	top is crystalline dolomite with burrows; bottom is highly porous chert breccia separated by white wispy seams and also has dolomitized burrows	porous chert breccia is more abundant than dolomite	clasts are 150 um to 2 mm	top is crystalline dolomite; bottom is in clast support	dolomite and silica

Core: Depth	Matrix	Cements	Internal Sediment	% Porosity/Type	Compaction
PM-17: 701.5	top is micritic matrix and bottom is silicious matrix	calcite overgrowths	none	tight	some overly close grains with pressure solution
PM-21: 470.8	matrix is densely grainstone of calcitic crinoids and bryozoans highly abraided and disarticulated with some clays; unsure what is making the microporosity (whatever it was--it was holding the clasts together before dissolution)	some calcite cements	internal sediment is the matrix coming in filling inbetween the clasts; clasts are made of same material but less grainy and more microporous	clasts are highly microporous; matrix has little microporosity	collapse breccia
PM-21: 481	spicules, sulfides, pits, microporous	calcite could be cement or could be original calcite	none	microporous silica; calcite areas are pretty tight--can't see porosity	minor stylolite
PM-21: 498.2	peloidal material with micrite	calcite overgrowths between grains	see internal sediment	none 0%	major stylolites, broken grains, mechanical fracturing
PM-21: 499.6	some micrite	some calcite almost pendant, forming in any open pore space	see internal sediment raining down on top	none	solution seams along grain boundaries, def. mechanical packing
PM-21: 571.8	top matrix is crystalline dolomite; bottom is white silica surrounding highly porous silica clasts	none	none	bottom is highly microporous	small open fracture and brecciated clasts

Core: Depth	Paragenesis
PM-17: 701.5	early silicification of bottom matrix and some fossil fragments; later calcite overgrowths
PM-21: 470.8	generally: subaerial exposure, solution collapse breccia, filled with marine sediment, dissolution of ?? To make microporosity
PM-21: 481	maybe silica replaced some calcite areas and left some alone and the burrows alone or calcite is cement coming in after silicification; but the burrows were prob. Calcite before silicification since they are untouched
PM-21: 498.2	stylolites cut grains,
PM-21: 499.6	internal sediment rains down on top. Form cements on bottoms of grains due to open shelter porosity. Some internal sediment could really be caliche
PM-21: 571.8	crystalline dolomite replaced original fabric and burrows; then silicification of some matrix and not the burrows; then brecciation of the silicified areas (or could be other way around)

Core: Depth	Grains	Abundance	Size	Grain Contacts	Mineralogy
PM-21: 695.2	Brachiopods	very few >10% grains	<2mm	none	calcitic fossils
PM-8: 398	highly abraided and disarticulated crinoids, gastropods, bryozoans, spicules	many of all; can't decipher all of them since they are so small	50-200 um	pkstone-grainstone, but no compactional features	mostly calcitic fossil fragments
PM-8: 435	spicules crinoids bryozoans	most few few	15-30 um ~600-800 um ~500 um	pkstone-grainstone	mostly to all silicified
PM-8: 447	highly abraided, disarticulated crinoids, bryozoans, and spicules with some dolomite	packstone-grainstone	20-150 um	some touching-- not overly close packing though	mostly calcitic fossil fragments and dolomite
PM-8: 447.5	bottom is grainstone of spicules, crinoids, bryozoans with some dolomite; top is similar composition but less grains and more dolomite	top and bottom are different by amount of grains and dolomite		very closely spaced grains	silica and calcite grains with dolomite cements
PM-8: 448	crinoids bryozoans gastropods	very grainy	0.5-3 mm	packstone	grains are mostly silica
PM-8: 502	crinoids bryozoans gastropods	many many many	~40 um- 5000 um: highly disarticulated	overly close packing, pressure solution	mostly calcite
PM-8: 543.6	Top: very fine bioclastic debris Bottom: larger bioclastic grains	Top: crinoids, spicules, gastropods Bottom: crinoids, spicules, gastropods	Top: 60-400 um Bottom: 800-2000 um	Top: grainstone but not overly packed Bottom: major pressure solution, overly close packing	all mauve-calcite
PM-8: 557	crinoids, gastropods, bryozoans	many of all	100 um up to 2 mm	packstone; not overly packed	grains are calcite with some silica and dolomite
PM-8: 578	crinoids	crinoid grains	100-2000 um	none	calcite
PM-8: 638	spicules crinoids bryozoans	tons! Few few	15-30um .5-1.5 mm .5-1 mm	normal	mostly silica with some crystalline dolomite at the bottom

Core: Depth	Matrix	Cements	Internal Sediment	% Porosity/Type	Compaction
PM-21: 695.2	15-100 um dolomite rhombs	none	none	none	none
PM-8: 398	matrix is silica; chalcedony	chalcedony	none	can't tell; not impreg.	none
PM-8: 435	micrite?	hard to see; unimpreg	none	probably some but can't see b/c not impreg.	none
PM-8: 447	some dolomite in matrix with calcite fossil fragments	calcite and chalcedony	none	assume microporous? Can't tell, not impregn.	none
PM-8: 447.5	(I'm assuming microporosity) with grainstones of calcite fragments and spicules	some dolomite cement; top has a lot of dolomite	none	I'm assuming microporosity	none
PM-8: 448	matrix is mostly silica (chalcedony)	calcite overgrowths on many of the fossils	none	can't tell?	don't see any
PM-8: 502	some clays? Not sure?	calcite overgrowths on fossils	possibly	none	pressure solution, broken grains, stylolites
PM-8: 543.6				hard to see, not impregnated	overly close grains, solution seams, broken grains
PM-8: 557	matrix is made up of smaller grains	dolomite, chaledony	none	assume microporous	none
PM-8: 578	dolomite ~20-50 um	calcite cements	none	impregnated	none
PM-8: 638	hard to identify	none	none	probably some but can't see b/c not impreg.	none

Core: Depth	Paragenesis
PM-21: 695.2	dolomite cuts into brach boundaries
PM-8: 398	high energy highly abraided disarticulated calcite grains; fractured; matrix later gets replaced by chalcedony and fills fractures: slide is laminated/layers of non porous chalc matrix to porous chal matrix to dark silica matrix
PM-8: 435	silicification
PM-8: 447	high energy deposit (possibly some burrows) with late dolomite
PM-8: 447.5	surface between top and bottom appears to be an erosional surface but not a hardground; top is highly dolomitized and has less grains; bottom is very high energy stuff highly abraided and disarticulated; dolomite was a later event
PM-8: 448	grains are silicified along with most of the matrix. Calcite overgrowths on fossils
PM-8: 502	top has ~2-3 graded beds of normal marine fauna with calcite overgrowths; separated by stylolite but a very sharp contact from the bottom; bottom is very hard to identify due to unimpreg. Sample
PM-8: 543.6	surface between top and bottom is very irregular, possibly exposure or just stylolite, possibly has pyrite on it as well.
PM-8: 557	some later cement by dolomite and chalcedony, some silicification of fossils
PM-8: 578	side is completely crystalline dolomite, has
PM-8: 638	top half has been silicified; bottom half is crystalline dolomite

Appendix 3
Fluid Inclusion Data

Homogenization temperature and final melting temperature of ice recorded for Q1, Q2, Q3, and dolomite samples. Blue cells denote consistent FIAs.

Q1	Th °C	Tmice °C
FIA 7	125.4	-3.3
	121.1	-3.6
FIA 2	71	
	98.5	
	96.7	
FIA 6	103.7	
	101.2	
	102.8	
	106.4	
FIA 5	113.4	
	116.5	
	121.9	
	114	
FIA 3	92.7	
	94.5	
	97	
	92	
	89.3	
FIA 4	81.3	
	91.5	
	101.5	
	95.2	
FIA 1	87	
	87.4	
	86.7	
	86.2	
	85.7	
Q2	Th °C	Tmice °C
FIA 4	128	-3.2
	124	-8.7
	103.2	-3.6
FIA 1	124.3	-8.7
	129.8	-5.8
	127	-3.3
	126.3	-2.8
	120	

	135.8	
	111.5	
	102.3	
	108.9	
FIA 2	119.8	
	100.8	
	99.4	
FIA 3	103.9	
Q3	Th °C	Tmice °C
	153.2	-21.7
	154.2	-13.9
	156.8	
FIA 1	150.5	
Dolomite	Th °C	Tmice °C
	138.2	-17
	127.4	-17.9
	152.6	-18.3
	132.1	-17.8
FIA 3	132.8	-17.6
	157.7	-18.8
	152	-17.2
FIA 4	155.7	-16.8
	120.2	-18.7
	127.6	-18.7
	132.5	-16.5
FIA 1	102.3	-17.2
	141.3	-18.4
	144.7	-18.9
FIA 2	148.3	-18.4